VARNA SCIENTIFIC AND TECHNICAL UNIONS
TECHNICAL UNIVERSITY - VARNA

SIXTEENTH INTERNATIONAL CONFERENCE ON MARINE SCIENCES AND TECHNOLOGIES

Dedicated to the 60th Anniversary of Technical University - Varna

PROCEEDINGS

ISSN 1314 - 0957

October 20th, 2022
Varna, Bulgaria

SIXTEENTH INTERNATIONAL CONFERENCE ON MARINE SCIENCES AND TECHNOLOGIES

Dedicated to the 60th Anniversary of Technical University - Varna

PROCEEDINGS

ISSN 1314 - 0957

October 20th, 2022
Varna, Bulgaria

VARNA SCIENTIFIC AND TECHNICAL UNIONS

BULGARIA
9000 VARNA
25, "TSAR SIMEON I" Str.

Phone: +35952 630 532
E-mail: nts@nts.varna.net
URL: nts.varna-bg.org
DOI: https://doi.org/10/7546/IO.BAS.2022.8

ISSN 1314 - 0957

Organized by:

VARNA SCIENTIFIC AND TECHNICAL UNIONS

AND

TECHNICAL UNIVERSITY - VARNA

With the Cooperation of:

BULGARIAN NATIONAL ASSOCIATION OF SHIPBUILDING AND SHIPREPAIR (BULNAS)

BULGARIAN ACADEMY OF SCIENCES (BAS):

INSTITUTE OF OCEANOLOGY - VARNA

BULGARIAN SHIP HYDRODYNAMICS CENTRE

PBM WOODWARD LTD

* * *

Main Topics of the Conference:

(1) Oceanology

(2) Ship Hydrodynamics

(3) Shipbuilding and Ship Repair

(4) Machinery and Propulsion Systems

INTERNATIONAL ADVISORY COMMITTEE

Carlos Guedes SOARES,
University of Lisboa, PORTUGAL

Mathias PASCHEN,
Universität Rostock, DEUTSCHLAND

Leonard DOMNISORU,
Dunarea de Jos University of Galati, ROMANIA

Ionel CHIRICA,
Dunarea de Jos University of Galati, ROMANIA

Volodymyr ZAYTSEV,
Admiral Makarov National University of Shipbuilding, Ukraine,

Yordan GARBATOV,
University of Lisboa, PORTUGAL

Pentscho PENTSCHEW,
Universität Rostock, DEUTSCHLAND

EXECUTIVE COMMITTEE

Chairman:
Stefan VACHKOV,
Chairman of the Varna Scientific and Technical Unions

Co-Chairmen:
Nikolai VALCHEV,
Head of Institute of Oceanology - Varna

Rumen KISHEV,
Bulgarian Ship Hydrodynamics Centre

Petar GEORGIEV,
Technical University - Varna

Scientific Secretary:
Stefan KYULEVCHELIEV,
Bulgarian Ship Hydrodynamics Centre

Organization Secretary:
Nedelcho VICHEV,
Varna Scientific and Technical Unions

Members:

Vencislav VALCHEV,
Rector of Technical University - Varna

Boyan MEDNIKAROV,
Head of "N. Vaptsarov" Naval Academy - Varna

Svetlin STOYANOV,
Chairman of the Bulgarian National Association of Shipbuilding and Shiprepair (BULNAS)

Ivan IVANOV,
Technical University - Varna

Nikola DUKOV,
Gas Flow Control, J. S. Co, Manager

Atanas PALAZOV,
Institute of Oceanology - Varna

Dimitar TODOROV,
ODESSOS Ship repair Yard, J. S. Co - Varna, Executive Director

Kiril PALAVEEV,
ULA Ltd. - Varna, Manager

Elena VELIKOVA,
Bulgarian National Association of Shipbuilding and Ship repair (BULNAS), Executive Secretary

C O N T E N T S

PLENARY

A NEW TECHNOLOGICAL APPROACH FOR EELGRASS REFORESTATION BASED ON TEXTILE PLASTIC-FREE GROWING MEDIA

Mathias PASCHEN[12], Daniela GLÜCK[13], Reinhard HELBIG[14]

Abstract. *It has been sufficiently proven that the existence of extensive eelgrass fields in coastal areas has positive economic and ecological as well as health-promoting effects. Eelgrass meadows of the species **Zostera marina** largely dissipate the energy of fluid flow close to the sea bed. This prevents, for example, scour formation of coastal structures or sanding-up of traffic channels. The oxygen-carbon balance of seaweed is many times better than that of rainforests. Likewise, recent research results say that eelgrass meadows significantly limit the spread of harmful bacteria of the species **Vibrionidae**. On the other hand, a significant decline in eelgrass meadows in the northern hemisphere has been noted for years.*

In this light, the authors set themselves the goal of designing a technology for efficient and sustainable reforestation of seagrass beds and testing it in the southern Baltic Sea. The basis of their technological approach is the well-known principle of "rolled turf". The seeds or young plants are placed on specially developed textile, plastic-free growing media. They are cultivated under controlled conditions, e.g. in greenhouses. After a few days to weeks, the growth media including plants will be fixed on the previously determined location on the seabed by means of diving operations. The paper presents the technological concept as well as initial results.

Key words: *Eelgrass, reforestation, seagrass, technology, textile plastic-free growing media.*

INTRODUCTION

Important publications are available that deal in particular with specific issues on the biology of seagrasses in the oceans and marginal seas and their ecological importance for both the health of the marine environment and the world's climate. The importance of a stable seagrass stock is well known regarding oxygen and carbon dioxide balance [6]. Unlike the flora in tropical rainforests, seagrasses are able to transport the climate-damaging CO_2 via their roots to the seabed, where it is permanently deposited. Additionally, fewer Vibrio bacteria are found in the vicinity of seagrass meadows in the Baltic Sea [6]. Seagrass beds also have a positive effect on stabilising the seabed against sediment movements (erosion and scouring) by significantly dampening the energy of near-bottom currents, see [3], [4] and [5]. Last but not least, healthy seagrass beds guarantee ideal spawning and nursery conditions for a large number of marine species.

The seagrasses *Zostera marina* and *Zostera noltii* occurring in the Baltic Sea region are listed as endangered species. Both nutrients entering the coastal areas of the Baltic Sea via inflows from the terrestrial zone and rising water temperatures due to climate change, especially in the summer months, are significant stress factors for these seagrasses and have a negative impact on the population and the spread of the natural seagrass meadows [1]. A natural recolonization of seagrass beds has already been observed in recent times due to an improvement in water quality caused by a measurable decrease in nutrient inputs in the western and southern Baltic Sea. However this natural recolonization takes place on large time scales. It can take decades even on suitable areas [6].

In this respect, supportive measures are necessary to sustainably push the process of reintroducing seagrass

[1] MariKom GmbH, [2] University of Rostock, Department of Maritime Systems,
[3] University of Rostock, Department of Bio-Sciences, [4] Saxon Textile Research Institute Chemnitz
Phone: +4915153418318; E-mail: info@maricom-germany.de

meadows at manageable costs. In many countries, efforts can be observed to accelerate the spread of plants by manually replanting plants removed from one site in another. Some of these efforts have produced satisfactory results. However, it is, in the long term, a time-consuming manual process and a costly method.

Glück [3] succeeded in providing experimental proof that seagrass plants can develop just as well on artificial habitats as on natural sediments. On that note the chance were given to develop a technological concept for seagrass field's restoration on the basis of the proven method of rolled turf to significantly reduce the manual effort under water.

The aim of the project is a validated technical concept for a technology that is suitable and acceptable for the afforestation of seagrass beds from both an ecological and a commercial point of view. The tasks associated with this are inevitably complex. Only individual steps are explained below.

MATERIAL AND METHODS

Explanation of the concept

The concept is based on the rolled turf principle. Textile, plastic-free growing carrier are the basis for planting seagrass meadows. Healthy seagrass plants collected as flotsam from the beach after storms or seagrass seeds are put into suitable plant carriers. In this way prepared carriers will be kept in basins onshore until the plants start growing or the seeds germinate under controlled conditions. When the plants reached an adequate size as well as a sufficient robustness against mechanical loads divers are going to spread the plant carrier including the seagrass plants on the seabed. Hereby the growing media will be fixed on the seabed by ground spikes. It is very important that there is a close contact between seabed and carrier. In other case the roots of the young seagrass plants will not have the possibility to grow into the sediment. Subsequently, all parts of the installation have to be checked regarding correct workmanship and to be documented typically by underwater photographs and videos.

In order to be able to observe both the progress of growth of the seagrass and the process of successive degradation of the growth carrier, monitoring should be done by means of ROV's or by divers.

Material and design of the textile plastic-free growing media

The material textile, plastic-free growth carriers has to be compatible with the marine environment as well as the seagrass. The growth carriers themselves can be practically designed in a strand, mesh or grid shape. Shape of carrier is not so important whether netlike or grid structure. Much more important is the design of the rope-like strand which keeps the seed respectively the young plants and it is the basis for manufacturing the carrier. On the one hand, material and design of the strand must ensure the required strength of the growth carrier to withstand current and wave induced loads until the seagrass plants are firmly anchored to the seabed. On the other hand, the strand should have such a structure that provides sufficient support to the plant without hindering its growth.

It is in the interest of sustainability to use such materials which are available in the region in sufficient quantities and at low costs. For this reason, experiments were carried out in particular with dead seagrass, hemp and flax fibres for manufacturing the strand. In addition, viscose fibres made of wood were also tested as a supplementary material.

The general construction of the strands is shown in Fig. 1. An example of a rope made from seagrass can be seen in Fig. 2.

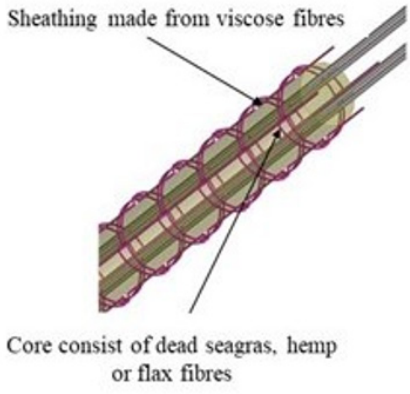

Fig. 1.
Structure of the textile strands developed

Fig. 2.
Finished strand, made from seagrass

The conceptual structure of a grid-shaped growth carrier is shown in Fig. 3. One example of a produced growing media is depicted in Fig. 4. In this case, the weft is manufactured from hemp. The warp consist of viscos fibre. The growing media consisting of rhombic meshes are similar in structure to the grid-like ones. Two mesh bars of each mesh are comparable to the warp threads in terms of their structure. The other two mesh bars consist of a strand that is comparable to the weft thread of the grid construction. The net-like growth medium shown in Fig. 4 is made of hemp and flax.

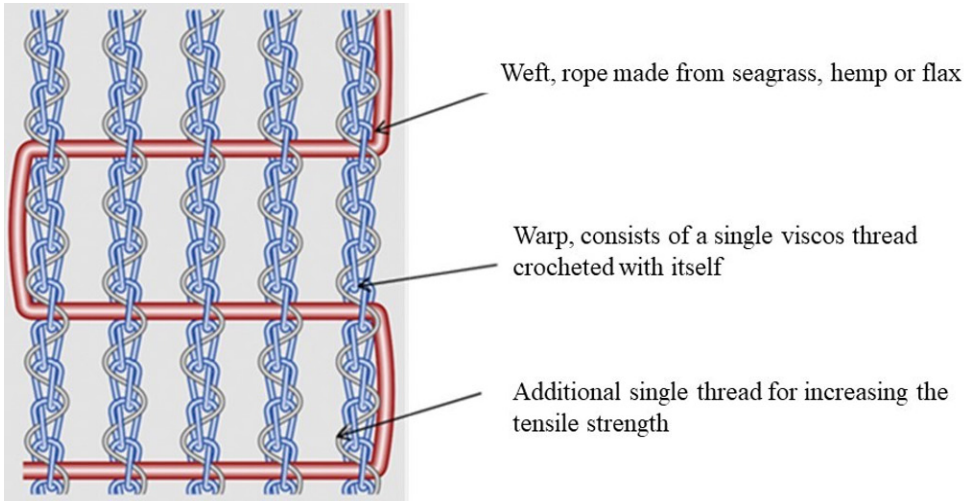

Fig. 3.
Detail design of the growing media in grid shape developed and used for the project

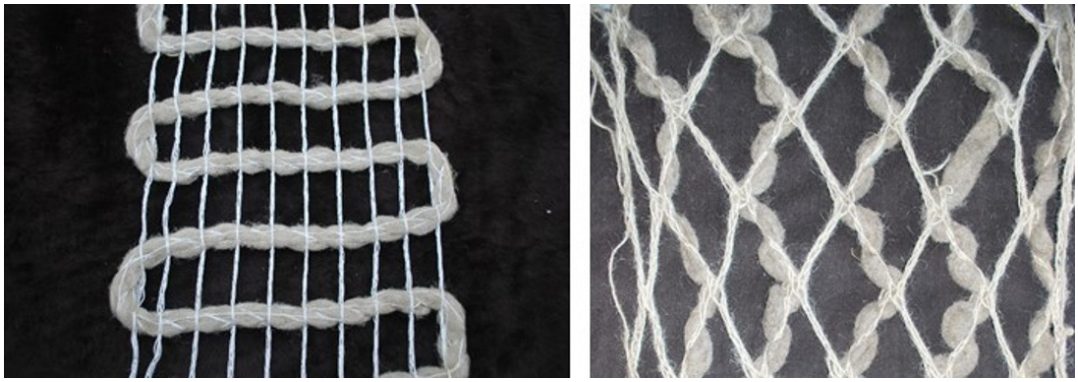

Fig. 4.
Example of a growth carrier in both grid shape (left) and net-like shape (right)

RESULTS AND CONCLUSION

First results

In mid-February 2022, the first trials began according to the concept described above. For this purpose, several basins filled with seawater (length: 4 m, width 1.25 m, height of the water column: approx. 35 cm) were installed in a greenhouse by an air temperature between 6°C to 8°C, later up to 20°C. Healthy seagrass plants collected from the beach after a storm were placed in different types of growing media by hand. The distance between the plants was about 20 cm by 20 cm.

The growth mediums and plants prepared in this way were kept in the greenhouse for 10 weeks. During this time, the condition of both the plants and the growth carriers was regularly checked. Selected parameters of the water body were measured.

About every 10th plant was marked with special markers to precisely follow its development. This way, it could be determined that more than 50 percent of the plants developed well. They showed recognisable root and leaf growth, see Fig. 5. Individual plants already developed seeds during this period. The rest of the plants died.

On 13 April 2022, the growth carriers including plants were deployed to a previously determined location with sandy soil in the Baltic Sea close to Rostock in approximately 7 metres depth (Rosenort reef) by two research divers. For this purpose, the growth mediums and plants were placed in trough-like transport containers before.

The installation went well due to good weather conditions, see Fig. 6. However, everyone involved was sceptical whether the plants would survive the heavy drop in temperature well (Baltic water temperature was below 6°C). On 18 May 2022, i.e. approximately five weeks after installation, the first monitoring took place. It could be seen that

- a great number of plants took a good development with regard to growth of roots and leaves, see Fig. 7 and 8,
- the viscous threads of the growth media were already partly in the process of degradation,
- unfortunately, the growing carrier also form a good habitat for green algae,
- a less number of plants didn't survive the procedure.

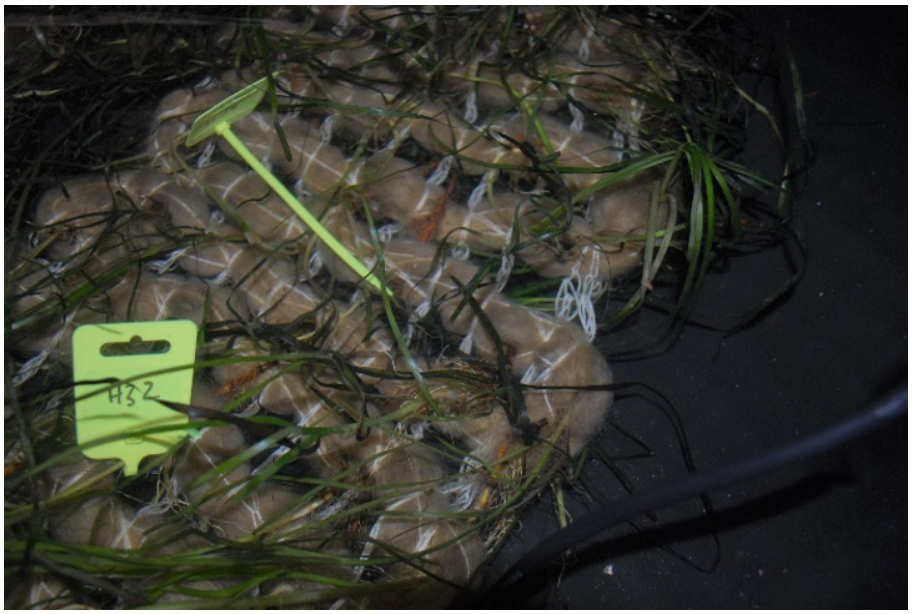

Fig. 5.
Seagrass plants placed in the growth carrier, two markers are visible.

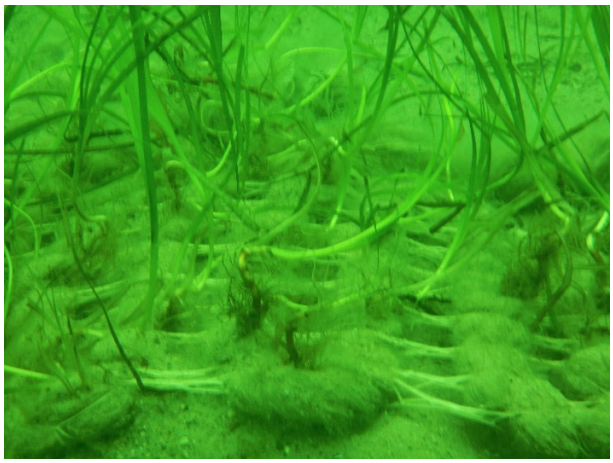

Fig. 6.
Photographic image immediately after installation

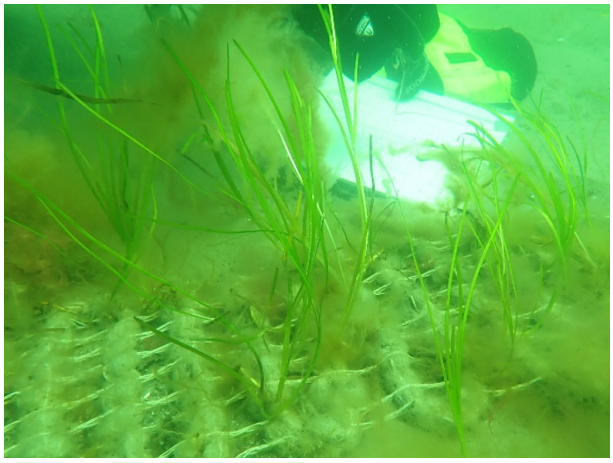

Fig. 7.
Monitoring on 18 May 2022, condition of the plants and growth medium is satisfactory

At the beginning of August 2022, there were days of very stormy weather with corresponding rough seas in the southern Baltic Sea. The monitoring on 16 August made the extent of this weather event clear. Numerous plants and growth mediums were destroyed. Of course, this was an unpleasant result. In terms of research, it led to further gains in knowledge.

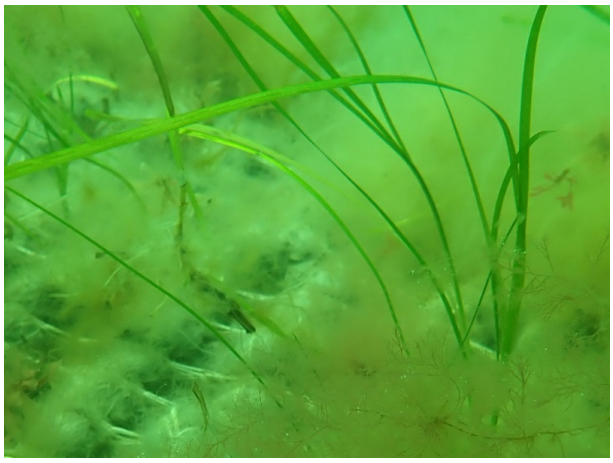

Fig. 8.
Monitoring on 18 May 2022, view on individual plants

CONCLUSION

It is internationally proven that the worldwide protection of seagrass meadows in general and the restoration of seagrass beds in the Baltic Sea in particular is of high priority under the aspect of "climate protection". In addition, there are numerous other reasons to do everything possible to protect and increase seagrass meadows. These have already been mentioned in the introduction to the paper.

With this project, the authors are taking up the challenge of developing a promising technology for the sustainable reforestation of seagrass beds based on textile, plastic-free growth media.

The results so far have clearly shown that the concept as a whole leads to the specified goal. It must also be accepted that there is still a need for further optimisation, particularly in the construction of the strands, which are important for seed germination and seedling development.

Likewise, the existing hydrological and meteorological conditions must be substantially taken into account in the choice of a suitable location.

ACKNOWLEDGEMENT

The authors would like to thank the Climate and Environment Foundation Mecklenburg - Western Pomerania (CEF) for funding this research and development project.

Thanks are equally due to the members of the project advisory board Dr. Heike Illing-Günther (STFI), Christin Klinger (CEF), Petra Mahnke (GMT) and Prof. Dr. Hendrik Schubert (University of Rostock) for their fruitful support.

REFERENCES:

[1] B o b s i e n, I. Mögliche Auswirkungen des Klimawandels auf den Blasentag (Fucus vesiculosus) und das Gewöhnliche Seegras (Zostera marina) in der Ostsee. Report. RADOST-Berichtsreihe 24. Landesamt für Landwirtschaft, Umwelt und ländliche Räume Schleswig-Holstein, Flintbek, 2014.

[2] G l ü c k, D. Keimungsverhalten von Seegras auf künstlichen Substraten**.** M.Sc.-Thesis, University of Rostock, Faculty of Mathematics and Natural Sciences, Institute of Biosciences, 2020.

[3] H a r b r e c h t, G.: Untersuchungen zur Kolkbildung an Monopiles und zur Migration von Objekten am Meeresboden. B.Sc.-Thesis, University of Rostock, Faculty of Mechanical Engineering and Marine Technology, Chair of Ocean Engineering, 2017.

[4] M e n z e l, P.; Paschen, M.: Kolkbildung und Kolkschutz an Monopile-Fundamenten. Lecture at the 112th Annual General Meeting of the Schiffbautechnische Gesellschaft in Potsdam in November 2017, published in: Yearbook of the Schiffbautechnische Gesellschaft, Vol. 111, pages 208 - 213.

[5] P a s c h e n, M.; Wranik, H.: Beurteilung der Wirksamkeit technischer Maßnahmen zur Verhinderung von Kolkbildung an zylindrischen Gründungsstrukturen von Offshore-Bauwerken auf Grundlage numerischer und experimenteller Analysen. Maritime Competence Centre for Industrial Research of Ocean Engineering GmbH, Report on the R&D project „Scour protection", 2016.

[6] R e u s c h, T.: Unterwasserwiesen im Klima-Labor speichern 30 Mal mehr CO_2 als die Tropen (Underwater meadows in the climate lab store 30 times more CO_2 than the tropics). Interview vom 7. Oktober 2021, abgedruckt in **ntv.**

OCEANOLOGY

USE OF MACROPHYTOBENTHIC COMMUNITIES AS IMPORTANT ELEMENTS, ACCORDING TO MARINE STRATEGY FRAMEWORK DIRECTIVE, FOR ASSESSMENT OF MARINE ENVIRONMENTAL QUALITY STATUS ALONG THE BULGARIAN BLACK SEA COAST

Kristina DENCHEVA

Abstract. *Marine Strategy Framework Directive was put in place to protect the marine ecosystem and biodiversity upon which our health and marine-related economic and social activities depend. To help EU countries achieve a good environmental status (GES), the directive sets out 11 illustrative qualitative descriptors. Macroalgae are included as elements in descriptors biodiversity and eutrophication. Macroalgae are important biological element in Water Framework Directive and Marine Strategy Framework Directive. Some indexes (indicators) were developed and applied for ecological quality and environmental status assessment. Macrophytobenthic communities as primary producers are very important elements of coastal water communities and are good indicators of ecological status because directly penetrate nutrients with their surface from sea water. The main goal of this paper is to apply some methods for assessment of coastal ecosystems ecological status for the aims of WFD and MSFD in 2021 year monitoring programe. From the final results, obtained from Ecological quality ratios of different ecological quality states and values of environmental status indicators, a good status in Galata - Emine region and in most polygons in Emine-Maslen nos region of Bulgarian coast was established. Lower status was assessed in Emine-Maslen nos region in Burgas bay (Burgas central, Sarafovo, Krajmorie) which is zone with high ecological risk because of strong influence of different contaminants. Ravda 2 polygon also was assessed as zone with no good status. Good correlation was established between ecological indexes and Secchi dept as indirect indicator for nutrient enrichment.*

Key words: *Ecological indexes, macrophytobenthic communities, MSFD, sea ecology.*

INTRODUCTION

Monitoring program, Descriptor 1,6 “Benthic habitats” examines biological diversity of benthic communities on the marine bottom. Regarding to Descriptor 1,6, good environmentall status has been achieved when biodiversity has been maintained, quality of habitats, distribution and abundance of species are in compliance with predominant physicogeographical, geographical and climatic conditions [12] Spatial extent of monitoring of macroalgae, according to initial assessment of marine environment, carried out in compliance with article 8 of MSFD is focused on wide type habitats in coastal zone and relevant regions of assessment (MRU) - 5 in coastal habitat.

Macroalgae on hard bottom, as element of benthic communities, include following parameters: species biodiversity, percent cover and biomass, depth distribution of macrophytobenthic communities.

Macroalgal communities are important element from Marine Strategy Framework Directive (MSFD) and Water Framework Directive. Because of important role in coastal communities as primary producers, first link in food chain and also not in last place, penetrating biogenic elements with whole surface, are good indicators of anthropogenic eutrophication.

Kristina Hristijanova Dencheva, Institute of Oceanology - BAS, Varna
Phone: 0894 653 511; E-mail: k.dencheva@io-bas.bg

MATERIALS AND METHODS

The assessment of marine environment status in regions of assessment (MRU) along the Bulgarian Black Sea coast, Descriptor 1,6, D5C6. D5C7 criteria-benthic habitats and biological element macroalgae, was carried out on the base of 1 conducted summer expedition, july - august months.

Space spread of 2021 year monithoring-macroalgae was focused on marine assessment regions (MRU)) Galata-Emine.and Emine-Maslen nos, situated in coastal habitats. In 2021 year, summer season sampling, monitoring was carried out, photo and video were taken in 21 polygons from coastal region of Black Sea. Destructive samples (252), and over 600 pictures were taken and processed and videos in the investigated polygons from representative reefs.

Methods for sampling of destructive and non-destructive samples, as well as these for laboratory analysis were described in intermediate reports, as well in the literature cited [2];[3]; [11];[15];[20].

Secchi disk depth was measured as associated parameter, indicating transparency of marine water.

In Table 1 are presented ecosystem elements and threshold values for Good status of marine environment of relevant indicators.

Inventory of elements and assessment approaches of Good ecological status (GES) and element threshold values, Descriptor1,6 and D5C7 criteria

Table 1

Element	Benthic habitats - macrophyte communities composition and abundance		Coverage macrophyte species			Macrophyte maximum depth		
Parameter from the BG Monitoring Programm	Proportion of Wet biomass of ESGI species	Ecological index-biomass (EI b.)	Ecological index coverage (v, cov)	Ph.crispa, Gelidium etc.	ESG II species C. albida, C. coelothrix etc.	Gongolaria barbata	Ericaria crinita f. bosphorica	Phyllophora crispa
Unit of the value	%	value	value	%	%	m	m	m
Parameter assessed in 2021-2022	≥ 0.6	≥ 0.644	≥ 0.644	≥ 35	≤ 15	≥ 10	≥ 4	≥ 17

Threshold values of indicators “maximal depth distribution of Gongolaria barbata, Phyllophora crispa, Gelidium spinosum, Zanardinia typus, Phyllophora crispa, as well as threshold values of cover of tolerant and sensitive species from lower infralittoral are not definitive and are subject to reassessment and may undergo changes.

Inventory of elements and assessment approaches of Good ecological status (GES) and element threshold values, Descriptor1,6 and D5C6 criteria

Table 2

Element	Benthic habitats - macrophyte communities composition and abundance		
Parameter from the BG Monitoring Programm	Proportion of Wet biomass of ESGII species	Ecological indexbiomass (EI b.)	Coverof tolerant species (lower infralittoral)
Unit of the value	%	value	%
Parameter assessed in 2021-2022	≤ 0.4	≥ 0.644	≤ 15

The assessment of ecological quality status of coastal marine regions was realized with Ecological index elaborated in compliance with European Water Framework Directive. High values of the Ecological index establish good environmental status and lower values respectively - no good status. The assessment of ecological status is on the base of elaborated classification system [2], revised and supplemented in the process of intercalibration - second phase in frames of GIG Black Sea [7];[8];[9];[10];[14];[15];[16] and approved with Regulation 4 /14.09.2012, [19].

Referent value was revised in last phase of intercalibration [2] and in result of this, the borders of ecological state classes for ecological index and ecological quality ratio were calculated (Table1).

Additional indicators were proposed - maximal depth distribution of Gongolaria *barbata*, and *Ericaria crinita f. bosphorica*, for upper infralittoral habitat, as well as cover of tolerant and sensitive species from lower infralittoral, and maximal depth distribution of *Phillophora nervosa,* threshold values of which were defined by Dimitar Berov, Institute of ecosystem research -Sofia.

Threshold values of Ecological index-biomass and ecological index - percent cover, proportion of biomass of sensitive and tolerant species - upper infralittoral were defined from Dencheva, Institute of Oceanology-BAS [10];[11];[18].

For assessment of ecological status of Marine environment, under the Marine Strategy Framework Directive threshold values of different indicators were used, published in the Monitoring program, Descriptor 1,6-benthic habitats [17]. (https://www.bsbd.org/msfd/2016/BLKBG_D1,6_SeabedHabitats_revised.pdf)

For every polygon, definition of final status, as a result of indicator values, was realized with “two out, all out” principle.

RESULTS AND DISSCUSION

The assessment of indicator values and environmental status were carried out in the investigated regions.

Region Galata - Emine

Polygons of observation Kara burun, Biala, Irakli and Emine were included in monitoring 2021 year, in Galata-Emine region. They were assessed in good status. (Table 3). This assessment was determined by the prevailed quantity sensitive macroalgae, mostly *Gongolaria barbata u Ericaria crinita f. bosphorica*. This region is characterized by low pressure, because of absence of large sources of contamination. From Table is obvious, that ecological indexes values, correspond to good status.

Indicator values assessment in different polygons, final assessment of Galata-Emine region, D5C7 criteria

Table 3

Name of marine assessment region	*Code of marine assessment region*	*Polygon*	*EI-(biomass)*	EI(vertical cover)	*Proportion of sensitive species (ESGI)*	*Maximal depth distribution of Gongolaria barbata*	*Maximal depth distribution of Ericaria crinite.f.bosphorica*
(BLK-BG-AA) Coastal	BLK-BG-AA-Galata-Emine	1.Kara burun	0.902	0.649	0.841		4.5
		2.Biala-Sv. Atanas	0.95	0.75	0.886	10.3	5.3
		3.Irakli 2	0.99	0.887	0.923		6.9
		4.Emine	0.999	0.851	0.931	11	7.1
			0.980	0.784	0.895	10.65	5.95
		Good					

Indicator values of assessment in different polygons, final assessment of Galata-Emine region, D5C6 criteria

Table 4

Name of marine assessment region	*Code of marine assessment region*	*Polygon*	*EI-(biomass)*	*Proportion of tolerant species biomass (ESGII)*	*Cover of tolerant (ESG II) from lower infralittoral*
(BLK-BG-AA) Coastal	BLK-BG-AA-Galata-Emine	1Kara burun	0.902	0.103	5
		2.Biala-Sv.Atanas	0.95	0.092	14.25
		3.Irakli 2	0.99	0.040	
		4.Emine	0.999	0.030	3.2
		Average value	0.980	0.066	8.73
		Good			

On Table 4 are presented values of indicators assessed, criteria D5C6 from relevant polygons in Galata-Emine region. It is obvious that all of them correspond to good status.

Region Emine – Maslen nos

Region Emine-Maslen nos includes polygons Nesebar, Ravda 1, Ravda 2, Pomorie 2, Sarafovo, Burgas centr. plaj, Krajmorie, Atia, Bivolite, Chervenka, Sveti Ivan, Sozopol, S.ozopol 2 (jug), Kolokita, Sveta Agalina sever, Sveta Agalina jug, Zmijski Fourteen polygons were in good status. Dominant are oligotrophic brown algae *Gongolaria barbata, Ericaria crinita f. bosforica*. Exeption are the tree polygons, situated in Burgas bay Krajmorie, Sarafovo and Burgas central plaj, which comprise the water area, being under effect of outgoing current from Mandra lake, flowing in Burgas bay, as well as untreated sewage waters, Burgas port and other sources of contamination from Burgas bay [21];[6];[7];[1]. In Krajmorie, Sarafovo and Burgas cenral plaj, tolerant species green and red algae are spread. Polygon Ravda 2 also was assessed in no good status. Availability of hydro technical construction, as well as intensive resort activity and outflow of sewage waters, contribute to this condition. In polygons Ravda1 and Ravda 2, Pomorie 2, the indicator ecological index-vertical cover, indicates no good status. In Ravda 2, indicator maximal depth distribution of Gongolaria barbata, establish no good status. (Table), The reason of this assessment were probably higher concentration of contaminants in result of resort activity and more closed character of marine waters, because of availability of hydro technical constructions.

In Krajmorie,Sarafovo, Burgas central plaj, all indicator values were low and correspond to no good status (Table 5).

Indicator values for assessment of environmental status in relevant polygons and final assessment of Emine-Maslen nos region, D5 C7 criteria

Table 5

Name of marine assessment region	*Code of marine assessment region*	*Polygon*	*EI-(biomass)*	EI (vertical cover)	*Proportion of sensitive species biomass*	*Maximal depth distribution of Gongolaria barbata*	*Maximal depth distribution of Ericaria crinita f. bosphorica*	*Cover of sensitive species (ESGI) from lower infralittoral*	*Final status*
(BLK-BG-AA) Coastal	BLK-BG-AA-Emine-Maslen nos	5.Nesebar	0.901	0.744	0.84	10			Good
		6.Ravda 1	0.813	0.619	0.758				Good
		7.Ravda 2	0.720	0.513	0.671	5.8			No good
		8.Pomorie 2	0.823	0.639	0.767				Good
		9.Burgas central plaj	0.08	0.091	0				No good
		10.Sarafovo	0.101	0.11	0				No good
		11.Krajmorie	0.343	0.248	0.239				No good
		12.Atia	1	0.965	0.84	10	8		Good
		13.Bivoli	0.999	0.889	0.8		5.2		Good
		14.Chervenka	0.836	0.644	0.779				Good
		15.Sozopol	0.997	0.888	0.799				Good
		16.Sozopol 2 (jug)	1	0.849	0.937				Good
		17. Sv. Ivan	0.954	0.821	0.889		4		Good
		18.Kolokita	1	0.972	0.961	8.2	6.8	36	Good
		19. Sv. Agalina sever	1	0.803	0.932	11	6	41.9	Good
		20. Sv. Agalina (jug)	0.992	0.813	0.925	10.5	7.4	36.7	Good
		21.Zmijski ostrov	1	0.844	0.962	10	8	38.67	Good
			Good						

From Table 6 is obvious, that in polygons Sarafovo, Burgas central plaj and Krajmorie, the status is no good, because of availability of large sources of contamination with multiannual impact in this region, which is assessed as zone in risk. The other 14 polygons were assessed in good status under all indicators. Exeption is Ravda 2- no good status of cover of tolerant species from lower infralittoral, but as a hole was assessed in good status.

Indicator values for assessment of status of relevant poligons, final assessment of Emine- Maslen nos region, Д5.С6 criteria

Table 6

Name of marine assessment region	*Code of marine assessment region*	*Polygon*	*EI- (biomass)*	*Proportion of tolerant species biomass*	*Cover of tolerant species(ESG II) fmrom lower infralittoral*	*Final status*
(BLK-BG-AA) Coastal	BLK-BG-AA-Galata-Emine	5. Nesebar 2	0.901	0.16		Good
		6. Ravda 1	0.813	0.242		Good
		7 .Ravda 2	0.720	0.329	17	Good
		8.Pomorie 2	0.823	0.233		Good
		9.Sarafovo	0.101	1	21.3	No good
		10. Burgas central plaj	0.08	1	52.96	No good
		11.Krajmorie	0.343	0.761		No good
		12. Atia	1	0.035		Good
		13. Bivoli	0.999	0.07		Good
		14.Chervenka	0.836	0.221		Good
		15. Sv. Ivan	0.954	0.111	14	Good
		16. Sozopol	0.997	0.071	2	Good
		17. Sozopol 2 jug	1	0.063		Good
		18. Kolokita	1	0.039	15	Good
		19. Sv. Agalina sever	1	0.068	14.5	Good
		20. Sv. Agalin jug	0.992	0.075		Good
		21Zmijski ostrov	1	0.038		Good
		Final status	Good			

CONCLUSIONS

The assessment of the two regions Galata- Emine and Emine-Maslen nos was not complete, because of no all polygons were included. The final assessment could be carried out after including of all polygons.

From Table 6 is obvious that the highest ecological quality ratios and indicator values indicating good status were estimated because of little or no sources of anthropogenic pressure in these polygons from Atia to Zmijski ostrov.

Probable pressures, which provoke the observed no good status of macrophytobenthic communities in Burgas central plaj, Sarafovo, Krajmorie, could be due to contaminants, which came from rivers in South part of Burgas town in coastal waters and direct flows from waste water treatment plants, from sewerage waters and underground waters.

REFERENCES:

[1]. B e r o v, D.2013. Community structure of braun algae of Cystoseira species and influence of anthropogenic factors on their distribution. Macroalgae as indicator of ecological status of coastal marine ecosystems in Black Sea.

[2]. B e r o v, D., Todorov, E., Marin, O., 2015 - Black Sea GIG - Coastal/Transitional waters - BQE. Technical report, 24 pp.

[3]. B e r o v, D., Hiebaum, G., Vasilev, V., Karamfilov, V., 2016. An optimised method for scuba digital photography surveys of infralittoral benthic habitats: A case study from the SW Black Sea Cystoseira-dominated macroalgal communities. Underw. Technol. 34.

[4] B e r o v, D., Karamfilov V., Biserkov S., Klajn S. 2018.Analisis of marine environment status.

[5] C o m m i s s i o n Decision (EU) 2018/229 of 12 February 2018 establishing, pursuant to Directive 2000/60/EC of the European Parliament and of the Council, the values of the Member State monitoring system classifications as a result of the intercalibration exercise and repealing Commission Decision 2013/480/EU (notified under document C(2018) 696)Text with EEA relevance.
[6] D e n c h e v a, K. 2008. Influence of the anthropogenic stress on macrophytobenthic communities Phytologia Balcanica 14 (3): 315-321.
[7] D e n c h e v a, K. 2010. State of macrophytobenthic communities and ecological status of the Varna Bay, Varna lakes and Burgas Bay PHYTOLOGIA BALCANICA 16 (1): 43 - 50.
[8] D e n c h e v a, K. 2011.Sensitivity of macrophytobenthic communities to anhropogenic pressures. Coastal and Transitional Waters Intercalibration Workshop, Constanca (ppt presentation).
[9]. D e n c h e v a, K., Dumitrescu, O. 2011.Intercalibration of macrophytobenthis-Black Sea GIG. Coastal and Transitional Waters Intercalibration Workshop, Casa Don Guanella, 17-18 November, 2011 (ppt presentation).
[10]. D e n c h e v a, K., Doncheva, V. 2014. Ecological Index (EI) - tool for estimation of ecological status in coastal and transitional waters in compliance with European Water Framework Directive. Proceedings of Twelfth International Conference On Marine Sciences And Technologies September 25th - 27th, 2014, Varna, Bulgaria, pp.219-226.
[11]. D e n c h e v a, K. 2018. USE OF MACROALGAE TO ASSESS ECOLOGICAL STATUS OF BULGARIAN COASTAL WATERS FOR THE AIMS OF EUROPEAN WATER FRAMEWORK DIRECTIVE Proceedings of 14 Interntional Black Sea Conference on Marine Sciences And Technologies.
[12] E u r o p e a n Commission. 2018. Reporting on the 2018 update of articles 8, 9 & 10 for the Marine Strategy Framework Directive. DG Environment, Brussels. pp 72 (MSFD Guidance Document 14).
[13] I n i t i a l assessment of marine environmental status, in compliance with article 8., 2021, 509 p.
[14] ISMEIMP - C-34-13/02. 04. 2015 year., Investigations on the State of the Marine Environment and Improving Monitoring Programs developed in compliance with MSFD.
[15] M e t h o d s of sampling of macroalgae. http://bgodc.iobas.bg/documents/2017/3_Methods_sampling_MSFD.pdf.
[16] M i n i s t e r i a l council dessision №1107/29.12.2016г. на Министерски съвет. План за управление на речните басейни в Черноморски район за басейново управление на водите (2016-2021г.) Раздел 4. Мониторинг и оценка на състоянието на повърхностните води, подземните води и зоните за защита на водите, Приложение 4.1.2 - Програма за хидробиологичен мониторинг на повърхностни води. Държ. в-к , брой 105/ 30.12.2016 г.
[17] M o n i t o r i n g program, Descriptor 1,6-benthic habitats (https://www.bsbd.org/msfd/2016/BLKBG_D1,6_SeabedHabitats_revised.pdf).
[18] O r f a n i d i s, S., Dencheva, K., Nakou, K., Basset 2012. A.Benthic macrophyte changes across an anthropogenic pressures gradient in Mediterranean and Black Sea water systems: structural vs. functional approaches. Current questions in water management (Eds. A Schmidt-Kloiber, A. Hartmann, J. Strackbein, Ch. K. Feld & D. Hering WISER final conference Tallinn, Estonia, 25-26 January 2012,147-149 p., ISBN 978-9949-484-19-5.
[19] R e g u l a t i o n No 4 from 14.09.2012 year for characteristic of surface waters. Issued from the Minister of environment and waters, effective from 5.03.2013 г., в сила от 5.03.2013 http://www3.moew.government.bg/files/file/Water/Legislation/Naredbi/Naredba_H4_za_harakterizirane_na_povyrhnostnite_vodi.pdf.
[20] R o e l f s e m a, C. and Phinn, S. 2009 A Manual for Conducting Georeferenced Photo Transects Surveys to Assess the Benthos of Coral Reef and Seagrass Habitats. Brisbane, Queensland, AUSTRALIA,33p.
[21] S t e f a n o v a, K., Todorova, V., Kamburska, L., Dencheva, K. 2005. Ecosystem of Blagk Sea along the Bulgarian coast-research and contemporary state- In Petrova A. (ed.) Contemporary status of biodiversity in Bulgaria-problems and perspectives.447-468p. Bulgarian bioplatform, Sofia (In Bulgarian).

ON THE CORRELATION OF HYDROLOGICAL AND HYDROCHEMICAL PARAMETERS WITH PHYTOPLANKTON BLOOMS IN THE NORTH-WESTERN PART OF THE BLACK SEA

Mariya GRANDOVA[1,2], Vasyl DIADYCHKO[3]

Abstract. *Control and prediction of microalgal blooms is the problem that disturb the researchers for many years. The studies of circumstances causing blooms were carried repeatedly, but the results differ depending on geographical region, blooming species and other factors. The material of the present study is the sample set taken for two decades (2003- 2019) at two stations in Odessa region (Ukraine). During this period we registered 332 blooms, some of them were multispecies. We analyze the correlation of the blooming microalgae biomass with the following parameters: temperature, salinity, pH, dissolved oxygen, ammonia, nitrate and nitrite, mineral, organic and total nitrogen, silicates, phosphates, organic and total phosphorus concentrations. We also studied separately the blooms of the main classes: Bacillariophyceae, Dinophyceae, Cyanophyceae and Prymnesiophyceae. The most interesting is strong correlation between organic nitrogen concentration and the biomass of blooming dinoflagellates that shows the necessity of organic nitrogen control for "red tides" prevention.*

Key words: *correlation, hydrological and hydrochemical parameters, North-Western Black Sea shelf, phytoplankton bloom.*

INTRODUCTION

The microalgal blooms cause great disruptions in marine communities. Massive development of microalgae led to hypoxia and death of bottom organisms. In the case of toxic species, it may be dangerous also for predators and even for people who eat marine products after bloom. Better understanding and prediction of blooms may help to prevent massive losses, especially in the areas with aquaculture enterprises.

There were several studies trying to find the correlations between phytoplankton blooms and different hydrochemical and hydrological parameters [2, 7, 9 - 13]. The results of these studies differed depending on the geographical region, the dominant blooming species and other factors, some of them were not evident yet. For example, the Onderka's study [12] of cyanobacteria blooms in eutrophic water body revealed that none of the variables (total phosphorus: total nitrogen ratio, nitrogen and phosphorus limitation, water temperature) used in the regression models seems to be dominating. On other hand, the study of Pinckney et al. [13] shows that the regression model with the main hydrological variables (salinity, diffuse attenuation coefficient (Kd), NO_x and NH_4^+) explained 71% of total variability associated with phytoplankton biomass in the moderately eutrophic Neuse Estuary. The models of Feki-Sahnoun et al. [2] show that the bloom occurrences of *Karenia selliformis* in the Gulf of Gabès (Tunisia) can be predicted based on salinity. The study of Lin et al. [9] on the blooms of *Karlodnium veneficum* in Chesapeake Bay shows that prey abundance was a primary factor in predicting *K. veneficum* abundance. Kahru et al. [7] considered that it is not possible to predict inter-annual fluctuations in cyanobacteria blooms in Baltic Sea from water chemistry, but found significant correlation with solar shortwave direct flux in July and the sea-surface temperature, also in July. Nevertheless, Mahmudi et al. [10] concluded the Poisson regression model suggested that all water quality factors measured (temperature, salinity, pH, DO, nitrate and phosphate) affected the abundance of *Trichodesmium sp.* (Cyanobacteria) in Ambon Bay and that, moreover, rising levels of nitrate and salinity will cause a surge in *Trichodesmium*. Ok et al. [11] even developed several simple equations that predict the maximum of chlorophyll a and the peak

[1]Ukrainian Scientific Centre of Ecology of the Sea, Odessa, Ukraine,
[2]Institute of oceanology, BAS, Varna, Bulgaria,
[3]Institute of Marine Biology, NAS, Odessa, Ukraine
Phone: +380999134751; E-mail: mariagrandova@gmail.com

day of bloom based on initial NO_3^- concentration and the ratio of the initial NO3 to Chl-α. They also suggested that the similar correlations will be suitable for other forms of mineral nitrogen, namely, to NH_4^+. So, one may see that the results obtained in different geological regions, in different hydrological conditions and based on different classes of phytoplankton may differ greatly. Thus, the study of the factors that preceded blooms are very important, especially considering that they have not previously been carried out in north-western part of the Black Sea.

MATERIAL AND METHODS

The material for the present study is the set of samples taken for about two decades (2003 - 2019) at two stations in Odessa region. The samples were taken weekly except of storming days when the sampling was dangerous. The stations were located in the coastal waters of Odessa, one of them in the water area that is semi-closed by wave breakers, and another one has free water exchange with the open waters. The samples were taken by Niskin bathometer, and processed by the usual methods of phytoplankton and hydrochemical analysis [4, 5]. The chemical analysis was carried out by the hydrochemical sector of UkrSCES.

As the indicator of bloom intensity, we take the biomass of blooming microalgae. Totally 332 bloom cases were analyzed, some of them were multispecies. The names of taxa are given according to AlgaeBase. We analyze its correlation with the following hydrological and hydrochemical parameters: water temperature, salinity, pH, dissolved oxygen, ammonia, nitrate and nitrite, mineral nitrogen (as the sum of the three previous parameters), organic and total nitrogen, silicates, phosphates, organic and total phosphorus concentrations. The raw results of sample processing are stored in the database of UkrSCES (www.blackseadb.org).

All the calculations, including Pearson correlation and linear trend equations, were made with the help of Microsoft Excel 2010.

RESULTS AND DISCUSSION

The first decades of XXI century were characterized with the continuing process of de-eutrophication of the Black Sea, and in particular in the north-western Black sea shelf. Nevertheless, according to the data of UkrSCES, together with the reduction in the concentration of nitrogen and phosphorus mineral forms, we observe the increase of their organic forms (table 1, the linear trend equation was given only for comparing the rate of decreasing/increasing of hydrochemical parameters).

We also observe a large decrease of silicon concertation. The reducing of dissolved silicate loads in the sea due to hydropower construction affects greatly the marine diatom populations and become a problem which has been concerning the researches for the several decades and has no easy solution [1, 6, 8].

All these changes influence the phytoplankton community, including the frequency and character of microalgae blooms.

The changes of average annual hydrochemical parameters in north-western Black Sea shelf (Odessa region, 2003-2019)*

Table 1

Parameter	trend direction	linear trend equation
Mineral nitrogen	decreasing	y = -1,6408x + 80,685
Organic nitrogen	increasing	y = 0,9861x + 509,75
Total nitrogen	decreasing	y = -1,6191x + 596,89
Silicon	decreasing	y = -12,081x + 622,22
Mineral phosphorus	decreasing	y = -0,3994x + 17,555
Organic phosphorus	increasing	y = 0,5141x + 13,654
Total phosphorus	decreasing	y = -0,4201x + 38,016
Salinity	increasing	y = 0,0729x + 14,171
PH	decreasing	y = 0,0105x + 8,3018
Dissolved oxygen	decreasing	y = -0,0986x + 11,227

*the data were received from UkrSCES database (www.blackseadb.org)

For the last two decades, we observed a great progress in reducing of the number of bloom incidents and their intensity. The dynamics of bloom cases with the appropriate trend line is shown on fig. 1.

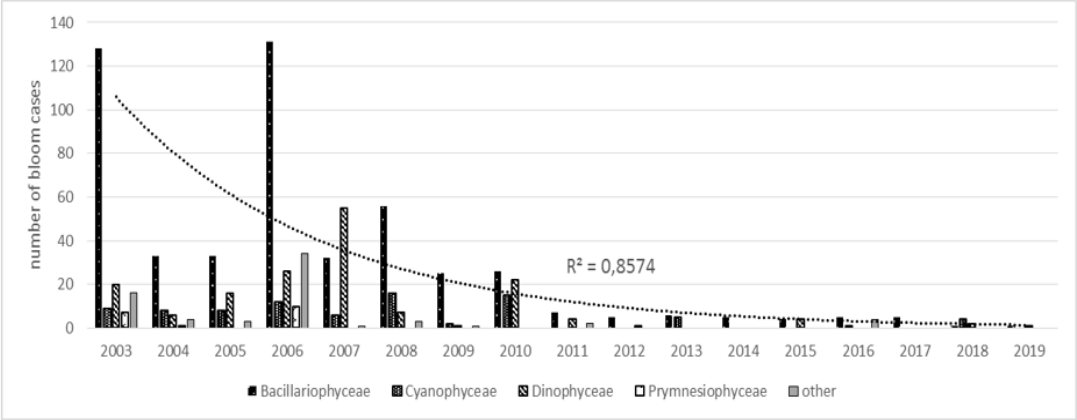

Fig. 1.
The number of microalgae blooms caused by representatives of the main phytoplankton classes in Odessa region (North-Western Black Sea shelf), 2003 -2019

At the beginning of the century, there were more than several tens of blooms per year, and most of them are caused by several species. If we count the bloom of each species as a separate bloom case, in the period 2003 - 2010 the number of bloom cases varied from 29 to 213 per year and the average was 97 ± 23. At the of the second decade the number of bloom cases varied from 2 to 13 per year, and the average was 7 ± 1.

The contribution of different classes to the blooms of microalgae has also changed (fig. 2). At the beginning of XXI century, the main part of blooms are caused by Bacillariophyceae, mainly by *Skeletonema costatum* (Greville) Cleve, 1873. At the last years, the share of diatom blooms became less (from 62% till 50%), but the share of Dinophyceae and especially of Cyanophyceae increased (from 18% till 25% and from 9 to 19%, respectively) (fig.2). The turning point may be considered the year of 2010, when the first huge bloom of *Nodularia spumigena* Mertens ex Bornet & Flahault, 1888 occurred that covered the main part of North-Western Black sea shelf [3].

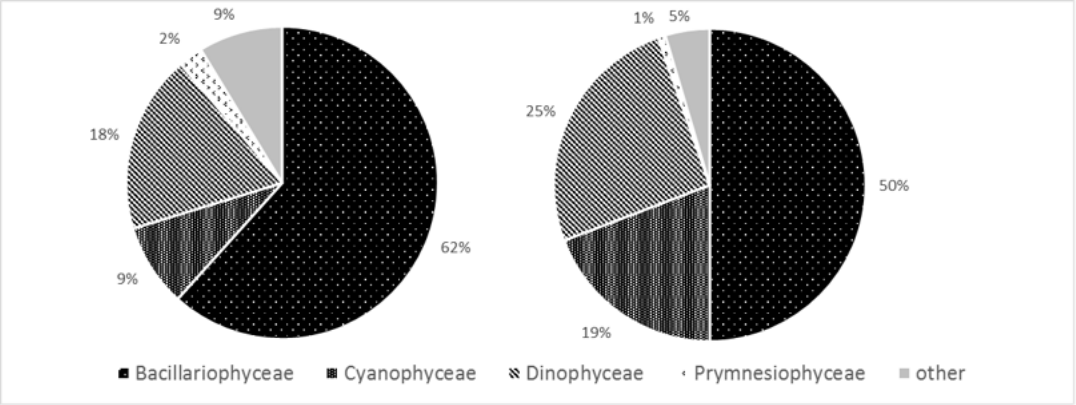

Fig. 2.
The contribution of representatives of different phytoplankton classes on the total number of blooms (left - 2003 - 2009, right - 2010 - 2019)

The characteristics of correlations between bloom intensity and hydrological and hydrochemical parameters for these two periods also differ. Correlation analysis of the whole set of samples showed no significant correlation with the analyzed hydrochemical and hydrophysical parameters two weeks before the bloom ($date_{14}$), a week before the bloom ($date_{-7}$), and the residual between the values of these parameters (($date_{-7}$ - $date_{-14}$) and ($date_{-0}$ - $date_{-7}$)). The main explanation of this fact is that the changes of phytoplankton

community provided the difference of factors preceding blooms. When we take into analysis the shorter periods, we observe more significant correlations with the certain environmental factors.

During the first decade of the 21th century, in 2003-2006 there was observed the significant correlation between the concentrations of silicon (positive correlation), dissolved oxygen (positive), pH (positive), and temperature (negative correlation) in the day of bloom ($date_0$), as it is shown in fig. 3. Then during the following four years, there was a period of transformation in marine phytoplankton community, and no significant correlation found. For the whole first decade, the significant correlation was found with dissolved oxygen (positive correlation), pH (positive correlation), temperature (negative correlation) and total nitrogen (positive correlation), the correlations with temperature (negative) and silicon (positive) were close to the significance limit. In the period of 2010-2019, we observe significant correlations with positive correlations with organic nitrogen, total nitrogen and silicon. These changes of correlation coefficients for different periods may be explained by the changes of blooming species mentioned before.

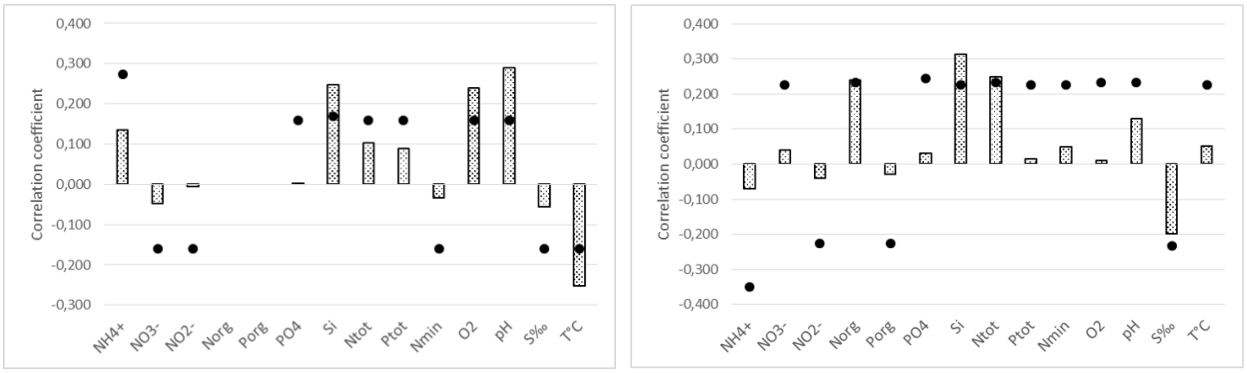

Fig. 3.
Coefficients of correlation of blooming species biomass and environmental factors in coastal waters of Odessa region (A - 2003 - 2006, B - 2010 - 2019).

*Dots indicate the limits of significance that depend of the quantity of samples where the parameter was measured.

Correlation analysis shows, that the blooms of different classes of microalgae are preceded by different parameters of environmental conditions. The strongest correlation was found between the concentration of organic nitrogen and the intensity of Dinophyceae blooms (fig. 4). This correlation is observed both in the $date_0$ and $date_{-7}$. This correlation is well explained by the fact that the most of the blooming dinoflagellates are heterotrophic.

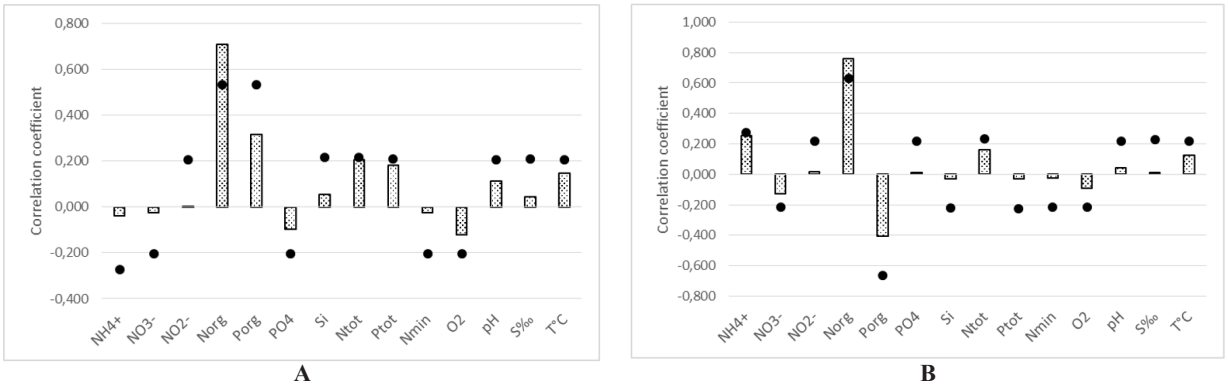

Fig. 4.
Coefficients of correlation of blooming dinoflagellate biomass and environmental factors in coastal waters of Odessa region in 2003-2019 (A - $date_0$, B - $date_{-7}$)

*Dots indicate the limits of significance that depend of the quantity of samples where the parameter was measured.

For Bacillariophyceae, there is a significant positive correlation between dissolved oxygen and negative correlation with temperature and concentration of organic phosphorus (fig. 5). These correlations were observed in $date_0$, $date_{-7}$ and $date_{-14}$. It is hard to say if the high concentration of dissolved oxygen really provide favorable conditions for diatoms or this correlation is the result of the fact that most diatom blooms take place in cold periods when the dissolved oxygen concentration is higher.

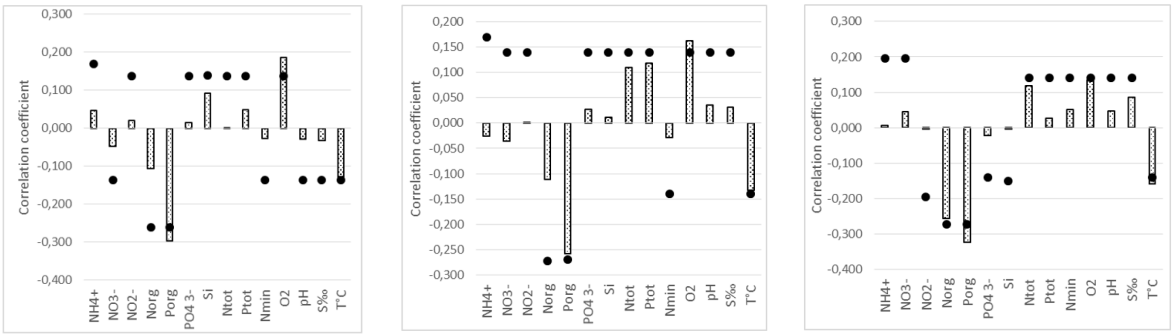

A B C

Fig. 5.

Coefficients of correlation of blooming diatom biomass and environmental factors in coastal waters of Odessa region in 2003-2019 (A - $date_0$, B - $date_{-7}$, C - $date_{-14}$)

*Dots indicate the limits of significance that depend of the quantity of samples where the parameter was measured.

For cyanobacteria blooms, there was observed a strong negative correlation with the residual of mineral phosphorus and total concentration in the date of bloom and a week before, and respectively, the positive correlation with pH residual (fig. 6).

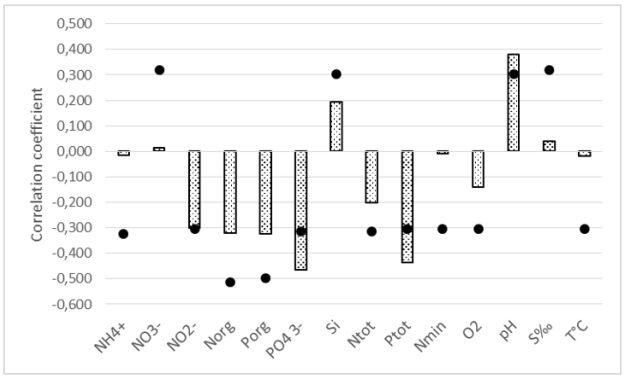

Fig. 6.

Correlation coefficients of blooming cyanobacteria biomass and environmental factors in coastal waters of Odessa region in 2003-2019 (residual ($date_0$ - $date_{-7}$))

*Dots indicate the limits of significance that depend of the quantity of samples where the parameter was measured.

Thus, we may say that the mineral phosphorus is consumed during the cyanobacteria bloom, although there were no significant correlation with initial concentrations of this nutrient. That may indicate that phosphorus concentration in the coastal waters of NWBS continues to be sufficient to meet the needs of cyanobacterial phytoplankton even during bloom.

For Prymnesiophyceae, there were no significant correlations found, maybe due to the small number of bloom cases.

CONCLUSION

The changes in hydrochemical parameters of marine environment led to the changes in marine biocenoses, including phytoplankton community. In the coastal waters of north-western part of Black Sea, we observed a decrease of silicon and mineral forms of nitrogen and phosphorus, but also an increase of their organic forms. This process was accompanied with the changes in microalgal community, including the number of blooms

and the set of blooming species. In the last decade, on the backdrop of decreasing number of bloom cases, the percentage of blooms caused by diatoms decreased, and the percentage of dinoflagellate and cyanobacteria blooms increased.

For the long periods, in north-western part of the Black Sea, it is impossible to choose the certain environmental parameters which precede the microalgal blooms. These parameters are changing throughout the decades and related with the species that develop bloom. For dinoflagellates, we observe a significant correlation between organic nitrogen concentration and bloom intensity (the biomass of blooming species). For diatoms, the correlation was negative for temperature and organic phosphorus and positive for dissolved oxygen. For cyanobacteria, were no significant correlations with the any of initial environmental parameters. It means, the for reducing the number of blooms, especially of red tides caused by potentially toxic dinoflagellates, it is necessary to control not only mineral, but first of all organic forms of nutrients.

ACKNOWLEDGES

We would like to give thanks to the UkrSCES colleagues that are responsible for hydrochemical analysis and for maintenance of database, and to the Institute of Oceanology "Fridtjof Nansen", Bulgarian Academy of Science, for the refuge from the war in Ukraine and possibility to continue the work on phytoplankton.

REFERENCES:

[1] C h e n, N., Wu, Y., Wu, J., Yan, X., and Hong, H. (2014), Natural and human influences on dissolved silica export from watershed to coast in Southeast China, J. Geophys. Res. Biogeosci., 119, 95- 109, doi: 10.1002/2013JG002429.

[2] F e k i - S a h n o u n, W., Hamza, A., Njah, H., Barraj, N., Mahfoudi, M., Rebai, A., et al. (2017). A Bayesian network approach to determine environmental factors controlling *Karenia selliformis* occurrences and blooms in the Gulf of Gabès, Tunisia. Harmful Algae 63, 119-132. doi: 10.1016/j.hal.2017.01.013.

[3] G r a n d o v a, M., Kovalishina, S., Ukrainskiy, V., Kaloshina, N. (2010). On the bloom of *Nodularia spumigena* in the coastal waters of Odessa Bay. International conference "Ecological problems of the Black Sea" - Odesa, 2010. - P. 317-320.

[4] G u i d e l i n e s for biological analysis of seawater and sediments (A. Tsyban ed.) // Leningrad: Hydrometeoizdat. - 1980. - 360 p.

[5] G u i d e l i n e s to the chemical analysis of seawater. RD 52.10.243-92 // Sankt-Petersburg: Hydrometeoizdat. - 1993. - 264 p.

[6] H u m b o r g, C., Conley, D. J., Rahm, L., Wulff, F., Adriana Cociasu, & Ittekkot, V. (2000). Silicon Retention in River Basins: Far-Reaching Effects on Biogeochemistry and Aquatic Food Webs in Coastal Marine Environments. Ambio, 29(1), 45–50. http://www.jstor.org/stable/4314993.

[7] K a h r u, M., Elmgren, R., Kaiser, J., Wasmund, N., and Savchuk, O. (2020). Cyanobacterial blooms in the Baltic Sea: correlations with environmental factors. Harmful Algae 92:101739. doi: 10.1016/j.hal.2019.101739.

[8] K a s p r z a k, S.M. Reservoir Hydroelectric Dams Silica Depletion Silica Shelled Diatom Phytoplankton A Gulf of Maine Catastrophe; 2018 // https://www.maine.gov/dep/ftp/projects/necec/public-interest/2019-02-14%20from%20Steve%20Kasprzak%20Attachment%204%20%20Reservoir%20Hydroelectric%20Dams%20Silica%20Depletion%20-%20A%20Gulf%20of%20Maine%20Catastrophe.pdf.

[9] L i n, C. H. M., Lyubchich, V., and Glibert, P. M. (2018). Time series models of decadal trends in the harmful algal species *Karlodinium veneficum* in Chesapeake Bay. Harmful Algae 73, 110-118. doi: 10.1016/j.hal.2018.02.002.

[10] M a h m u d i, M., Serihollo, L. G., Herawati, E. Y., Lusiana, E. D., and Buwono, N. R. (2020). A count model approach on the occurrences of harmful algal blooms (HABs) in Ambon Bay. Egypt. J. Aquat. Res. 46, 347-353. doi: 10.1016/j.ejar.2020.08.002.

[11] O k Jin Hee et al (2021). Phytoplankton Bloom Dynamics in Incubated Natural Seawater: Predicting Bloom Magnitude and Timing. Frontiers in Marine Science, Vol. 8. doi: 10.3389/fmars.2021.681252.

[12] O n d e r k a, M. (2007). Correlations between several environmental factors affecting the bloom events of cyanobacteria in Liptovska Mara reservoir (Slovakia) - a simple regression model. Ecol. Modell. 209, 412-416. doi: 10.1016/j.ecolmodel.2007.07.028.

[13] P i n c k n e y, J. L., Millie, D. F., Vinyard, B. T., and Paerl, H. W. (1997). Environmental controls of phytoplankton bloom dynamics in the Neuse River Estuary, North Carolina, USA. Can. J. Fish. Aquat. Sci. 54, 2491-2501.

NATURAL METHOD OF MANAGEMENT (CONSTRUCTION, MAINTENANCE AND INCREASE) OF FREE BEACHES

Gencho GEORGIEV, Lyubomir DIMITROV

Abstract. *The disadvantage of the free beach is the lack of methodology for sufficiently accurate assessment of the consumption of sediments from the coastal zone. However, the factors influencing these processes and their main dependencies are already known, which in a relatively short period of time cause major changes in the outline of the coastline and the relief of the seabed. Based on this, the main essence of the proposed method is to solve the opposite problem: artificial creation of conditions for dynamic resilience through intervention formation of the main factors influencing the equilibrium profile of the underwater coastal slope and sediment balance management in the desired direction.*
Key words: *Artificial beach; free beach; sea beach.*

OBJECTIVES AND HYPOTHESES

The increasing shortage of sand in coastal areas, the progressive coastal erosion and landslide processes in certain areas, as well as the unforeseen accumulation of beach material as a result of man-made intervention in natural processes along the Black Sea coast, provoke the search for new sources of this material and the creation of environmentally friendly, scientifically based methods for its redistribution and maintenance over a period of many year.

The purpose of the proposed in this work method is to create a theoretical basis, as well as sizing methodology and algorithm for creating, maintaining and growing artificial "free" beaches by means of:

► Investigation of suitable deposits of sand with the required grain size composition of:

▪ natural underwater shoals located at a shallow depth and close to the shore;

▪ paleo beds of coastal river valleys;

▪ buried sands along old coastlines formed during low sea level stand of the Black Sea;

► Overcoming the lack of a methodology for a sufficiently accurate assessment of the flow of sediments from the coastal zone, by creating a theoretical basis, a sizing methodology and an algorithm for solving the inverse problem: artificially creating conditions for dynamic stability by forming the equilibrium profile of the underwater coastal zone slope and manage the sediment balance in the direction we want.

The proposed project for the development of an environmentally friendly method and algorithm for the management (creation, maintenance and growth) of free beaches is a novelty in the world hydrotechnical science and practice. It is in line with the European priorities for the protection of the natural resources of the Black Sea and represents a scientific solution offering a significant ecological effect, low cost and short implementation periods.

ACTUALITY AND SIGNIFICANCE OF THE SCIENTIFIC ISSUES

Seashore fortification is an ancient human problem. Mastering the coast of sea basins, people were forced to protect the built material culture of society from the destructive action of sea waves. In solving this problem, the desire to immediately limit and stop the wave impact naturally arises. Brick, stone, concrete or reinforced concrete embankments were built and are still being built today. However, this approach does not always lead to positive results and in all cases requires a large expenditure of labor and funds and entails the following disadvantages:

▪ the use of artificial facilities turns out to be effective and economically profitable only for small sections of the coast;

Eng. Georgiev Gencho Dinev PhD, Professor Eng. Dimitrov Lyubomir Ivanov PhD
Institute of Oceanology - Bulgarian Academy of Sciences, Bulgaria
E-mail: g.georgiev@io-bas.bg; geos@io-bas.bg

▪ the built facilities have relatively limited areas of action in their immediate vicinity;

▪ depending on the direction of the wave and the coastal currents, destruction of the neighboring sections of the coast is often observed as a result of a change in the hydrodynamic situation in the area of the constructed facilities;

▪ the accumulation of sediments is always at the expense of the neighboring areas: the influence of the built facilities on the natural balance of natural processes is almost always unfavorable;

▪ when the complex of coastal fortifications turns out to be ineffective, its reconstruction and repair are too expensive and unjustified (modern achievements of science and practice do not allow to accurately and accurately determine the lithodynamic picture in the area of the constructed fortifications, which leads to ambiguity in expectations effect).

A sea beach is an accumulation landform, representing a distinct part of the coastal zone, extending from the uppermost limit of the maximum wave inundation to the area of origin of the surf current, covered with sand, gravel and other sedimentary or rock formations as a result of natural or artificially induced as a result of human activity processes of interaction of the sea with the land. The territory of the sea beach also includes the sand dunes, sand hairs and sea terraces located immediately behind the beach strip or falling on the sea beach.

An artificial beach is a sand wash or loose shore strengthening facility, built with sediment retaining auxiliary hydrotechnical facilities such as bunds, dams, dashes, etc.

A free beach is an artificial beach, built without sediment retaining auxiliary hydrotechnical facilities such as bunkers, dams, dashes, etc.

Artificial and free beaches, as coastal protection facilities, have been widely used and have proven their advantages and nature-compatibility in the world practice of marine hydrotechnical construction. Artificial beaches are created in areas with a shortage of alluvial materials, where it is impossible to form a natural beach profile. The seaming of the sea shores by means of a free beach is achieved by removing the direct impact of sea waves on the shore - the energy of the disturbance is absorbed by the beach. Pouring sand allows you to immediately get a wide beach. This improves the situation not only in the fortified section, but also in the adjacent sections where sand is transported by natural or with the help of the proposed management method (creation, maintenance and growth) of free beaches sediment migration. If the free beach does not bring a positive result, it does not worsen the state of the coast. The need for a construction site and concrete works on the seashore is completely excluded. The use of free beaches allows to reduce several times the initial investment of funds and to distribute the total capital investments for shore fortification over a longer period. It is only after a few decades that the amount of total funds invested in the creation and regeneration of the free beaches equals that required for the construction and maintenance of the traditional shore fortification facilities.

Fig. 1.
An Example of a free beach

A disadvantage of the free beach is the lack of methodology for a sufficiently accurate assessment of the flow of sediment from the coastal zone. However, even now the factors affecting these processes and their main dependencies are known, which in a relatively short period of time cause major changes in the outline of the coastline and the relief of the seabed. Proceeding from this, the main essence of the proposed project is the solution of the opposite task: artificially creating conditions for dynamic stability by means of interventional formation of the main factors influencing the equilibrium profile of the underwater coastal slope and managing the sediment balance in the desired direction.

For the solution of this task and for the purposes of marine hydraulic engineering, the propagation of the disturbance over the shallow water sections of the bottom and the quantitative evaluation of the transformation of the wave elements are of particular interest. It has been proven beyond doubt that the transversal and longitudinal movement of sediments in the coastal zone mainly depends on the wave energy, the direction of wave propagation, the configuration of the shoreline, the type of sediment material and the degree of bottom roughness. Decisive factors for the transverse drift are the wave energy, which is quadratic in relation to the wave height and the depth of collapse, which in turn is a function primarily and also of the wave height. The maximum of the intensity of the longitudinal coastal displacement of the sediments is reached when the wave approaches the coast at some critical angle $350 < \alpha < 500$. The coastal and bottom longitudinal displacement of the sediments also depend on the power of the wave E/2T - directly proportional to the energy (wave height).

For the solution of this task and for the purposes of marine hydraulic engineering, the propagation of the disturbance over the shallow water sections of the bottom and the quantitative evaluation of the transformation of the wave elements are of particular interest. It has been proven beyond doubt that the transversal and longitudinal movement of sediments in the coastal zone mainly depends on the wave energy, the direction of wave propagation, the configuration of the shoreline, the type of sediment material and the degree of bottom roughness. Decisive factors for the transverse drift are the wave energy, which is quadratic in relation to the wave height and the depth of collapse, which in turn is a function primarily and also of the wave height. The maximum of the intensity of the longitudinal coastal displacement of the sediments is reached when the wave approaches the coast at some critical angle $350 < \alpha < 500$. The coastal and bottom longitudinal displacement of the sediments also depend on the power of the wave E/2T - directly proportional to the energy (wave height).

If we consider breakwater berms, underwater breakwaters, sandwashes and shallow water areas of the bottom specially created in front of facilities, these are examples of the practical use of artificially induced transformation and breaking of waves for the purpose of protecting the facility or the shore.

We can have a significant effect on the mastery of wave energy and its purposeful use by building in front of the engineering facilities or the coast of artificial bottom sand relief forms and facilities managing the transformation of the wave and the movement of sediments in the coastal zone.

With the construction of sand relief forms and facilities on the seabed, successive zones of divergence and convergence of wave propagation will be created, which will lead to the quenching of wave energy and its targeted use for the growth and multi-year maintenance of existing or created with suitable grain size composition , roughness and slope free beaches.

STATUS OF RESEARCH ON THE PROBLEM

The creation of a nature-based, science-based method and algorithm for the management (creation, maintenance and growth) of free beaches is a novelty for research on the problem and has no analogue in the field of earth sciences.

A major disadvantage of the free beach is the difficulty of finding suitable quarries of sand with a grain size composition greater than or equal to the natural average diameter of the beach. The correct selection of the profile and grain size composition is based on the accurate knowledge of the situation in the fortified section over a relatively long period of time. Knowledge of the Bulgarian coast of the Black Sea does not meet modern needs. In addition, world science has not given a satisfactory answer to the problems posed in this field by practice. This necessitates the strengthening of research of a regional nature in our country. The intensive study of the seasonal and mode characteristics of the waves and the beaches along our coast is necessary. The issue of uncovering feeder provinces and quarries is important.

In our country there is an as yet unproven view that such careers are absent. There is a lack of sufficient research in this area, but the initial observations and results of some studies at IO-BAS give encouraging results. Broadly speaking, there are three main options for developing such careers:

- from natural underwater shafts located at a shallow depth in front of the coast. In front of the accumulative sections, they are usually found at depths of 6 to 10 meters, and in front of the abrasive sections at 10 - 15 meters. A large supply of suitable beach material lies between the so-called zero bottom line, which separates the transfer of sediment material normal to the coast and to the deep sea, and the bottom line marking the end of sediment movement. The subject of the proposed project is the creation of a physical model and method for the purposeful intervention formation of this area with the aim of influencing the main factors determining the transverse and longitudinal movement of sediments in favor of maintaining and growing the coastline;

Fig. 2.
An Example of a hard protection of free beach from Playa de Las Teresitas beach

- from the paleobeds of the coastal river valleys of the Batova, Provadiyska, Kamchia, Dvoinitsa, Hadjiyska, Sredetska rivers;

- from buried sands along old coastal pine trees on the Bulgarian coast of the Black Sea. Given that today in the world there are technologies for extracting sands from depths of more than 70 meters, these reserves should not be considered „buried“ at all.

What has been stated so far determines the need to deepen the knowledge of the regional hydrological and lithological processes along the shores of the Black Sea.

The scientific research included in the project is oriented towards issues of international importance and for this reason is characterized by high international visibility. These studies have their place as far as they pursue important social challenges such as the growth of the country‘s territory and the provision of extensive beaches for the development of tourism, which will increase the significance of the achieved scientific results.

The development will reflect the adoption of amendments and additions to the Law on the Organization of the Black Sea Coast, regulating the conduct of scientific research at the request of state or local bodies and determining the management decisions that necessarily require the prior conduct of a targeted scientific study or an opinion from a competent scientific organization , unit or scientist.

The implementation of the proposed project will create specific mechanisms for the rapid commissioning and conduct of scientific research in response to urgent specific needs and problems of national or regional importance.

Fig. 3.
An Example of creation of a beach by so called "transverse bypass"

REFERENCES:

[1] G e o r g I e v, G., Protection of the Bulgarian Black Sea Coast without Coastal Structures. Bulletin of National Oceanographic Committee, October 1984.
[2] G e o r g I e v, G., Numeral Model of Diffraction in Marine Limited Shallow Water. First National Session" The Use of IT (PC) in Hydro-techniques". September 1986, Primorsko, Bulgaria.
[3] G e o r g I e v, G., Numeral Decision and Optimizing of Modulated Marine Coast Protection Structures with Computer. First National Session "The Use of IT (PC) in Hydro-techniques" **September 1986,** Primorsko, Bulgaria.
[4] G e o r g I e v, G., New Structures of Coastal Protection Facilities. Fourth IMAEM (International Maritime Association of East Mediterranean) International Congress. May 1987, Varna.
[5] G e o r g I e v, G., Conformable to Nature Method for Building up, Preserving and Growth of Free Beaches. Fourth National Scientific Applied Conference on Scientific Assurance of the Preventive Activity and Protection of the Population at Calamities and Damages. November 1997, Sofia, Bulgaria.
[6] G e o r g I e v, G., Dimitar Dimitrov, Draft Amendment Project Law on the Development of the Black Sea Coast Third Scientific Conference with International Participation "Geography, Regional Development and Tourism" 2020 27-29 November 2020 Shumen.

NATURAL METHOD FOR MANAGEMENT OF WAVE TRANSFORMATION AND CONSTRUCTION OF FREE BEACHES

Gencho GEORGIEV

Abstract. *The disadvantage of the free beach is the lack of methodology for sufficiently accurate assessment of the consumption of sediments from the coastal zone. However, the factors influencing these processes and their main dependencies are already known, which in a relatively short period of time cause major changes in the outline of the coastline and the relief of the seabed. Based on this, the main essence of the proposed method is to solve the opposite problem: artificial creation of conditions for dynamic resilience through intervention formation of the main factors influencing the equilibrium profile of the underwater coastal slope and sediment balance management in the desired direction.*
Key words: *Artificial beach, free beach, sea beach.*

INTRODUCTION

An artificial beach is a sand wash or loose shore strengthening facility, built with sediment retaining auxiliary hydrotechnical facilities such as bunds, dams, dashes, etc.

A free beach is an artificial beach, built without sediment retaining auxiliary hydrotechnical facilities such as bunkers, dams, dashes, etc.

Artificial and free beaches, as coastal protection facilities, have been widely used and have proven their advantages and nature-compatibility in the world practice of marine hydrotechnical construction. Artificial beaches are created in areas with a shortage of alluvial materials, where it is impossible to form a natural beach profile. The seaming of the sea shores by means of a free beach is achieved by removing the direct impact of sea waves on the shore - the energy of the disturbance is absorbed by the beach. Pouring sand allows you to immediately get a wide beach. This improves the situation not only in the fortified section, but also in the adjacent sections, where sand is transported by natural or with the help of the proposed method of creating free beaches sediment migration. If the free beach does not bring a positive result, it does not worsen the state of the coast. The need for a construction site and concrete works on the seashore is completely excluded. The use of free beaches allows to reduce several times the initial investment of funds and to distribute the total capital investments for shore fortification over a longer period of time. It is only after a few decades that the amount of total funds invested in the creation and regeneration of the free beaches equals that required for the construction and maintenance of the traditional shore fortification facilities.

A disadvantage of the free beach is the lack of methodology for a sufficiently accurate assessment of the flow of sediment from the coastal zone. However, even now the factors affecting these processes and their main dependencies are known, which in a relatively short period of time cause major changes in the outline of the coastline and the relief of the seabed. Proceeding from this, the main essence of the proposed project is the solution of the opposite task: artificially creating conditions for dynamic stability by means of interventional formation of the main factors influencing the equilibrium profile of the underwater coastal slope and managing the sediment balance in the desired direction.

STATUS OF RESEARCH ON THE ISSUE

The creation of a nature-based, science-reasoned method and algorithm for creating free beaches is a novelty for research on the problem and has no analogue in the field of earth sciences.

A major disadvantage of the free beach is the difficulty of finding suitable quarries of sand with a grain size composition greater than or equal to the natural average diameter of the beach. The correct selection of the profile and grain size composition is based on the accurate knowledge of the situation in the fortified section

Eng. Gencho Dinev Georgiev PhD, Institute of Oceanology - Bulgarian Academy of Sciences, Bulgaria
E-mail: g.georgiev@io-bas.bg; geos@io-bas.bg

over a relatively long period of time. Knowledge of the Bulgarian coast of the Black Sea does not meet modern needs. In addition, world science has not given a satisfactory answer to the problems posed in this field by practice. This necessitates the strengthening of research of a regional nature in our country. The intensive study of the seasonal and mode characteristics of the waves and the beaches along our coast is necessary. The issue of uncovering feeder provinces and quarries is important.

In our country there is an as yet unproven view that such careers are absent. There is a lack of sufficient research in this area, but the initial observations and results of some studies at IO-BAS give encouraging results.

SUBJECT OF THE PROPOSED PROJECT

The proposed method is aimed at processing and accumulating the natural underwater shafts located at a shallow depth in front of the coast. They are usually found in front of the accumulative sections at depths of 6 to 10 meters, and in front of the abrasive sections at 10 - 15 meters. A large supply of suitable beach material lies between the so-called zero bottom line, which separates the transfer of sediment material normal to the coast and to the deep sea, and the bottom line marking the end of sediment movement. The subject of the proposed project is the creation of a physical model and a method for the purposeful interventional formation of this area with the aim of influencing the main factors determining the transverse and longitudinal movement of sediments in favor of the maintenance and growth of the coastline.

SOLVE THE PROBLEM

For the solution of this task and for the purposes of marine hydraulic engineering, the propagation of the disturbance over the shallow water sections of the bottom and the quantitative evaluation of the transformation of the wave elements are of particular interest. It has been proven beyond doubt that the transversal and longitudinal movement of sediments in the coastal zone mainly depends on the wave energy, the direction of wave propagation, the configuration of the shoreline, the type of sediment material and the degree of bottom roughness. Decisive factors for the transverse drift are the wave energy, which is quadratic in relation to the wave height and the depth of collapse, which in turn is a function primarily and also of the wave height. The obtained curves of the distribution of sand consumption along the beach profile prove that the consumption as well as the speed of the longitudinal coastal currents do not depend on the slope of the underwater coastal slope of the sandy bottom in the shallow water area [1]. The maximum of the intensity of the longitudinal coastal displacement of the sediments is reached when the wave approaches the coast at some critical angle $35^0 < \alpha < 50^0$. The coastal and bottom longitudinal displacement of the sediments also depend on the power of the wave E/2T - directly proportional to the energy (wave height).

We can have a significant effect on the mastery of wave energy and its purposeful use by building in front of the engineering facilities or the coast of artificial bottom sand relief forms and facilities that manage the transformation of the wave and the movement of sediments in the coastal zone.

With the construction of sand relief forms and facilities on the seabed, successive zones of divergence and convergence of wave propagation will be created, which will lead to the quenching of wave energy and its targeted use for the growth and multi-year maintenance of existing or created with suitable grain size composition , roughness and slope free beaches.

The theoretical justification of these processes is based on two hypotheses: 1) the possibility of applying the optical law of Snellius when the waves pass through the boundary between areas with different but constant depths in each area; 2) for the constancy of the wave energy flux within the limits of each ray tube.

Consider a section in front of the coast with a relatively constant depth H_o. We assume that a monochromatic wave with period τ, initial length λ_o and an initial front parallel to the coastline propagates along the section.

From the hypothesis of constancy of the flow of wave energy along the extension of each ray tube, it follows that the height of the wave during propagation in the central part of the section with depth H_o will remain unchanged along the entire length of the section.

How should the depth of the section be modified so that, with a minimum amount of bottom excavation, the maximum reduction in wave height per unit of wave travel is obtained? The simplest solution to the posed question is the increase of the depth along the bottom of the section to H_2 ($H_2 > H_o$) within the limits of a rhombus with side length a and peaks located at both ends of the section along the wave propagation. In Fig. 1 the bottom deepening area is shaded. The length of the rhombus in the direction of wave propagation is equal

to L = 2.a.sinα (where α is the angle between the limit of depth variation and the perpendicular to the axis of the rhombus, and the total area of the bottom depression is:

(1) $$S = \mathbf{a}.(2.\cos \boldsymbol{\alpha} \,.\, \sin \boldsymbol{\alpha})$$

With such deepening of the bottom, initially parallel to the axis of the rhombus, the wave rays will deviate from this direction twice, in different directions. This will happen once when crossing the boundary from depth H_0 to H_2 and a second time when crossing the boundary from H_2 to H_0. Ultimately, the output distance between the wave rays $\mathbf{l_o}$ in the region of the second refraction of the wave rays will acquire a value $\mathbf{l_1 > l_o}$, and at a distance **R** from the top of the rhombus the distance between the refracted wave rays will be $\mathbf{l_2 > l_1}$. Using the law of conservation of the flow of wave energy between wave beams, it will be obtained that the coefficient of reduction of the wave height at a distance **R** from the beginning of the bottom deepening region will be:

(2) $$\mathbf{Kr_2} = \sqrt{\frac{lo}{l2}}$$

Based on Fig. 1 we solve a not very complicated trigonometric problem as a result of which we get the following results:

(3) $$\mathbf{l_1 = 2.(2a - l_0.\ tg\alpha} \; - \frac{2a.ctg\alpha - lo}{tg\Delta 1\alpha + ctg\alpha}) . \frac{[\sqrt{a^2.(1-sin\alpha}\,) - lo/2]}{\sqrt{\left(a - \frac{lo}{2cos\,\alpha}\right)^2 - [\sqrt{a^2.(1-sin\alpha}\,) - lo/2]^2}};$$

(4) $$\mathbf{Kr_1} = \sqrt{\frac{lo}{l1}};$$

and as a final result:

(5) $$\mathbf{l_2 = 2.(2a - l_0.\ tg\alpha} - \frac{2a.ctg\alpha - lo}{tg\Delta 1\alpha + ctg\alpha}) . \frac{[\sqrt{a^2.(1-sin\alpha}\,) - lo/2]}{\sqrt{\left(a - \frac{lo}{2cos\,\alpha}\right)^2 - [\sqrt{a^2.(1-sin\alpha}\,) - lo/2]^2}} + 2.\{R - \sqrt{a^2 + sin\alpha} \; -$$

$$- \sqrt{\left(a - \frac{lo}{2cos\,\alpha}\right)^2 - [\sqrt{a^2.(1 - sin\,\alpha}\,) - lo/2]^2} + (2a - l_0.\ tg\alpha - \frac{2a.ctg\alpha - lo}{tg\Delta 1\alpha + ctg\alpha})\}.tg\,(\Delta\alpha_1 + \Delta\alpha_2);$$

(6) $$\mathbf{Kr_2} = \sqrt{\frac{lo}{l2}};$$

A very important condition in solving the problem is the dumping of excavated sand masses directly on the shore in front of the section and obtaining a ready-made free beach with a grain-metric composition similar to the underwater coastal slope of the section.

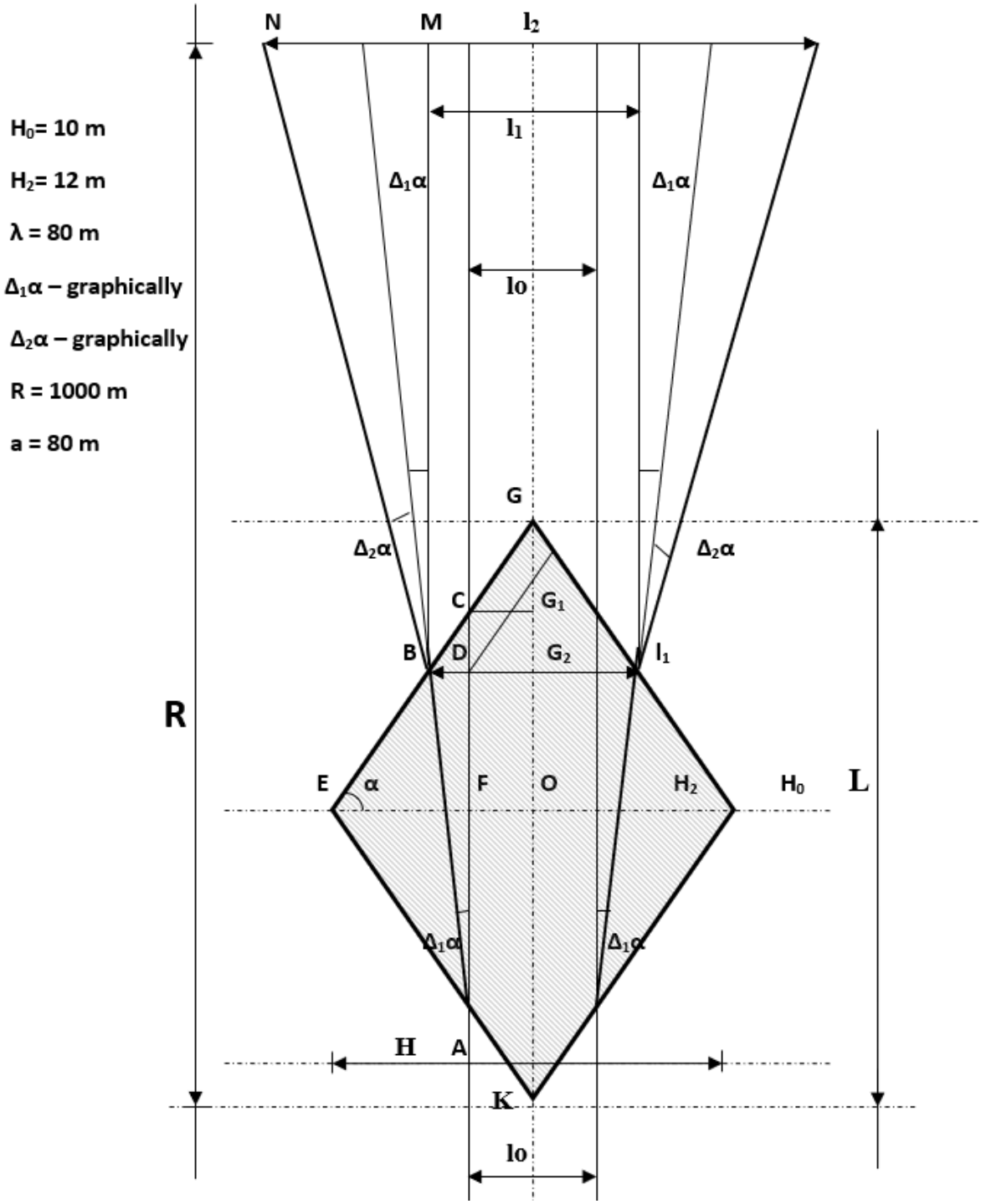

Fig. 1.

It is also convenient to use the formula for constructing the wave beams [2]:

(6) $$\Delta_{i+1}\alpha = \arcsin\{[\,(1+0{,}032\,\lambda_0/d_{i+1})\,/\,(1+0{,}032\,\lambda_0/d_i)].\,\sin\Delta_i\alpha\}$$

where $\Delta_{i+1}\alpha$ - angle of refraction; $\Delta_i\alpha$ - angle of incidence;
$d_{i,\,i+1}$ - water depth.

(7) $$EG = a;\ OG/a = \sin\alpha\ ;$$

The proposed method for managing the transformation of disturbance and the movement of sediments in the coastal zone in the part of its theoretical justification is based on the hypotheses formulated at the beginning of the report. The applicability of Snellius optical law and the constancy of the energy flow within the limits of the beam tube is theoretically justified in this case, when the horizontal dimensions of the deepened trench compared to the length of the incident wave are large and the depths vary smoothly. In our case, the horizontal dimensions of the deepening trench are commensurate with the length of the impact wave, and the depths of the boundaries of the deepening change sharply. In this regard, the proposed method of damping the wave energy will be more effective as the ratio **λ / H** is smaller.

Sizing the effect of wave energy attenuation will be complicated when the natural depth is not constant but varies within the development section. As a first approximation, we can safely assume that the results of the proposed sizing will be significant in this case as well, when the depths of the excavated bottom of the section follow the natural slope of the bottom.

CONCLUSION

What has been stated so far determines the need to deepen the knowledge of the regional hydrological and lithological processes along the shores of the Black Sea.

The scientific research included in the project is oriented towards issues of international importance and for this reason is characterized by high international visibility. These studies have their place as far as they pursue important social challenges such as the growth of the country's territory and the provision of extensive beaches for the development of tourism, which will increase the significance of the achieved scientific results.

The development will reflect the adoption of amendments and additions to the Law on the Organization of the Black Sea Coast, regulating the conduct of scientific research at the request of state or local bodies and determining the management decisions that necessarily require the prior conduct of a targeted scientific study or an opinion from a competent scientific organization , unit or scientist.

The implementation of the proposed project will create specific mechanisms for the rapid commissioning and conduct of scientific research in response to urgent specific needs and problems of national or regional importance.

REFERENCES:

[1] K o m a r, P. D. The mechanics of sand transport on beaches. - J. Geophis. Res., v 76, N 3, 1971.

[2] S m I r n o v a, T.G., Pravdivets Yu.P., Smirnov, G.N. Beregozaschitnye sooruzhenia. Publisher Associations of construction universities. Moscow 2002.

[3] G e o r g I e v, G., Protection of The Bulgarian Black Sea Coast without Coastal Structures. Bulletin of National Oceanographic Committee, October 1984.

[4] G e o r g I e v, G., Numeral Model of Diffraction in Marine Limited Shallow Water. First National Session" The Use of IT (PC) in Hydro-techniques". September 1986, Primorsko, Bulgaria.

[5] G e o r g I e v, G., Numeral Decision and Optimizing of Modulated Marine Coast Protection Structures with Computer. First National Session "The Use of IT (PC) in Hydro-techniques" September 1986, Primorsko, Bulgaria.

[6] G e o r g I e v, G., New Structures of Coastal Protection Facilities. Fourth IMAEM (International Maritime Association of East Mediterranean) International Congress. May 1987, Varna.

[7] G e o r g I e v, G., Conformable to Nature Method for Building up, Preserving and Growth of Free Beaches. Fourth National Scientific Applied Conference on Scientific Assurance of the Preventive Activity and Protection of the Population at Calamities and Damages. November 1997, Sofia, Bulgaria.

SHIP HYDRODYNAMICS

DETERMINING THE SPEED-POWER CURVE IN EEXI WITH SCARCE OR MISSING SHIP DATA

Stefan KYULEVCHELIEV

Abstract. *The impending certification of EEXI is becoming a matter of emergency for shipowners. The speed-power curve is an important element in calculating EEXI. Very often lack of ship data is a serious problem, especially for ships in service built in the pre-EEDI period. For such cases the Guidelines of MEPC offer approximate formulae based on average values for samples of existing ships. This is a very rough estimation which may underestimate the real EEXI value. The paper advocates the admissibility of empirical methods for powering performance prediction in calculating EEXI. A case study is performed justifying this proposal.*
Key words: *CFD, EEXI, empirical methods, speed-power curve, Vref.*

INTRODUCTION

Pursuing the targets of reducing carbon intensity set in its Greenhouse Gas Strategy, the International Maritime Organization (IMO) adopted amendments to MARPOL Annex VI to introduce a new energy efficiency standard for in-service vessels: the 'Energy Efficiency Existing Ship Index' (EEXI). It is due to enter into force on 01 November 2022. All vessels in service will need to demonstrate compliance by their next scheduled survey - annual, intermediate or renewal - whichever is the first on or after 01 January 2023.

The speed-power curve is one of the most important inputs for precise calculation of EEXI.

The paper summarizes the requirements of the certification organizations regarding the speed-power curve, the applicable methods of its calculation and the verification of their results recognized by Verifiers.

Very often lack of ship data is a serious problem, especially for ships in service built in the pre-EEDI period. For such cases the Guidelines of MEPC offer approximate formulae based on average values for samples of existing ships. This is a very rough estimation which may underestimate the real EEXI value.

Another possibility could be the use of CFD. This option is discussed in more details in the paper: needed (often missing) ship and propeller data; scaling; reliability and validation of results; computing resources. The geometrical data of hull and propeller necessary for CFD simulation is the type of information most commonly missing for older ships.

The paper moves an option for estimating the speed-power curve of a ship using established and validated empirical prediction methods for all elements of powering performance: resistance, propulsive factors and propeller open-water characteristics. This approach can be applied with only minimum or partial information about the ship.

The proposed approach is demonstrated with a case study of a specific ship with minimum of information about the ship. The results are compared with the predictions based on model testing and prove to justify the method. Analyses like the presented one can be used to validate the method for any ship.

MEPC REGULATIONS REGARDING THE SPEED-POWER CURVE

Important basic parameters in the EEXI formula [1] are the power of the main engine(s) $P_{ME(i)}$, ship speed *Vref* at specified *Capacity*.

By definition [4], ***deadweight*** should be used as *Capacity* for bulk carriers, tankers, gas carriers, LNG carriers, ro-ro cargo ships (vehicle carriers), ro-ro cargo ships, ro-ro passenger ships, general cargo ships, refrigerated cargo carrier and combination carriers. *Deadweight* should be taken for the summer load draught that is the maximum summer draught as certified in the stability booklet.

For containerships, passenger ships and cruise passenger ships the definitions of *Capacity* are different.

Assoc. Prof. Dr. Stefan Kyulevcheliev, Bulgarian Ship Hydrodynamic Centre - Bas, Varna, Bulgaria
Phone: +359 887744132; E-mail: Kyulef@yahoo.com

The power of the main engine(s) $P_{ME(i)}$ is defined as

(a) 75% of the original installed power (*MCR*), or

(b) 83% of the limited installed power (*MCRlim*) in cases where overridable Shaft/Engine Power Limitation is installed in accordance with [3],

whichever is lower.

The ship speed *Vref* is the speed for the defined *Capacity* with the power $P_{ME(i)}$ defined as above.

Five options are envisaged for determining *Vref* depending on the available information.

Option 1. For ships falling into the scope of the EEDI requirement, the ship speed *Vref* should be obtained from an approved speed-power curve as defined in [5].

Option 2. For ships not falling into the scope of the EEDI requirement, the ship speed *Vref* should be obtained from an estimated speed-power curve as defined in [2].

Option 3. For ships not falling into the scope of the EEDI requirement but whose sea trial results, which may have been calibrated by the tank test, under the EEDI draught and the sea condition as specified in [4], the ship speed *Vref* may be obtained from the sea trial report.

Option 4. For containerships, bulk carriers or tankers not falling into the scope of the EEDI requirement but whose sea trial results, which may have been calibrated by the tank test, under the design load draught and sea condition as specified in [4], the ship speed *Vref* may be obtained from the sea trial report.

Option 5. In cases where the speed-power curve **is not available or the sea trial report does not contain the EEDI or design load draught condition**, the ship speed *Vref* can be approximated by *Vref,app* to be obtained from statistical mean of distribution of ship speed and engine power, as defined below:

(1) $$V_{ref,app} = (V_{ref,avg} - m_V) \times \left[\frac{\sum P_{ME}}{0.75 \times MCR_{avg}}\right]^{\frac{1}{3}} \quad [\text{knot}]$$

where,

Vref, avg is a statistical mean of distribution of ship speed in given ship type and ship size, to be calculated as follows:

(2) $$Vref,avg = A \times B^C$$

where

mV is a performance margin of a ship, which should be 5% of *Vref,avg* or 1 knot, whichever is lower; and

MCRavg is a statistical mean of distribution of MCRs for main engines and *MPPavg* is a statistical mean of distribution of MPPs for motors in given ship type and ship size, to be calculated as follows:

(3) $$MCRavg \text{ or } MPPavg = D \times E^F$$

where:

the coefficients A, B and C and D, E and F are given in [1].

Option 6. Notwithstanding the above, in cases where the energy saving device (ESD) is installed, the effect of the device may be reflected in the ship speed *Vref* with the approval of the verifier, based on the following methods in accordance with defined quality and technical standards:

a) sea trials after installation of the device; and/or

b) dedicated model tests; and/or

c) numerical calculations.

All possible situations, which may occur with data of different level of availability, are comprehensively covered in the IACS Record 172 [6].

PROBLEMS WITH DETERMINING EEXI OF SHIPS WITH MISSING DATA

The practice shows that very often, especially for ships in service built in the pre-EEDI period, data for applying some of the *Options 1* to *4* is not available. It may happen, for example, when the ship has changed its owner one or several times since it is launched and the data from its design and sea trial stage lost in time.

What can be done in such cases?

The Guidelines [1] offer *Option 5*, as called above: the approximate formulae (1) to (3) based on average values for samples of existing ships. These formulae are designed to give a conservative estimate of EEXI value - they include a margin of about 5% in the EEXI value, i.e. the EEXI value may improve up to 5% if more accurate method is applied.

Another possibility is to perform new model tests for the EEXI conditions. This is naturally considered expensive and slow by the Shipowners.

Third possibility, gaining popularity lately, involves CFD analysis. This option is also associated with high costs and several months. However, the costs are lower and the period is shorter compared to carrying-out model tank tests anew.

Under the pressure of the deadlines for the introduction of the EEXI Regulations, many ship-owners started inquiries for calculating *Vref* by CFD. In response many consulting companies and hydrodynamic facilities are actively offering this service.

Formally, there is no implicit mention of using CFD in the Guidelines, except for *Option 6*: installed ESD. It seems, however, that the Classification societies are inclined to accept calculations involving CFD. An indication of that is the fact that the Classification societies are offering such a consulting service themselves.

Of course, the Classification societies set very strict and comprehensive requirements on the basis of [7] to the validation of the CFD results. “Blind” computations are required for parent or sister hull, or a similar ship.

The most reliable, and most expensive, options - dedicated model tests or CFD simulation - require a complete and precise 3D model of the hull and of the propeller. The case of partial geometry, e.g. offset tables of hull and propeller, will need a reconstruction of the surfaces, which would lead to additional costs and time with a risk of inaccuracies.

There is a practical contradiction here: “If there is no information about a ship to apply the *Options 1* to *4*, what is the chance that detailed geometrical information, necessary for CFD analysis or model tests, will be available?”

Even in the case of installed ESD, where application of CFD is fully legitimate according to the Guidelines, the situation is ambiguous. If the ESD has been retrofitted, then its designer must have already proven its efficiency either by model testing or CFD. Then it seems that the use of CFD is reasonable to support the decision of installing ESD with using the case without ESD for validation.

CASE STUDY OF THE APPLICATION OF APPROXIMATE EMPIRICAL METHODS WITH MINIMUM INFORMATION ABOUT THE SHIP

The methods for determining the reference speed, *Vref*, specified in the Guidelines and officially recognized by the Verifiers (Classification societies) rely on data of different levels of completeness and reliability/ uncertainty. From complete model tests and sea trials, through calibrating partial data to EEXI conditions, CFD simulations (where accepted) to simple approximate formulae based on statistics.

A question arises then, which the author would like to put for debate: “Couldn’t approximate methods for prediction of powering performance (speed-power curve) be of comparable accuracy with the accepted methods or even better than some of them”. If so, can’t they be accepted by the Verifiers?

In terms of necessary data for EEXI estimation, this is an interim solution.

The proposal is checked in this section. A case study was performed with a ship, for which complete information is available - geometry of hull and propeller, model test results and full-scale performance prediction.

A situation was simulated where only very scarce information is available, namely:

- Main particulars;
- A sketch of the Body Plan of the ship;
- Diameter of the propeller;
- Rudder dimensions;

- MCR and RPM of the main engine.

The investigated ship is a 300K VLCC with the following proportions: LPP/B = 5.365, B/T = 2.927, CB = 0.797. The MCR of the engine is 26460 kW.

The body plan of the ship is shown in Fig. 1.

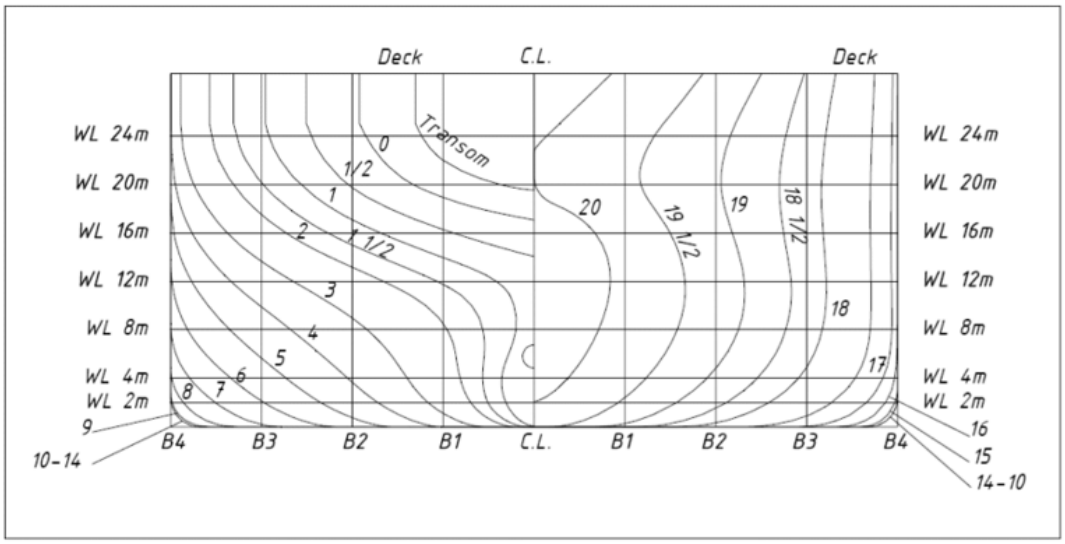

Fig. 1.
Body plan of the case-study ship

The resistance and propulsive factors were predicted by the Holtrop's method [8, 9].

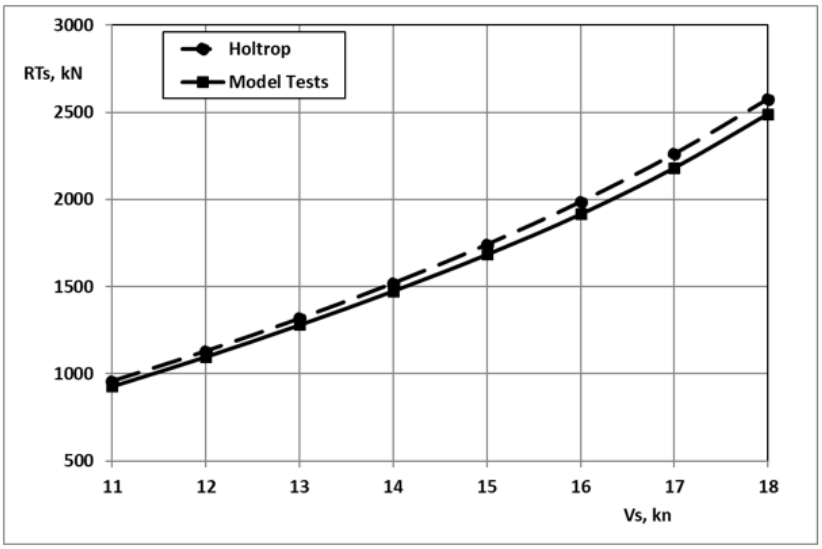

Fig. 2.
Resistance prediction

Not knowing the design point of the actual propeller, a B-series propeller was designed for 85% MCR and fixed diameter D = 10.70 m.

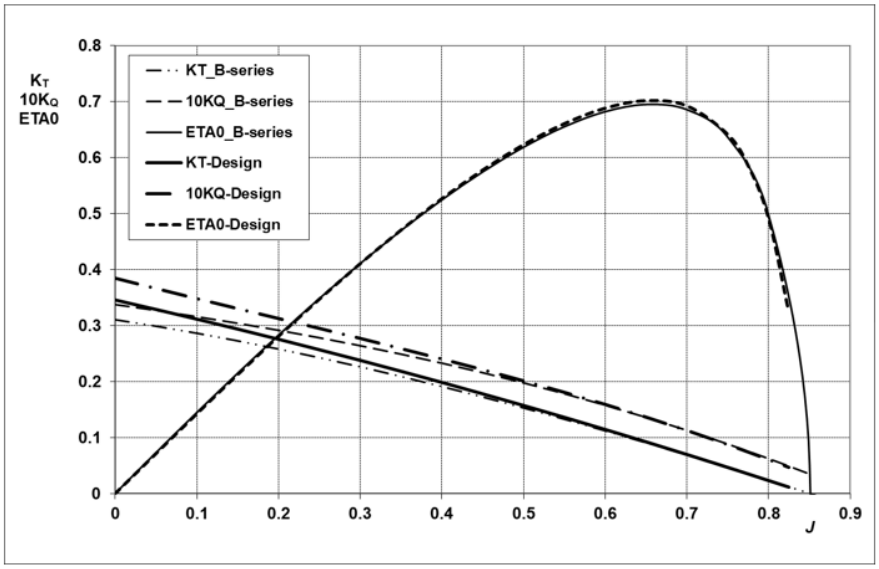

Fig. 3.
Hydrodynamic characteristics of the B-Series propeller

The parameters of the B-series propeller are:

	B-series propeller	Actual design propeller
Diameter D, m	10.70	10.70
Pitch ratio P/D	0.759	0.776
Expanded blade-area ratio A_E/A_0	0.463	0.450
Number of blades Z	4	4

The speed-power curve obtained with the calculated resistance and the selected B-series propeller is illustrated in Fig. 4. The actual speed-power curve of the ship predicted from model tests (index MT) is included in the figure for comparison.

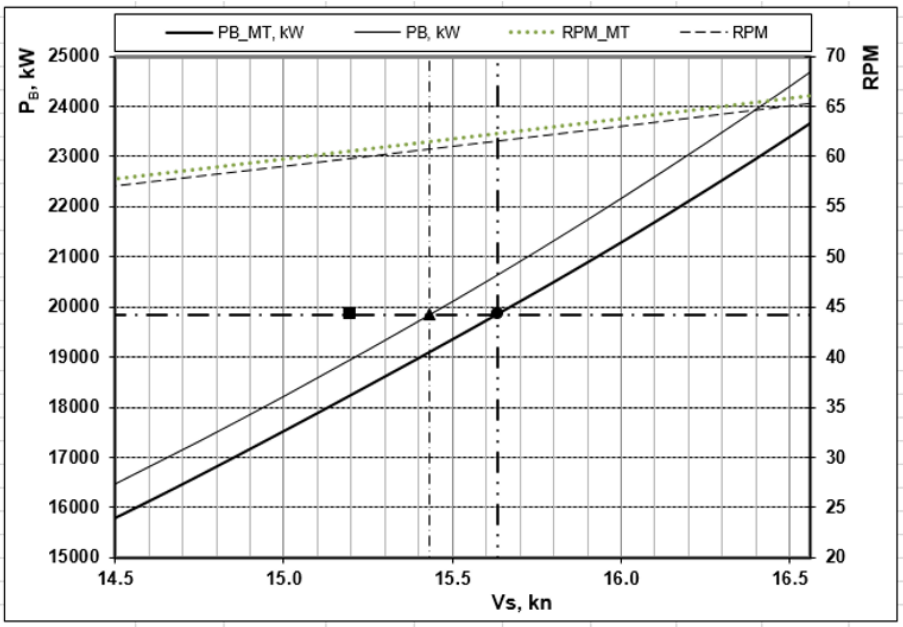

Fig. 4.
Speed-power curve

The reference speed *Vref* necessary for evaluating EEXI corresponds to P_{ME} = 85%MCR.
The square marker in the figure indicates *Vref,app* calculated by the statistical formulae (1) to (3).
The values for *Vref* obtained by the three different methods are:

Predicted from model tests	15.63 kn
Approximate methods	15.43 kn
Formulae (1) - (3)	15.20 kn

CONCLUSIONS

As expected, since the statistical formulae (1) - (3) have been designed to be conservative, the discrepancy of their result from the model tests prediction is the largest.

The estimation with the approximate methods shows twice better accuracy. Actually the accuracy is quite satisfactory and close to the tolerences usually claimed by model basins for model tests accuracy.

Besides the case study shows that a satisfactory estimation can be achieved with lack of detailed data for the ship and the propeller.

To the knowledge of the author, based on recent publications, the alternative approach - CFD simulations - do not offer much better accuracy of prediction, especially concerning propeller open water characteristics and self-propulsion. Moreover, CFD simulations require complete geometry information, which is often missing, and larger computing resources.

One may argue that the results of the test case was just a matter of good luck. This may be true, but, if empirical prediction methods were accepted, the requirement can be imposed that they should be validated on similar ships by a blind test similar to the case study presented here.

REFERENCES:

[1] Resolution MEPC.333(76), GUIDELINES ON THE METHOD OF CALCULATION OF THE ATTAINED ENERGY EFFICIENCY EXISTING SHIP INDEX (EEXI), 2021.
[2] Resolution MEPC.334(76), GUIDELINES ON SURVEY AND CERTIFICATION OF THE ATTAINED ENERGY EFFICIENCY EXISTING SHIP INDEX (EEXI), 2021.
[3] Resolution MEPC.335(76), GUIDELINES ON THE SHAFT/ENGINE POWER LIMITATION SYSTEM TO COMPLY WITH THE EEXI REQUIREMENTS AND USE OF A POWER RESERVE, 2021.
[4] Resolution MEPC.308(73), GUIDELINES ON THE METHOD OF CALCULATION OF THE ATTAINED ENERGY EFFICIENCY DESIGN INDEX (EEDI) FOR NEW SHIPS, 2021.
[5] Resolution MEPC.254(67), GUIDELINES ON SURVEY AND CERTIFICATION OF THE ENERGY EFFICIENCY DESIGN INDEX (EEDI), 2014.
[6] IACS Record 172, EEXI IMPLEMENTATION GUIDELINES, 2022.
[7] ITTC Procedure 7.5-03-01-01, Uncertainty Analysis in CFD Verification and Validation, Methodology and Procedures, 2021.
[8] Holtrop, J., “A Statistical Re-Analysis of Resistance and Propulsion Data”, International Shipbuilding Progress, Vol. 31, No. 363 Nov 1984.
[9] Holtrop, J. and Mennen, G.G.J., “An Approximate Power Prediction Method”, International Shipbuilding Progress, Vol. 29, No. 335, Jul 1982.
[10] Oosterveld, M.W.C. and Oossanen, P. van, “Further Computer-Analyzed Data of The Wageningen B-Screw Series”, International Shipbuilding Progress, Vol. 22, No. 251, July 1975.

DETERMINATION OF THE AERODYNAMIC COEFFICIENTS OF THE STEERING COMPLEX OF THE CAR-PASSENGER FERRY "MARAL" BY THE NUMERICAL METHOD

Volodymyr ZAYTSEV, Valeriy ZAYTSEV,
Dmytro ZAYTSEV, Victoria LUKASHOVA

Abstract. *When developing mathematical models of the plumage of hovercrafts, it is often assumed to separately determine the forces and moments of resistance of the annular nozzles of propellers, propellers and the steering complex (aerodynamic rudder with a flap, taking into account the stabilizer-pylon). However, this approach does not take into account the mutual influence of all elements of the propeller-steering complex of the car-passenger ferry (CPF) "Maral" on the total resistance of the vessel, which may lead to slightly incorrect results.*

In the report, the aerodynamic coefficients of the steering complex of the car-passenger ferry "Maral" are determined by a numerical method to solve the aerodynamic mathematical model of the aerodynamic rudder with a flap, taking into account the pylon stabilizer, the propeller, the annular propeller nozzles in standard situations (in the hover mode of the ship), taking into account their mutual influence.

Key words: *Aerodynamic coefficients of the steering complex, aerodynamic rudder with flap, CPF "Maral", propeller, propeller annular nozzles, steering complex, stabilizer-pylon.*

INTRODUCTION

When creating mathematical models of the hovercraft plumage, it is usually assumed that the forces and moments of resistance of the annular nozzles of propellers, propellers and the steering complex (aerodynamic rudder with a flap, taking into account the stabilizer-pylon) are determined separately. Mathematical models for calculating the resistance of hovercraft plumage are usually conditionally divided into parts. That is, mathematical models of empennage usually include only the consideration of an aerodynamic rudder with a flap, taking into account the pylon stabilizer, and the annular attachments are considered separately. In this case, it is assumed that the total resistance will be equal to the algebraic sum of the indicated resistances [1 – 5].

However, this approach does not take into account the mutual influence of all elements of the hovercraft propeller-steering complex on the total resistance of the vessel, which can lead to somewhat incorrect results.

In the study, it was decided to consider the general problem of an aerodynamic mathematical model of an aerodynamic rudder with a flap, taking into account the pylon stabilizer and an annular nozzle with a propeller in the hover mode of the vessel.

The drag coefficients obtained as a result of blowing one empennage complex for neighboring complexes will be corrected by introducing a mutual influence coefficient. Such a coefficient can be obtained as a result of selective joint blowing of three empennage complexes at several empennage attack angles.

Volodymyr Zaytsev, Prof., Doctor of Technical Sciences, Chief of department,
Dept. of Marine Technology and Ocean Engineering, Shipbuilding Institute,
Admiral Makarov National University of Shipbuilding (NUOS), Nikolaev, UKRAINE
Valeriy Zaytsev, Docent, Doctor of Technical Sciences, Educational and Scientific Center of Hydromechanics, Shipbuilding faculty, Admiral Makarov National University of Shipbuilding (NUOS), Nikolaev, UKRAINE
Dmytro Zaytsev, Docent, Candidate of Technical Sciences, Educational and Scientific Center of Hydromechanics, Shipbuilding faculty, Admiral Makarov National University of Shipbuilding (NUOS), Nikolaev, UKRAINE
Victoria Lukashova, assistant, Dept. of Marine Technology and Ocean Engineering, Shipbuilding Institute, Admiral Makarov National University of Shipbuilding (NUOS), Nikolaev, UKRAINE
Phone: +380-067-515-75-53; E-mail: zvv1949@gmail.com

NARRATION

An aerodynamic model of the steering complex of the automobile-passenger ferry (APF) "Maral" is considered (Fig. 1). It was decided to consider the general problem of the aerodynamic mathematical model (the APF "Maral" empennage) of an aerodynamic rudder with a flap, taking into account the pylon stabilizer and an annular nozzle (AN) with propellers in standard situations in the hover mode of the ship (Fig. 2) [6].

The drag coefficients that will be obtained as a result of blowing one empennage complex (3 such complexes are installed on the APF "Maral") will be corrected by introducing a mutual influence coefficient. Such a coefficient will be obtained as a result of selective joint blowing of three empennage complexes at several empennage attack angles.

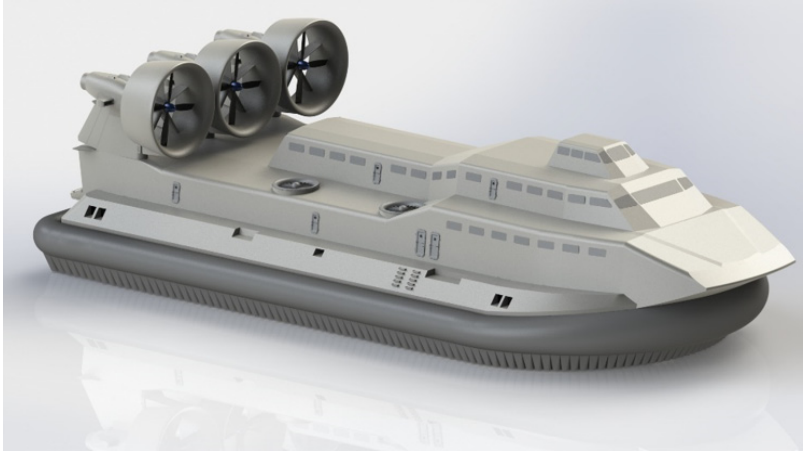

Fig. 1.
Automobile-passenger ferry "Maral"

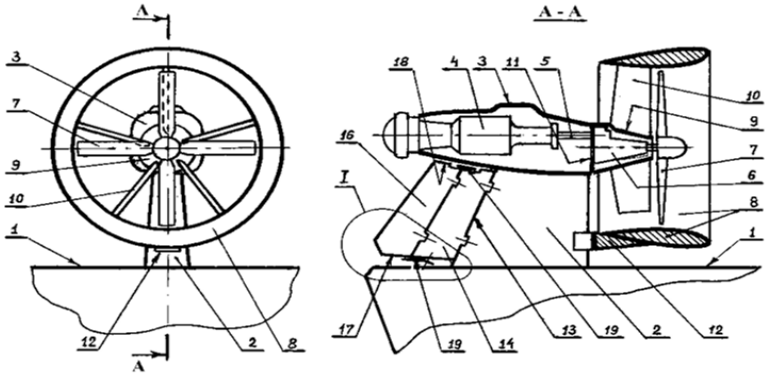

Fig. 2.
APF "Maral" propulsion and steering complex

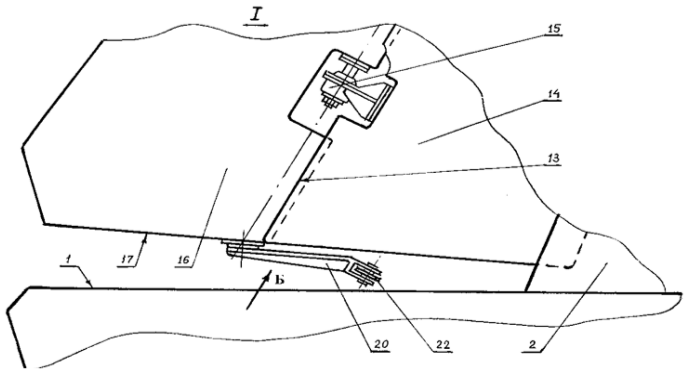

Fig. 3.
APF "Maral" propulsion and steering complex (component 1)

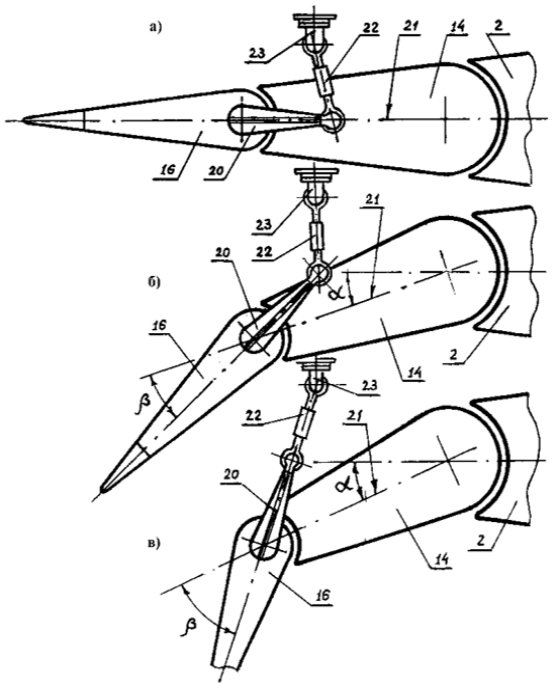

Fig. 4.
APF "Maral" propulsion and steering complex (view along arrow Б)

Figures 2 - 4 indicate:

1 - upper deck APF "Maral"; *2* - pylon-stabilizer; *3* - gondola; *4* - traction engine (TE); *5* - intermediate shaft; *6* - reduction gear; *7* - pulling propeller; *8* - annular nozzle (AN); *9* - fairing; *10* - blades (spokes) of the straightening apparatus (BSA); *11* - bow end of the gondola; *12* - special box part that supports AN; *13* - aft edge of the pylon; *14* - aerodynamic steering wheel (ASW); *15* - hinge connecting ASW to pylon; *16* - flap; *17* - lower end of the flap; *18* - upper end of the flap; *19* - double-lever hinge mechanism (DLHM); *20* - tiller (first lever of DLHM); *21* - longitudinal axis located in the plane of symmetry of the flap; *22* - second lever of DLHM; *23* - fixed bracket.

As a rule, the drag coefficient of hovercraft air rudders $C_{X.Aero\_Rud}$ and $C_{Y.Aero\_Rud}$ and plumage is determined by the results of blowing them in a wind tunnel. However, this method of determining this coefficient is very costly both in terms of time and money.

With the development of computer technology and engineering software, it became possible to significantly reduce these costs. This can be done using software packages that implement the finite volume method (FVM), such as ANSYS CFX or SolidWorks FlowSimulation.

To do this, first of all, you need to create a 3D model of APF "Maral" propulsion and steering complex (PSC) (Fig. 5).

Then, based on the PSC APF "Maral" 3D model, it is necessary to create its simplified 3D model, from which all unnecessary details, such as rudder drive elements, etc., will be excluded. As a result of the transformations, we obtain a simplified 3D model of PSC APF "Maral" (Fig. 6) for further creation of its computational model (Fig. 7).

A simplified 3D PSC model is placed with given rudder angles in a box that represents the environment around the object under study. Two additional objects have been added to the calculated 3D model: *1* - a body of circular cross section, the diameter of which corresponds to the outer diameter of the propeller AB-98; this body is designed to simulate the airflow generated by a propeller; *2* - a rectangular horizontal surface on which the PSC is mounted, it simulates the upper deck of the ship, on which the pylon with AN and rudder is installed. The calculated 3D PSC model is shown in fig. 7.

All work on the creation of a 3D calculation model is carried out in the SolidWorks software product.

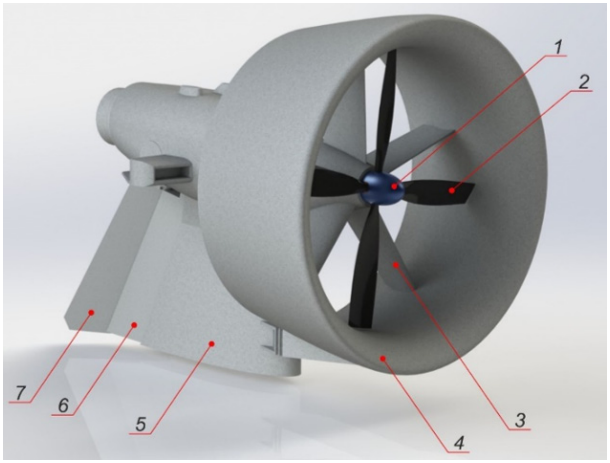

Fig. 5.
General view of the 3D model of PSC APF "Maral" assembly
1 - propeller fairing; *2* - propeller AB-98;
3 - straightener; *4* - annular nozzle; *5* - pylon;
6 - air steering wheel; *7* - air rudder flap

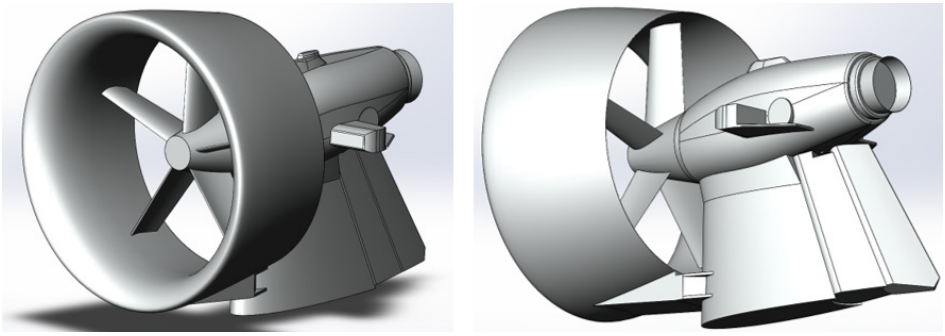

Fig. 6.
Simplified 3D model of PSC APF "Maral" assembly

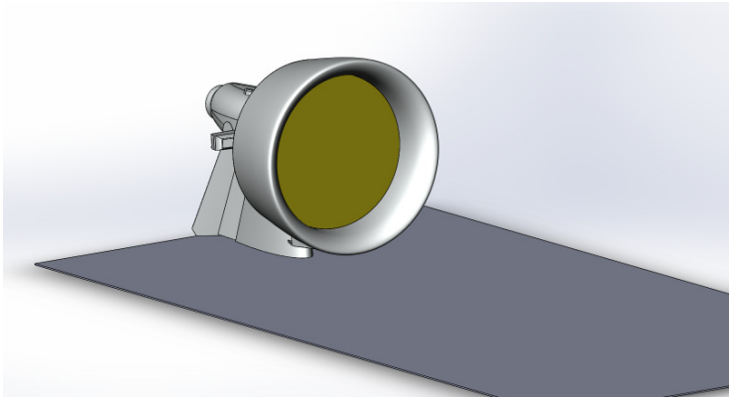

Fig.7.
PSC APF "Maral" 3D calculation model

Further preparation of the numerical experiment is carried out using the FlowSimulation module, which is an integral part of the SolidWorks software. First of all, the dimensions of the calculation area are set (Fig. 8) with the following dimensions: length - 60.0 m; width - 20.0 m; height - 14.5 m.

Then the general settings of the task are performed: task type - external flow; fluid medium - air (Air); flow type - laminar and turbulent; adiabatic walls; wall roughness - 5 microns; pressure - 101.325 kPa; temperature - 293.2 K.

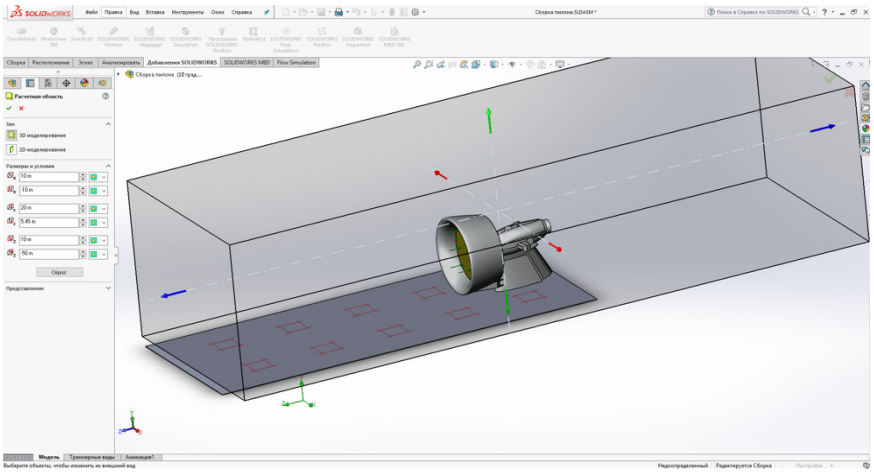

Fig. 8.
PSC APF "Maral" computational domain

Boundary conditions are set. For a plane that simulates the surface of a hovercraft deck, the "Real wall" property is set. A virtual propeller is created in the SolidWorks engineering database and assigned propeller AB-98 parameters. In the calculation model, the input and output surfaces of the propeller are specified.

An initial global mesh of finite volume elements is created inside the computational domain. The mesh generator of the FlowSimulation module has a large number of settings that allow you to create an optimal global mesh (Fig. 9). To improve the accuracy of calculations and obtain reliable results on the surfaces of the calculation model, it is necessary to create a local grid. The local grid is a region of smaller finite volume elements compared to the global grid elements, and they are located in the near-wall region of the computational model.

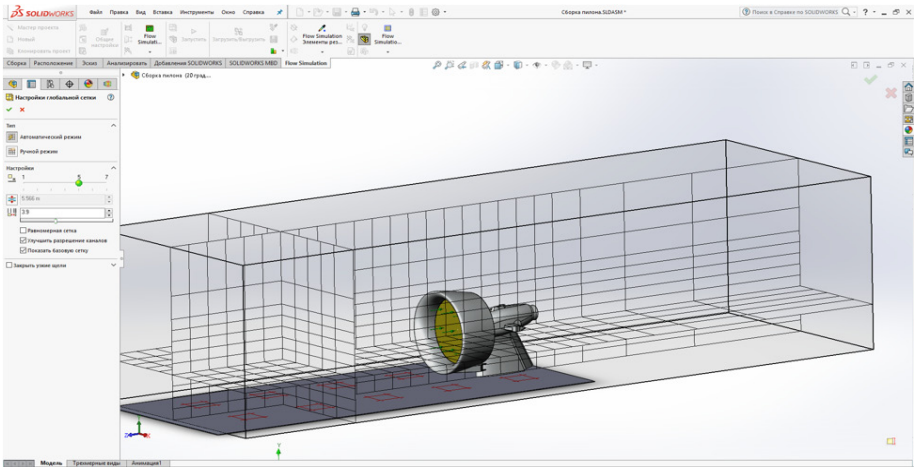

Fig. 9.
Initial global mesh

When creating a finite element mesh, it is necessary to obtain the maximum quality of the elements. The automatic finite element meshing procedure does not provide the required element quality and creates an excessive amount of poor quality finite elements. Such a finite element mesh will increase the duration of the calculation, worsen the convergence of the results, and the reliability of the results will not be too high. The built-in tools for creating a finite element mesh, the mesh generator "Meshing", allow you to achieve the maximum quality of the mesh elements.

In order to obtain the results of interest to us, as well as to monitor the convergence of the calculation, it is necessary to set goals. To solve the problem, it is necessary to know the forces on the surfaces of the air rudder and its flap, the moments relative to the axis of rotation of the rudder and the axis of rotation of the flap. With the help of the corresponding menu, goals were set for the objects of interest to us.

To determine the aerodynamic drag coefficients of air rudders in the entire range of their rudder angles, it is

necessary to prepare such a problem for each rudder angle that we will study, from the extreme left position to the extreme right position. For this study, the following rudder angles were adopted: 0 degrees; 5, 10, 15, 20, 24 degrees to port; 5, 10, 15, 20, 24 degrees to starboard.

After completing the settings in the preprocessor, you can begin to solve the problem, which is performed automatically at the user's command and usually does not require the user to be constantly near the personal computer.

The results of the performed calculation for each task (for each rudder angle) are recorded in a separate project folder. The FlowSimulation module has a large set of tools for processing simulation results. It allows you to get an image of a grid of finite volume elements, which was built in the course of solving the problem (Fig. 10).

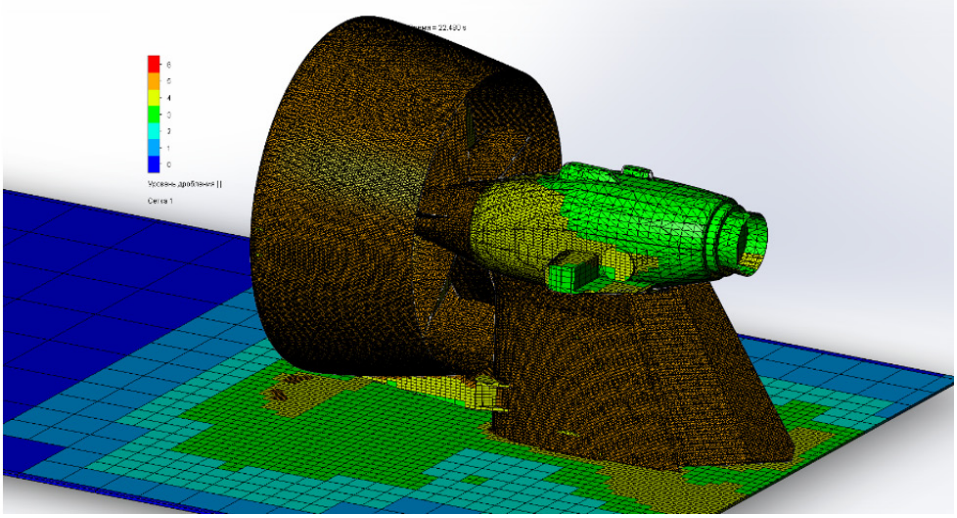

Fig. 10.
Grid of finite volume elements for rudder angle 20° to starboard

Results processing tools allow you to build diagrams in various sections both on surfaces and display such parameters as flow velocity, pressure, temperature, density, vorticity, etc. on them.

Figure 11 shows the diagram of the distribution of velocities in a horizontal section in the area where the main air flow from the propeller passes through the air rudder.

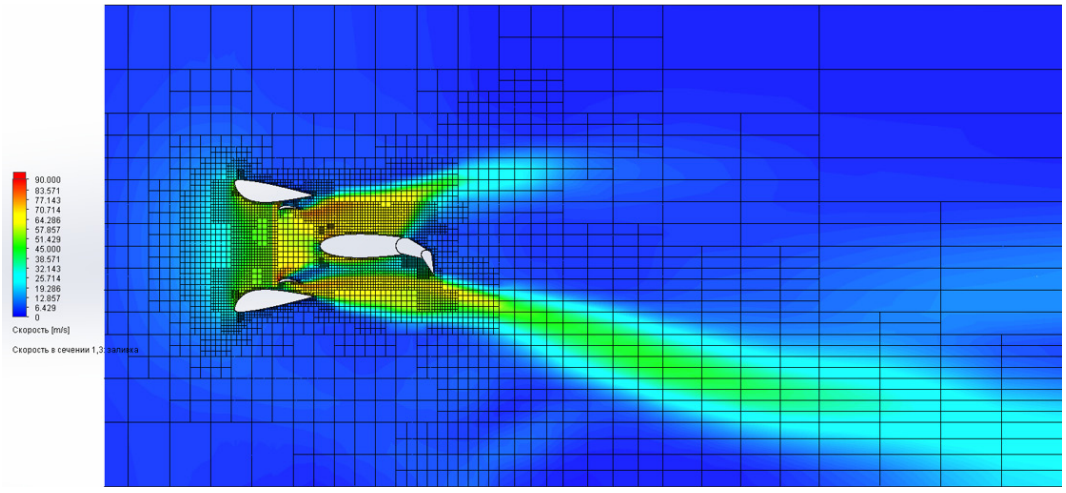

Fig. 11.
Velocity distribution diagram in a horizontal section at a distance of 7.5 m from the main plane for a rudder angle of 24° to port

The picture of the pressure distribution over the surface of the rudder and flap is shown in Fig. 12.

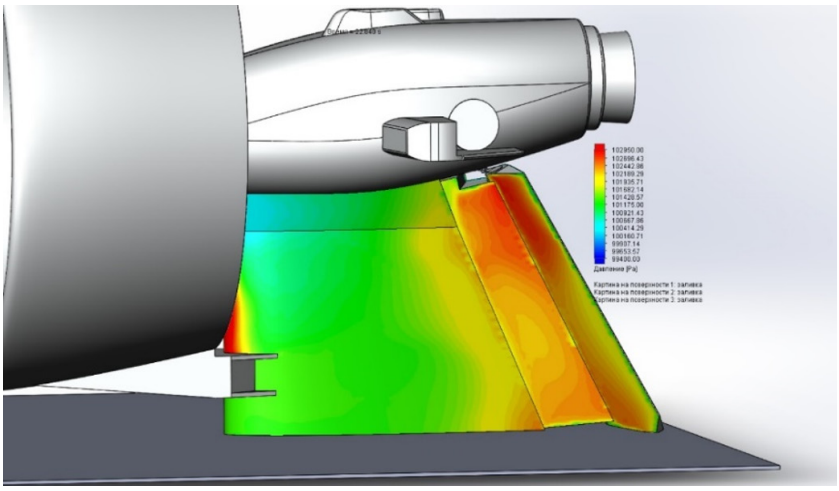

Fig. 12.
Pressure distribution along the rudder and flap for a rudder angle of 24° to port

In addition, all calculation results for all targets are recorded in a separate file, the data of which can be imported into MS Excel. The final calculation data for all rudder angles in the SolidWorks coordinate system are presented in Table 1.

Results of a numerical experiment on blowing the rudder with a flap at different rudder angles in the SolidWorks software coordinate system

Table 1

Target name	Dimension	Port side					0°	Starboard				
		24°	20°	15°	10°	5°		5°	10°	15°	20°	24°
Rudder												
R_P	N	3928	3132	2048	1494	1118	1005	1388	2069	2894	3788	4330
$R_{Xsw.P}$ (X)	N	-3872	-3130	-2027	-1351	-612	248	1087	1982	2872	3786	4301
$R_{Ysw.P}$ (Y)	N	208	18,8	-113	-222	-313	-312	-263	-148	-49,9	124	256
$R_{Zsw.P}$ (Z)	N	-629	-108	269	599	882	923	823	575	358	-55,9	-420
Flap												
R_{3K}	N	3469	2933	1894	1274	540	193	690	1293	1949	2649	3321
$R_{Xsw.3K}$ (X)	N	-1812	-2240	-1725	-1246	-537	142	687	1283	1847	1983	1623
$R_{Ysw.3K}$ (Y)	N	1245	779	314	99,9	-31,2	-53,8	-25,2	72,2	278	771	1264
$R_{Zsw.3K}$ (Z)	N	-2683	-1725	-717	-246	48,4	118	57,9	-139	-559	-1578	-2607
M_{3K}	N*m	1307	951	523	322	106	-34,1	-110	-219	-445	-783	-1329
Rudder with flap												
R_{P+3K}	N	6738	5730	3784	2624	1518	1170	2002	3296	4728	6063	6825
$R_{Xsw.P+3K}$ (X)	N	-5685	-5370	-3752	-2597	-1149	390	1774	3266	4718	5769	5925
$R_{Ysw.P+3K}$ (Y)	N	1453	798	201	-122	-344	-365	-288	-75,5	228	895	1520
$R_{Zsw.P+3K}$ (Z)	N	-3312	-1834	-449	354	930	1041	881	435,5	-201	-1634	-3027
$M_б$	N*m	5368	4621	2923	1890	757	-244	-1017	-1891	-2976	-4113	-5172

Based on the results of the numerical experiment, we determine the necessary aerodynamic drag coefficients for the rudder complex.

The initial data for calculating the aerodynamic drag coefficients for the rudder complex are given below: air flow velocity - 50 m/s; rudder area - 3.76 m^2; flap area - 4.05 m^2; area of the complex - 7.81 m^2; air density - 1.225 kg/m^3; rudder chord - 1.153 m; flap chord - 1.219 m; total chord - 2.372 m.

Aerodynamic drag coefficients separately for the rudder are shown in Table 2.

Rudder drag coefficients

Table 2

Target name	Port side					0°	Starboard				
	24°	20°	15°	10°	5°		5°	10°	15°	20°	24°
Rudder											
$C_{.руля}$	0,682	0,544	0,356	0,260	0,194	0,175	0,241	0,359	0,503	0,658	0,752
$C_{Y.руля}$	0,673	0,544	0,352	0,235	0,106	0,043	0,189	0,344	0,499	0,658	0,747
$C_{Z.руля}$	-0,036	-0,003	0,020	0,038	0,054	0,054	0,046	0,026	0,009	-0,022	-0,045
$C_{X.руля}$	-0,109	-0,019	0,047	0,104	0,153	0,160	0,143	0,100	0,062	-0,010	-0,073

The aerodynamic drag coefficients separately for the flap are given in Table 3.

Flap drag coefficients

Table 3

Target name	Port side					0°	Starboard				
	24°	20°	15°	10°	5°		5°	10°	15°	20°	24°
Flap											
$C_{.закр}$	0,559	0,473	0,305	0,205	0,087	0,031	0,111	0,209	0,314	0,427	0,535
$C_{Y.закр}$	0,292	0,361	0,278	0,201	0,087	0,023	0,111	0,207	0,298	0,320	0,262
$C_{Z.закр}$	-0,201	-0,126	-0,051	-0,016	0,005	0,009	0,004	-0,012	-0,045	-0,124	-0,204
$C_{X.закр}$	-0,433	-0,278	-0,116	-0,040	0,008	0,019	0,009	-0,022	-0,090	-0,255	-0,420
$C_{.M.Z.закр}$	0,173	0,126	0,069	0,043	0,014	-0,005	-0,014	-0,029	-0,059	-0,104	-0,176

The aerodynamic drag coefficients of the rudder complex are shown in Table 4.

Drag coefficients for the rudder complex

Table 4

Target name	Port side					0°	Starboard				
	24°	20°	15°	10°	5°		5°	10°	15°	20°	24°
Rudder complex											
$C_{.компл}$	0,563	0,479	0,316	0,219	0,127	0,098	0,167	0,276	0,395	0,507	0,571
$C_{Y.компл}$	0,475	0,449	0,314	0,217	0,096	0,033	0,148	0,273	0,395	0,482	0,495
$C_{Z.компл}$	-0,121	-0,067	-0,017	0,010	0,029	0,031	0,024	0,006	-0,019	-0,075	-0,127
$C_{X.компл}$	-0,277	-0,153	-0,038	0,030	0,078	0,087	0,074	0,036	-0,017	-0,137	-0,253
$C_{.M.Б}$	0,189	0,163	0,103	0,067	0,027	-0,009	-0,036	-0,067	-0,105	-0,145	-0,182

CONCLUSIONS

The described technique made it possible to determine the drag coefficients of the APF "Maral" rudder propeller complex, taking into account the mutual influence of the annular nozzle, propeller, and aerodynamic rudder.

The application of the described technique in the design of hovercrafts will make it possible to create more reliable ships of this type, and in simulation modeling, it will make it possible to more accurately predict their behavior in various operating modes.

REFERENCES:

[1] V o y t k u n s k y, Ya. I. Handbook on the theory of the ship. Ship propulsion and controllability. Ed. 2nd, revised and supplemented / Voytkunsky Ya. I., Pershits, R.Ya., Titov, I. A. - L .: Shipbuilding, 1973. - 512 p.
[2] R u s e t s k y, A. A. Propulsors of ships with dynamic principles of maintenance: a tutorial. - L .: Shipbuilding, 1979. - 240 p.
[3] H a n d b o o k of ship theory / Ed. V. F. Droblenkov. - M.: Military Publishing House, 1984. - 592 p.
[4] H a n d b o o k of ship theory: in 3 volumes / [ed. ME AND. Voytkunsky]. - L.: Shipbuilding, 1985. - V.1: Hydromechanics. Resistance to the movement of ships. Ship movers. - 768 p.
[5] H a n d b o o k of ship theory: in 3 volumes / [ed. ME AND. Voytkunsky]. - L.: Shipbuilding, 1985. - V.3: Controllability of displacement ships. Hydrodynamics of ships with dynamic principles of maintenance. - 544 p.
[6] O s t a p e n k o, S.Ya., Bogatov, L. I., Pavlov, G. A. Patent of Ukraine №80803. IPC: B60V 3/00; B60V 1/00. Propulsion and steering complex of a hovercraft; Published: 11/12/2007.

SHIPBUILDING AND SHIP REPAIR

DEVELOPMENT OF SHORT SEA SHIPPING AND MULTIMODAL TRANSPORT OF BLACK SEA REGION

Petar GEORGIEV*

Abstract. *The development of Short Sea Shipping and related multimodal transport is of particular importance for Europe. The topic is of special importance in relation to the current situation connected with the waning Covid-19 pandemic, the war in Ukraine and related energy and transport problems. The article reviews new facts and circumstances to be considered when preparing in-depth analyses for the transport of goods in the Black Sea region and Bulgaria's participation in multimodal corridors. Based on the described facts, corresponding conclusions were made.*
Key words: *Black Sea, multimodal transport, short sea shipping, transport corridors.*

INTRODUCTION

After the full liberalization of cabotage services in Europe after 2002 an EU-flag ship is eligible to undertake cabotage trades in any EU state. In such way it was possible for short sea shipping (SSS) to start competing effectively with land-based transport. Unfortunately, it still cannot completely replace the land-based transport, but the statistics show a constant development. Organizational and legal problems are still an obstacle.

There are five major regional markets, each with its own characteristics; the Black Sea, the Mediterranean, the Atlantic Range, the North Sea, and the Baltic (Figure 1).

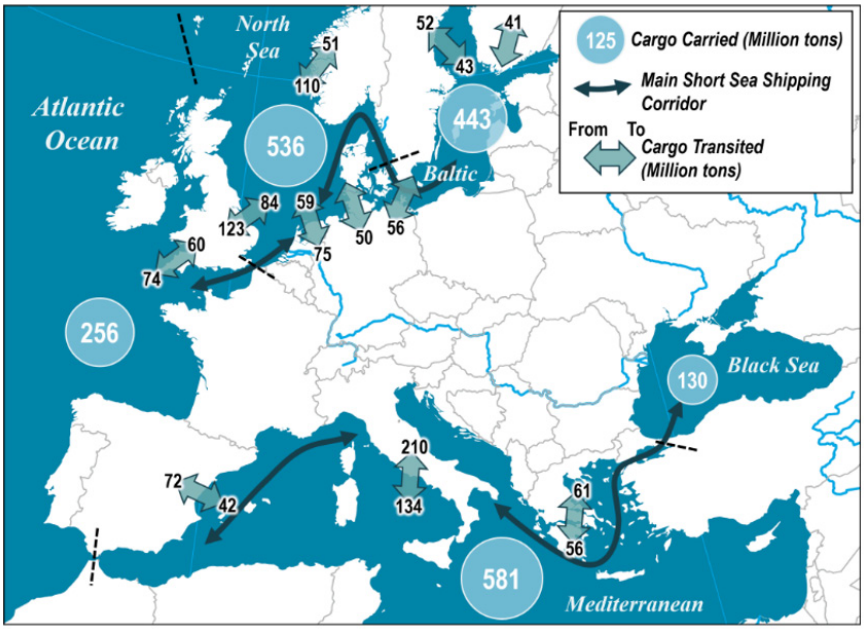

Fig. 1.
The European Short Sea Shipping Market [1]

The main measures to improve short sea shipping are related to [1]:

• **Technical and infrastructural aspects**: shorter turnaround time in ports, more efficient customs operations and administrative procedures, and more favourable port pricing.

***Technical University of Varna**

• **Commercial aspects**: better integration of short sea shipping in supply chain practices through information and reliability improvements.

• **Political aspects**: policies to internalize the external costs of transport modes, ending preferential treatment by customs procedures in favour of overland traffic. This also includes harmonizing rules for land and sea carriage of hazardous goods.

Authors in [2] investigated influence of factors as length of the coastline, Gross domestic product (GDP), number of ports, volume of rail infrastructure on SSS in European countries. Due to the small number of countries (n = 25 countries) involved in the statistical processing of the data, the conclusions drawn should be taken with caution. A longer coastline does not necessarily imply a larger SSS volume and more important is the number of large ports. The GDP per capita is more important factor and it is included as a factor in the multivariate linear regression model for total SSS volume, liquid bulk SSS volume and dry bulk SSS volume. The number of SSS ports (in total as well as only small or large SSS ports) correlated strongly with total SSS volume. A higher rail length relates to a smaller SSS volume in dry bulk and containers transport. According to the authors, other factors also affect the volume of SSS such as: overall maritime traffic per country, peripherality of the country, and proximity to major sea routes.

The paper presents facts and considerations regarding the current state of SSS, the impact of the war in Ukraine, cargo flows in the Black Sea region, maritime transport across the Black Sea, and the possibilities for multimodal transport from the ports of Bulgaria. The aim is that this information serves various interested parties in the preparation and implementation of the maritime policy of Bulgaria and maritime and multimodal transport through Bulgaria.

CURRENT STATE OF SHORT SEA SHIPPING

SSS in Europe

Unfortunately, the SSS highest level in 2019 compared with the economic downturn in Europe in 2009 are coming down in late 2020 probably due to Covid-19 [3]. The decreasing is 6.6 % compared to 2019. The predominance of short sea shipping of goods over deep sea shipping for Bulgaria, Romania and Turkey in the Black Sea region and EU (27 countries) is shown in Figure 2. Some geographical considerations and many inhabited islands play important roles for this percentage. The share of SSS is lower in countries with major ports with intercontinental trade such as France, Portugal, Germany, Belgium, the Netherlands, Spain, and Slovenia. With share less than 63 %. The explanation for the high percentage of Bulgaria can be sought in the geographical location and the depth of the Bulgarian ports from 11.1 to 12.0 meters. For comparison, the maximum depth of the port in Constanta is 16.1meters, which allows the docking of deep-sea going ships.

Italy was the major SSS country with a share of 14.4 % of the total tonnages of EU short sea shipping in 2020 followed by Netherlands and Spain. Almost all EU Member states (except of Italy, Sweden, Latvia, Estonia, France, Croatia) have increased the volume of SSS compared to 2010. This is clear from the 2019/2010 freight ratio (Figure 3). For Bulgaria, this percentage increasing is 38%. In addition, all EU Member States registered a fall in SSS between 2019 and 2020 except Malta, Croatia, Cyprus, and Sweden. Bulgaria recorded one of the biggest decreases (-17%) (Figure 3).

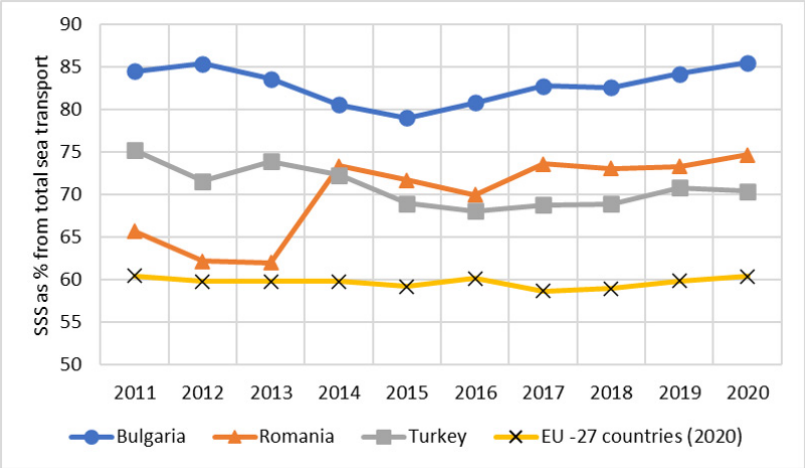

Fig. 2.
Percentage of SSS from the total sea transport for countries in the Black Sea region (elaborated based on [3])

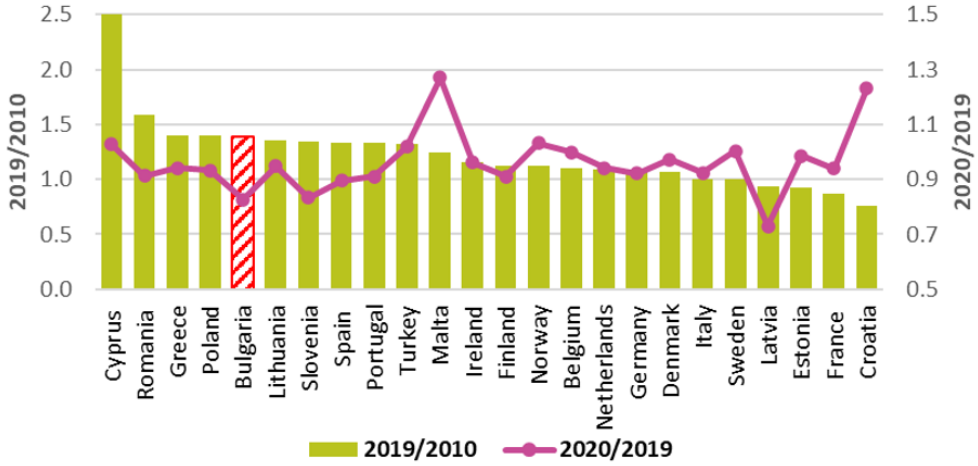

Fig. 3.
Comparison of SSS freight for 2019/2010 (left axis) and 2020/2019 (right axis) (elaborated based on [3])

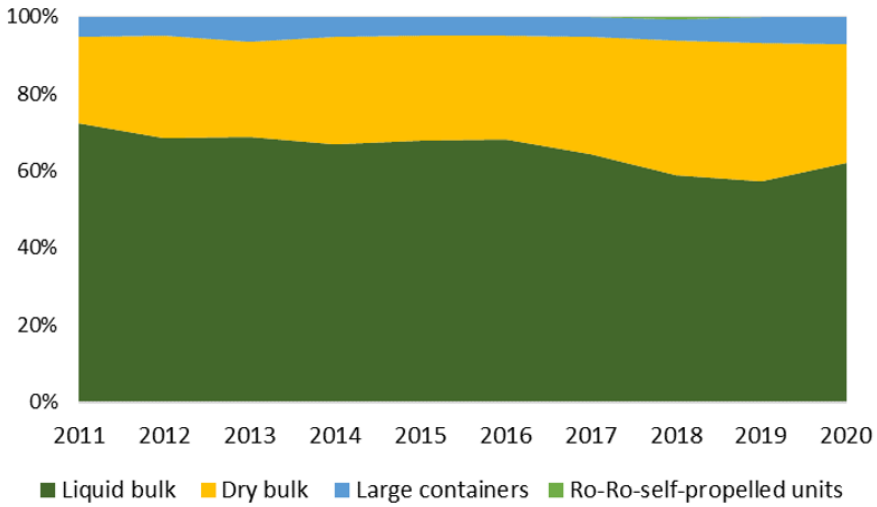

Fig. 4.
Volume of transported goods by SSS for the last ten years in the Black Sea (elaborated based on [3])

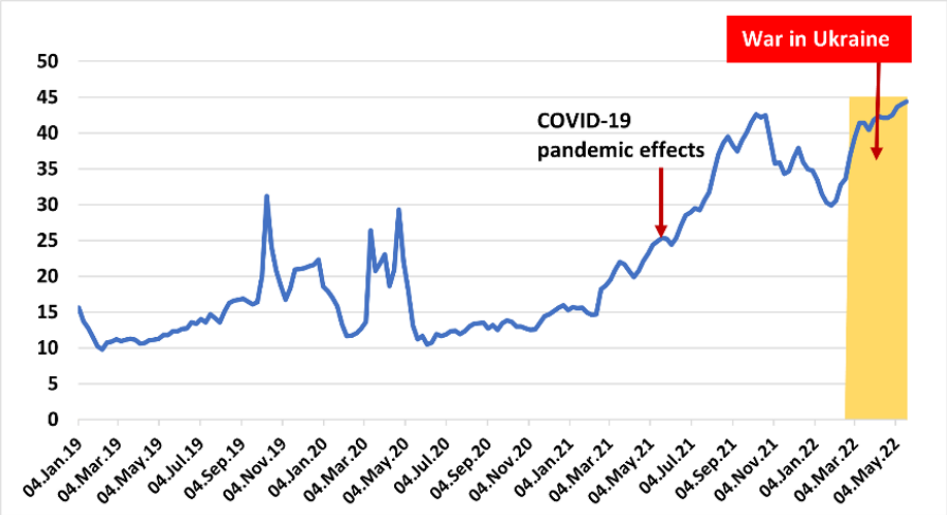

Fig. 5.
***ClarkSea Index* in thousand USD/day for last 3 years (elaborated based on [4])**

The liquid bulk remained the dominant type of cargo in EU short sea shipping, The same is valid for the Black Sea too (Figure 4). The percentage of liquid cargoes is greater than 60 % for the last 10 years with exemption for 2018 and 2019. The maximum volume of Ro-Ro movable self-propelled units is 830,000 tonnes for 2018 (0.6% for the year).

Influence of war in Ukraine

The war in Ukraine in two of the Black Sea countries has a global impact. The UNCTAD says the war in the Ukraine is stifling trade and logistics of the country and the Black Sea region, increasing global vessel demand and the cost of shipping around the world [4].

The price of shipping is rising, that it is clear from *ClarkSea Index*[1] values (Figure 5). The presented data are for the major shipping sectors, including tankers, bulkers, containerships, and gas carriers. This is because of the transport hurdles in the Black Sea region as disruptions in regional logistics, the halting of port operations in Ukraine, the destruction of important infrastructure, trade restrictions, increased insurance costs and higher fuel prices. According to the report [4] , by the end of May 2022, the global average price for very low sulphur fuel oil had increased by 64% since the start of the year.

Since the start of the war (8th week of 2022), weekly port calls have gone from 60 to almost zero in Ukraine (Figure 6). Port calls are significantly less than 2021 for Russian Federation and have decreased in Türkiye since pre-war. Meanwhile, dry bulk vessel calls have seen small increases at ports more visible in Bulgaria and less pronounced in Roman, reflecting the re-routing of some of the trade from Ukraine.

Regarding container transport, since the terminal in Constanta is overloaded, requests are increasingly being received from Ukrainian freight forwarders interested in transporting cargo through Varna (Figure 7) Containers for Ukraine must be reloaded onto a truck for onward delivery, which takes time, slowing down the overall container turnover and increasing transportation costs [6].

[1] *ClarkSea Index* is a weighted average index of earnings for the main vessel types where the weighting is based on the number of vessels in each fleet sector

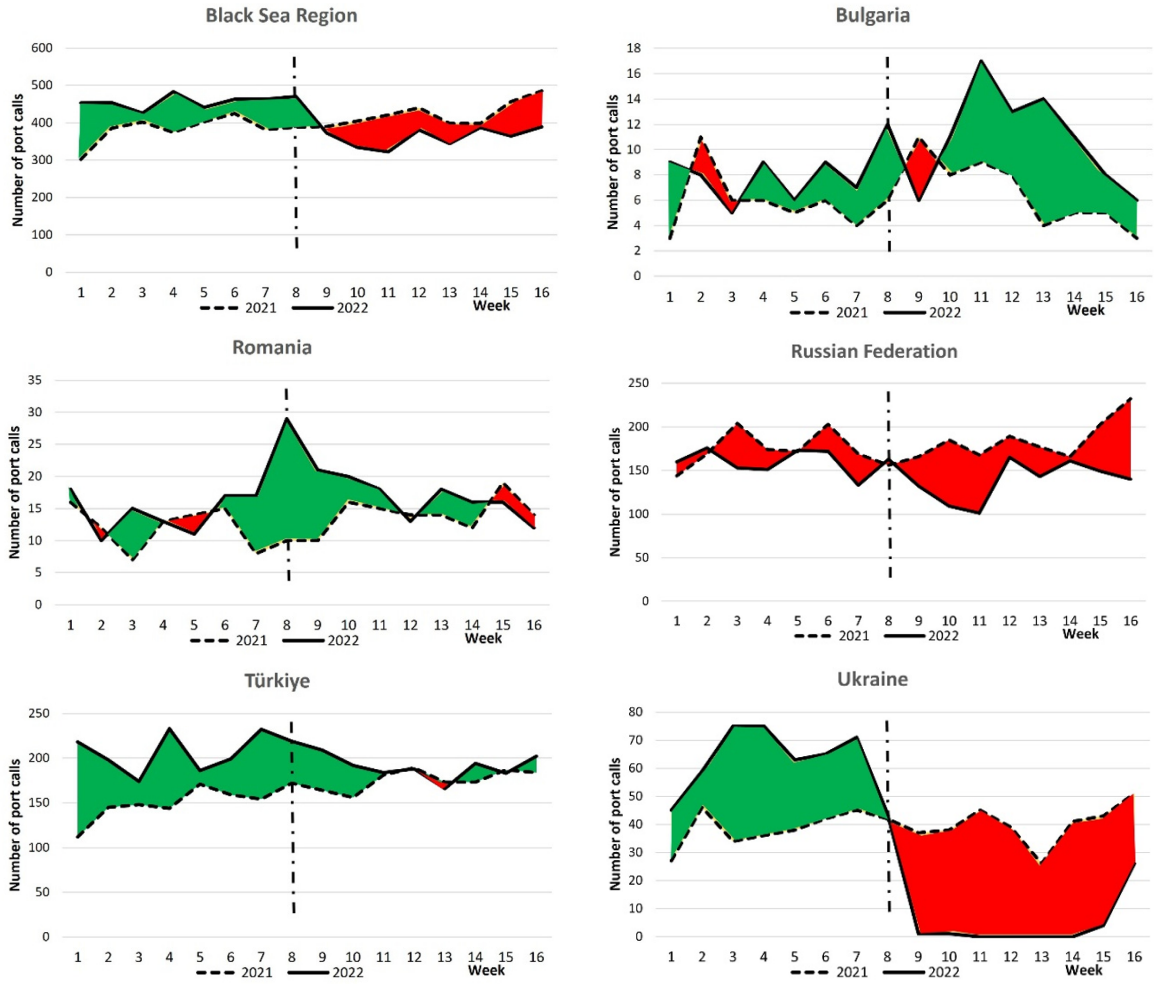

Fig. 6.
Number of port calls of dry bulk in the Black Sea region, by week, 2021 and 2022 (elaborated based on [5])

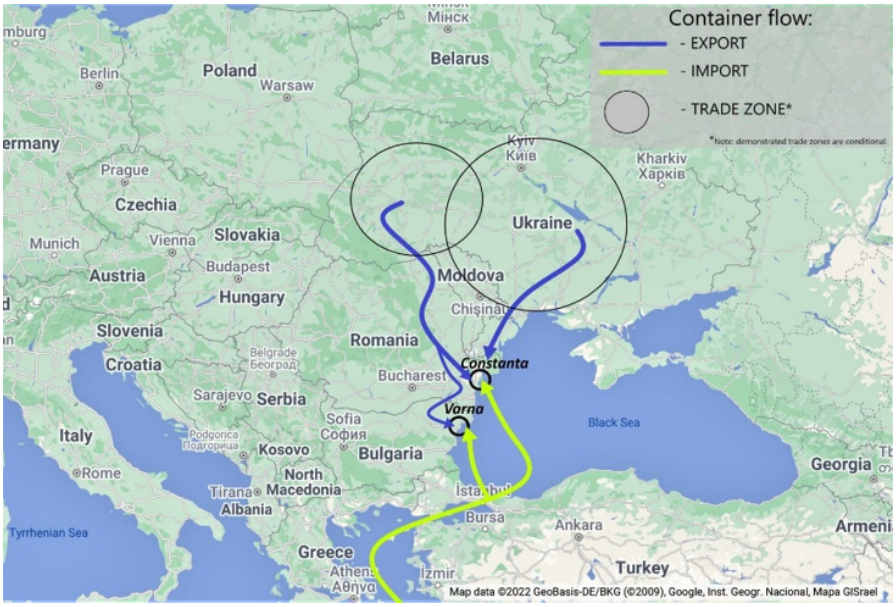

Fig. 7.
Routes of container transport after the 24 of February 2022 [6]

A good decision to improve the situation in the Black Sea region was the adoption of the initiative "Black Sea Grain Initiative" [7]. The Joint Coordination Centre (JCC) established in the frame of the initiative has responsibility for four main tasks: 1) monitoring the movement of commercial vessels to ensure compliance; (2) focusing on only the export of bulk commercial grain and related food commodities; (3) ensuring the on-site control and monitoring of cargo from Ukrainian ports; and (4) reporting on shipments facilitated through the Black Sea Grain Initiative. The route of the ships with grain cargo is shown in Figure 8. The first shipment of grain to leave Ukraine under a wartime deal appears to have ended up in Syria [9]. The 26 years old m/v "Razoni" (DWT = 29292 t, L x B = 186.6 x 25 m), loaded with 26,000 tons of corn was the first vessel shipped under this initiative.

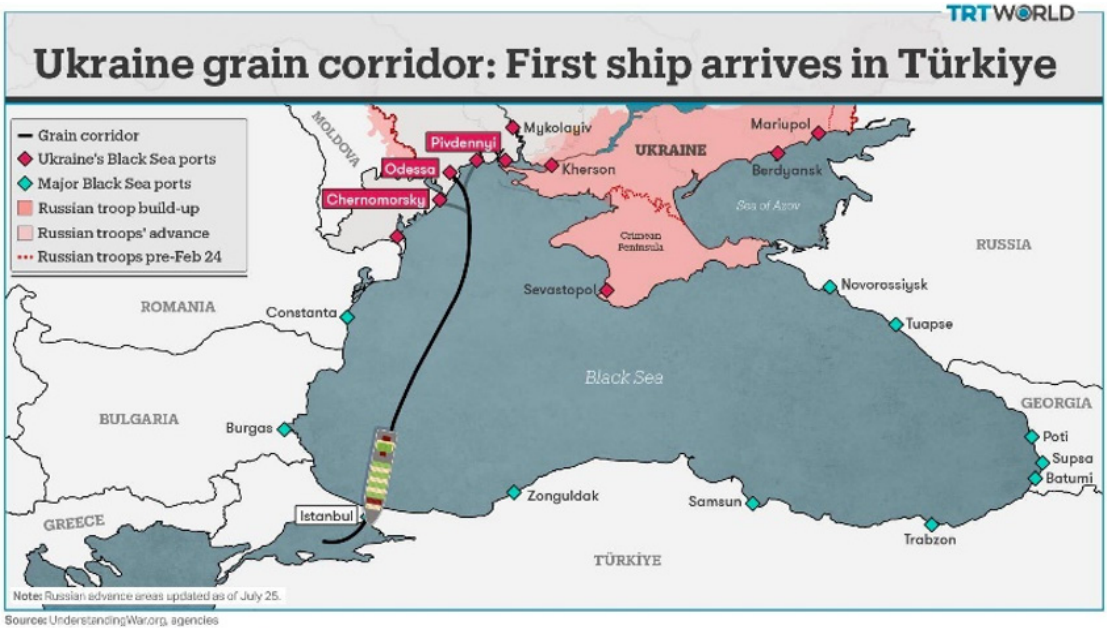

Fig. 8.
Route of grain cargo from Ukrainian ports [8]

CARGO CORRIDORS AND FRIGHT RATES

In 2021, 26.3 million containers (TEU) were transported on the Europe-Asia-Europe route, which is 84% of Trans-Pacific one and 3.3 times more than the Transatlantic route [10]. During the last 18 months, container freight rates started to grow and a year ago they reached their maximum of nearly 10,370 USD. The reasons can be found in the insufficient number of empty containers and the economic revival after the pandemic. This corresponded also to the maximum available carrying capacity. There is currently a steady decline and ship owners are planning to increase their capacity by buying new containers and building new ships.

The Central Asia Regional Economic Cooperation (CAREC) Program is a partnership of 11 countries: Afghanistan, Azerbaijan, the People's Republic of China, Georgia, Kazakhstan, Kyrgyz Republic, Mongolia, Pakistan, Tajikistan, Turkmenistan, and Uzbekistan [12].

There are six CAREC corridors that link the region economic hubs to each other and connect the landlocked countries to other Eurasian and global markets. The joining of Georgia to CAREC in 2017 expands the multimodal network connectivity to the Black Sea ports and the land border with Turkey.

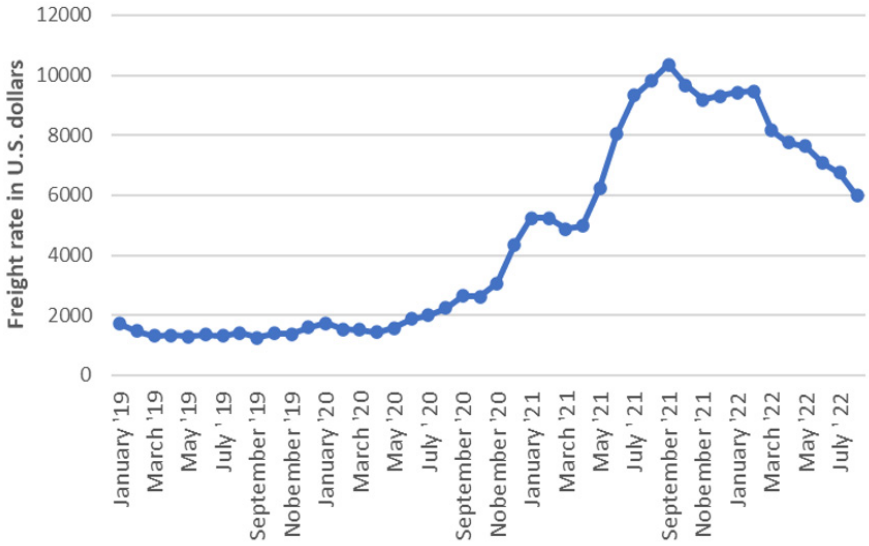

Fig. 9.
Global container freight rate index from January 2019 to August 2022 [11]

The corridor No. 2, called Middle Corridor (Figure 10), is a result of founded in January 2017 the International Association "Trans-Caspian International Transport Route" (TITR). The corridor is of interest of Bulgaria and its parameters [13] are presented in Table 1.

Parameters of TITR

Table 1

Route	Countries/Cities	Distance	Time
Trans-Caspian Route	Lianyungang (PRC) - Aktau/Kuryk (Kazakhstan) - Azerbaijan - Georgia - Turkey / Ukraine / Poland / Romania / Italy / other EU countries	9400-11000 km	13-21days
Sea Route	Lianyungang (China) - Suez (Egypt) - Istanbul (Turkey)	16400 km	35-45 days

*PRC - People's Republic of China

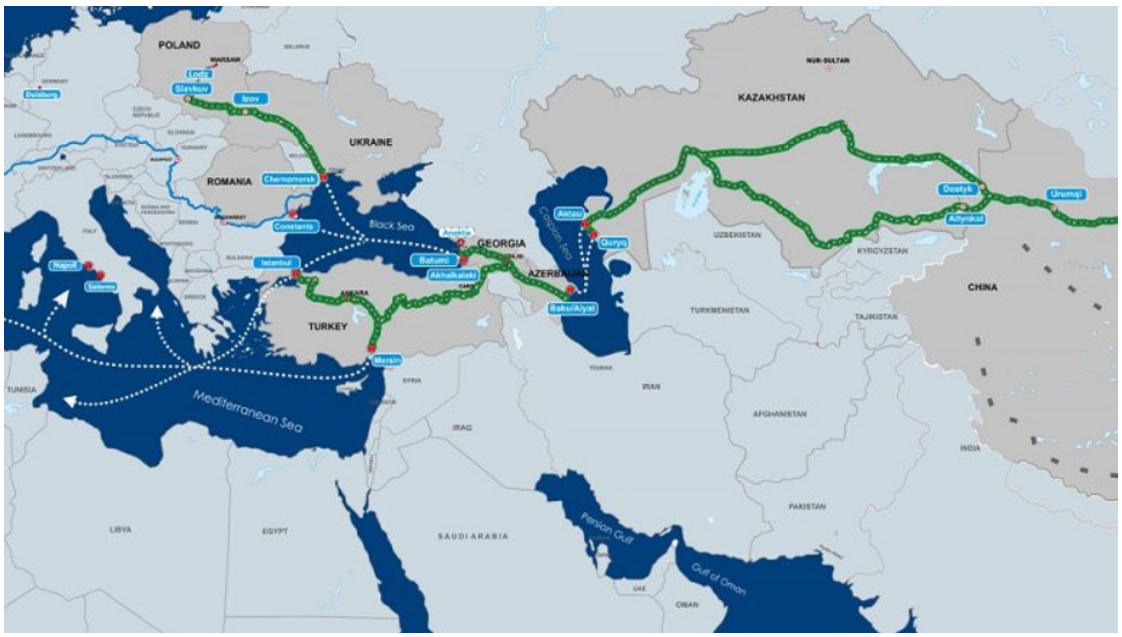

Fig. 10.
Trans-Caspian International Transport Route [14]

Summary of ports serving CAREC countries on the TITR route [1]

Table 2

Sea	Port Name	Port Capacity (mtpa)	Combined Throughput (mt)	Conatainer Capacity ('000 TEU pa)	Containerized Throughput ('000 TEU)
Caspian Sea	Aktau	15.0	3.2	25.0	14.3
	Kuryk	6.0	2.4	100.0	0.0
	Baku-Alat	15.0	4.6	500.0	35.1
	Bandar-Azali	7.0	1.0	40.0	3.3
	Astrakhan	12.1	2.2	10.0	2.6
Black Sea	Samsun	23.0	12.2	125.0	67.0
	Varna	15.0	9.5	300.0	139
	Constanta	100.0	66.0	1,800.0	666.0
	Odessa	50.0	21.7	1,400.0	650.0
	Rostov- on-Don	28.0	22.9	50.0	0.0
	Novorossiysk	200.0	154.0	1,600.0	755.0
	Batumi	20.0	2.9	200.0	116.1
	Poti	63.0	6.3	550.0	510.0

mt= metric tonne; pa = per annum

The capacity of the Caspian and Black Sea ports is presented in Table 2. The natural continuation of this corridor is through the Black Sea to the ports of Bulgaria and Romania.

In the analysis of the existing transport corridors, some infrastructure bottlenecks in rail transport should also be considered [15] as follows:

• PRC–EU trains carry 42-44 FEU while. Kazakhstan and Russian trains have usually 32 wagons with capacity for 4 TEU per wagon (total 64 FEU).

• Georgia Railways has capped capacity on block trains: to 29 wagons for 58 TEU (29 FEU) and 1,900 tons per train, because Rikoti Pass and Akhalkalaki pass on the Tbilisi- Kars line caps capacity to 36 TEU (18 FEU) only or 18 wagons per train.

• TITR fares per Km are comparable with those of UTLC[2], though transit time is longer despite shorter distance.

• Neither Poti nor Batumi ports have efficient rail connection down to the dockside container terminal.

The Middle Corridor is an essential lifeline for some major industrial complexes located far inland in Central Asia such as fertilizers plant in Mary (Turkmenistan) and TALCO aluminium plant in Tursunzade (Tajikistan). This becomes especially important considering the war in Ukraine.

One final fact to consider when analyzing maritime transport corridors in the Black Sea region is the cost of crossing the Bosporus. Türkiye has increased the transit fee for using the Bosporus and Dardanelles fivefold and the new toll was set at $4 per tonnage. The new regulation will enter into force on Oct. 7, 2022, [16].

[2] United transport and Logistics company corridor - located in the north passing through Kazakhstan, Russia, and Belarus. https://3seas.eu/

Fig. 11.
Extended Baltic-Black-Aegean Seas Corridor [17]

MULTIMODAL CORRIDORS FROM BULGARIA

By the end of July, the EC decided to extend four European Transport Corridors to the territory of Ukraine and Moldova - including the ports of Mariupol and Odesa. The proposal will improve transport connectivity of these two countries to the EU [17]. The extension of the Baltic-Black -Aegean Seas Corridor is shown in Figure 11. To overcome a substantial obstacle the Ukrainian Railway Company (UZ) intends to build an UIC 1.435mm gauge track to the Polish border [18]. It will allow to remove replacing the bogies.

The idea of a railway corridor between Greece and Bulgaria, which would connect the ports of Thessaloniki, Alexandropoulos, Burgas, Varna, and Ruse, is not new (Figure 12). It received confirmation of readiness from both sides for more active work in mid-September 2019 [19].This corridor will carry out multimodal transport from the Mediterranean to Europe in a north-south direction

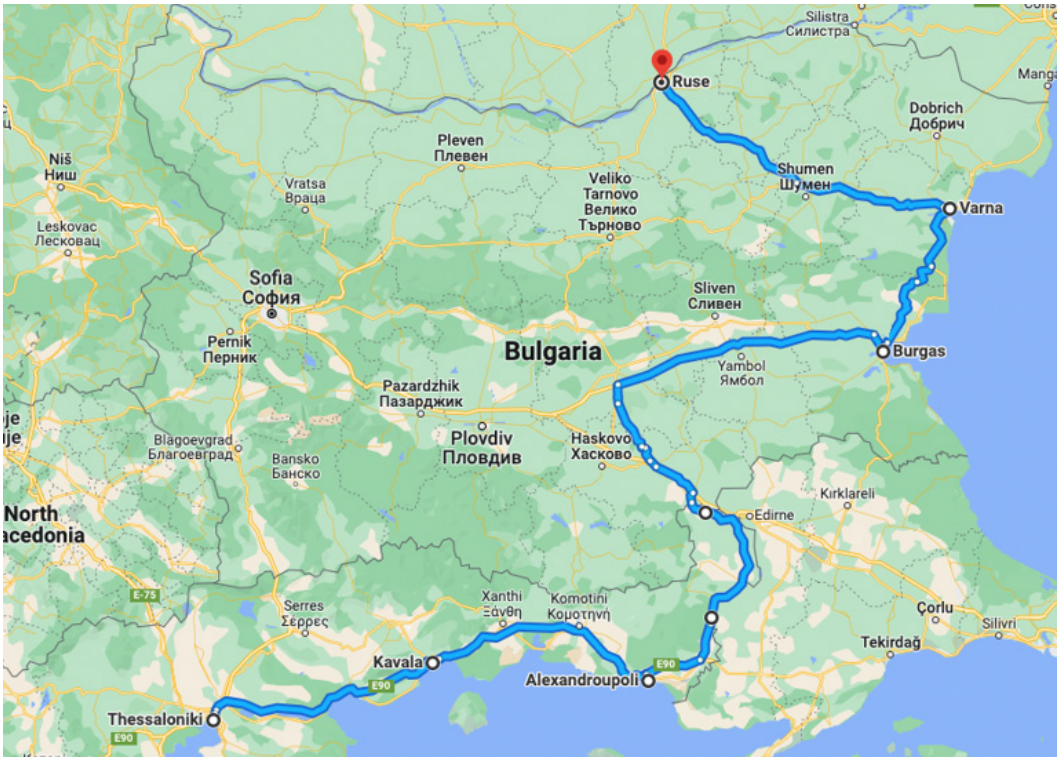

Fig. 12.
The rail transport corridor between the ports of Bulgaria and Greece [20]

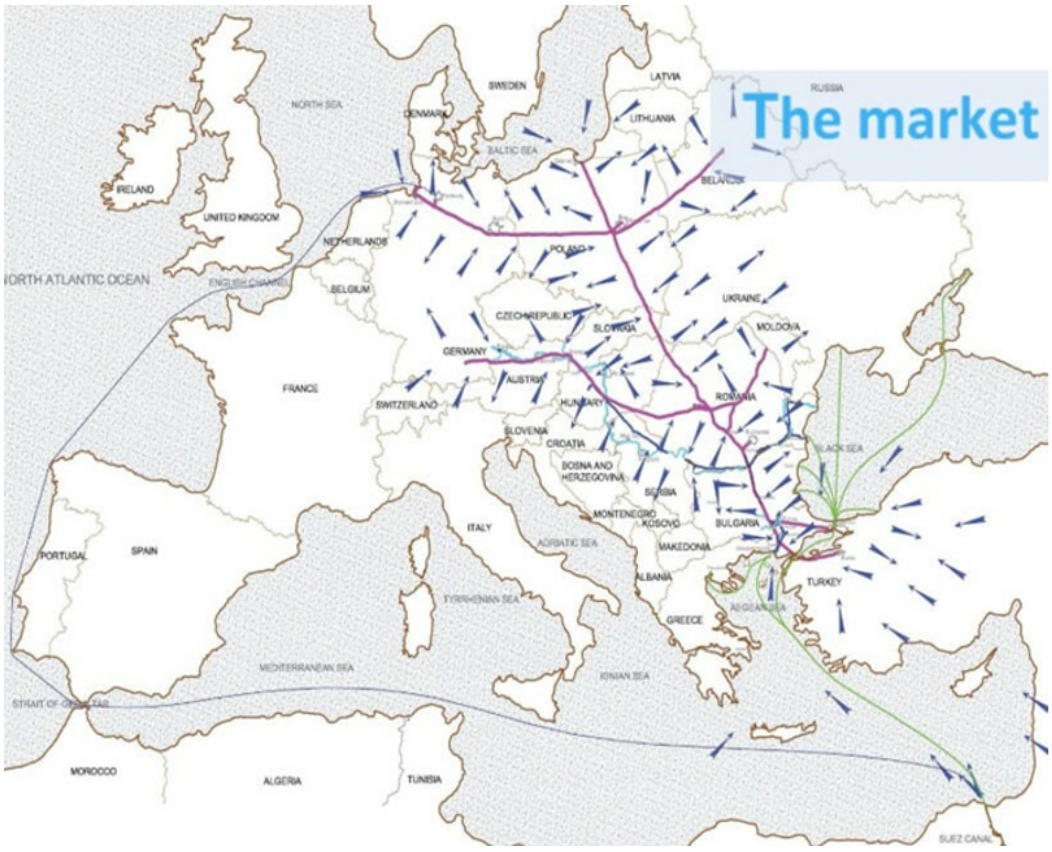

Fig. 13.
South North Stream Railway line (SNS) [22]

Similarly, the Three Seas Initiative (3SI)[3] is developing infrastructure for transport, along the North-South axis, by supporting cross-border and transnational projects. Corridors from Port of Varna to Port of Gdansk by train and by track have distance of about 2000 km and railway transport has advantage in terms of greenhouse gas and other emissions [21].

During the Three Seas Summit and Business Forum in Riga (Latvia, 2022) became clear that, The Three Seas Initiative Investment Fund (3SIIF) has acquired a significant share of the Port of Burgas that is the closest European Union port to the Bosporus Strait.

A quiet new idea for South North Stream Railway line (SNS) (Figure 13) is proposed by Large Infrastructure Projects [22]. The ABS+De project (ABC+De stands for Aegean to Baltic Sea Connection & Danube) foresees a high velocity railway line with a huge capacity to carry out transportation tasks between the new ultra large port of Maroneia on the Aegean Sea and port Wisla at the Baltic Sea. The railway track is in six project countries - Greece, Bulgaria, Romania, Hungary, Slovakia, and Poland, all of which are part of the European Union. Some of main parameters are as follows: Total length is 1,626.22 km, Track gauge 1435 mm - Standard European Railway, Number of tracks: 2 or 3 at some stretches, Distance between stations: 16 300 m - 29 200 m, Total locomotive power per freight train: 21 600 kW, Commercial speed for freight trains - 200 km/h; Commercial speed for high-speed trains - 400 km/h; Train length max. 1800 m, Train weight - max. 8500 t

CONCLUSIONS

Majority of counties in Europe increased the volume of transported cargoes by the Short Sea Shipping in the period 2010- 2109. In Croatia, Cyprus, Malta, Sweden, and Turkey there is a growth in SSS freight for 2020 compared to 2019 as well. The percentage of SSS from the total sea transport for Bulgaria is high (above 80%) due to the distance from the main sea motorways and the limited water depth in the ports.

Lliquid cargo remains the most transported commodity in the Black Sea, but for the last 10 years the volumes have been continuously decreasing, although not to a significant extent.

As could be expected, the war in Ukraine had a negative impact on maritime transport not only in the region but also in the world. With the beginning of the war, the freight rates increased worldwide, and for the Black Sea region, port calls in Russia decreased compared with the previous year and in Ukraine they were practically zero. A certain increase in port calls is observed for Romania and especially for Bulgaria because of redistribution of cargo flows. With joint efforts, a solution was found to the problem of grain export from Ukraine.

In the months after the abatement of Covid -19, container transport has an increasingly large share in maritime transport. The peak for freight rates was 12 months ago due to a shortage of empty containers and ship capacity. The situation is now normalizing, but ship owners are starting to plan to buy new containers and building ships.

The transport corridors between Asia and Europe continue their development, with increased countries joining their efforts in this direction. The strategic plan for the year 2030 of the Central Asia Regional Economic Cooperation (CAREC) Program is indicative. Trans-Caspian International Transport Route, which reaches the Georgian ports of Poti and Batumi, remains of interest to Bulgaria. The sea transport of goods through the Black Sea to the ports of Bulgaria is important link in the multimodal chain.

An important result of the war in Ukraine is the extension of the European Transport Corridors to the territory of Ukraine and Moldova - including the ports of Mariupol and Odesa, which requires a switch to standard 1.435mm gauge track in these countries.

Continues the work on new multimodal corridors through the territory of Bulgaria. An agreement has been reached for a corridor connecting the ports of Greece and Bulgaria and new project for South North Stream Railway line connecting the newly constructed port of the Aegean and Baltic seas is under way.

ACKNOWLEDGMENTS

This work was performed within the Research Plan of the Technical University of Varna, funded by the State Budget under the contract NP13 for 2022.

[3] https://3seas.eu/

REFERENCES:

[1] R o d r i g u e, J-P. (2020) The Geography of Transport Systems, New York: Routledge, Fifth Edition, ISBN 978-0-367-36463-2, Retrieved from: https://transportgeography.org/contents/chapter5/maritime-transportation/short-sea-shipping-europe/
[2] V a n den Bos, G., Wiegmans, B. Short Sea shipping: a statistical analysis of influencing factors on SSS in European countries. *Journal of Shipping and Trade*. 3, 6 (2018). https://doi.org/10.1186/s41072-018-0032-3.
[3] E u r o s t a t. Maritime transport statistics - short sea shipping of goods. Data from January 2022.
[4] UNCTAD. The war in Ukraine is in two of the Black Sea countries, but its impact is global. 22 June 2022. Retrieved from: https://unctad.org/news/war-ukraine-raises-global-shipping-costs-stifles-trade.
[5]UNCTAD (2022). Maritime Trade Disrupted: The war in Ukraine and its effects on maritime trade logistics, UNCTAD/OSG/INF/ 2022/2), 28 Jun 2022. Retrieved from: https://unctad.org/ukraine-in-focus/maritime-trade-disrupted.
[6] https://theloadstar.com/congested-port-of-constanta-passes-ukraine-freight-gauntlet-to-varna/.
[7] B o s a c k, M. McA. (2022). Understanding the Black Sea Grain Initiative, Parley Policy Cable No. 14 (July 28, 2022), Retrieved from: https://www.parleypolicy.com/post/understanding-the-black-sea-grain-initiative.
[8] https://twitter.com/trtworld/status/1554732206769201152/photo/1.
[9] https://www.timesofisrael.com/first-ship-carrying-grain-out-of-ukraine-spotted-docking-in-syrian-port/.
[10] https://www.statista.com/statistics/253988/estimated-containerized-cargo-flows-on-major-container-trade-routes/.
[11] https://www.statista.com/statistics/1250636/global-container-freight-index/.
[12] ADB. (Asian Development Bank). (2020). CAREC Transport Strategy 2030. ISBN 978-92-9262-000-4 (electronic), http://dx.doi.org/ 10.22617/SPR200024-2.
[13] A b d i k e r i m o v, G. Transit and Transport cooperation between Kazakhstan and European Union: Prospects for the development of Middle Corridor. Round Table, Brussels, On 15th June 2022.
[14] https://traveltomorrow.com/the-middle-corridor-might-be-the-answer-to-reconnect-asia-and-europe/.
[15] ADB (2021). Ports and logistics scoping study in CAREC countries. ISBN 978-92-9262-757-7 (electronic) http://dx.doi.org/10.22617/ SPR210103-2.
[16] https://www.dailysabah.com/business/transportation/turkiye-hikes-strait-transit-fees-to-4-per-tonnage.
[17] EC. COM (2022) 384 final, ANNEX 2 - PART 8/8, ANNEX to the amended proposal for a REGULATION OF THE EUROPEAN PARLIAMENT AND OF THE COUNCIL on Union guidelines for the development of the trans-European transport network, amending Regulation (EU) 2021/1153 and Regulation (EU) No 913/2010 and repealing Regulation (EU) 1315/2013, Brussels, 27.7.2022.
[18] https://mediarail.wordpress.com/ukraine-wants-to-connect-to-europe-in-1-435mm/.
[19] https://www.mtc.government.bg/en/category/1/bulgaria-and-greece-continue-project-thessaloniki-kavala-alexandroupolis-burgas-varna-ruse-railway-corridor.
[20] https://www.railfreight.com/railfreight/2022/04/13/greece-bulgaria-share-plans-for-new-rail-line-and-hub/?gdpr=accept.
[21] G e o r g i e v, P., G a r b a t o v, Y. Multipurpose vessel fleet for short Black Sea shipping trough multimodal transport corridors. 2021. *Brodogradnja*, Vol.72, Number 4, 2021, pp 79-101, http://dx.doi.org/10.21278/brod72405.
[22] https://www.largeinfraprojects.eu/

SHIPYARD CONSTRUCTION, REPAIR AND RECYCLING EMISSIONS IMPACT ON ENVIRONMENTAL POLLUTION

Petar GEORGIEV*, Angel ANGELOV*, Yordan GARBATOV**

Abstract. *The study analyses the shipyard activity emissions and their impact on environmental pollution in keeping air pollution on an acceptable level for human life. Different shipyard manufacturing processes, including metal cutting, forming, welding, surface preparation, dry or wet abrasive blasting for removing the old paint and rust, repainting the hull, dismantling, and recycling the ships at the end of their service life, generate air pollutant emissions. The present study identifies the level of air pollution concentration generated from different shipyard activities and analyses how any individual activity is related to existing regulations for air pollution in the shipbuilding and repair industry. The study is conditional on the installed shipbuilding and repair technology implemented in one shipyard.*
Key words: *Emission, energy efficiency, manufacturing, ship, shipyard.*

INTRODUCTION

IMO's work on greenhouse gas (GHG) emissions began nearly 25 years ago. The International Conference of Parties to the MARPOL Convention adopted Resolution 8 on CO_2 emissions from ships [1]. According to the Resolution the Marine Environment Protection Committee (MEPC) was invited to consider what CO_2 reduction strategies might be feasible and to establish the amount and relative percentage of CO_2 emissions from ships as part of the global inventory. Several specific technical and operational reduction measures have been introduced over the years. Specialists are very familiar with Energy Efficiency Design Index (EEDI - in effect since 2013)[1] in the design of ships, Energy Efficiency Operational Indicator (EEOI) and Energy Efficiency of Existing Ship Index (EEXI - to come into force on January 1, 2023)[1] and Carbon Intensity Indicator (CII)[1] concerning the operation of existing ships.

In the last 15 years, attention has started to be paid to the emissions from shipping and the building and repair of ships. Modern shipbuilding and ship repair yards are located adjacent to or within coastal cities, making an important issue not only for the impact on the climate but also on the health of citizens [2], [3]. There are few studies, and a quick review could highlight several more significant research whose number has increased in recent years (Table 1).

[1] https://marine-offshore.bureauveritas.com/needs/carbon-indexes

*** Technical University of Varna,**
**** Centre for Marine Technology and Ocean Engineering (CENTEC),**
Instituto Superior Técnico, Universidade de Lisboa, Lisbon, Portugal

References for research of emissions from shipbuilding and ship repair activities

Table 1

Ref.	Year of Publication	Type of Pollution/ Research
[4]	2007	Volatile organic compounds (VOC)[2]
[5]	2013	Volatile organic compounds (VOC)
[6]	2015	Oxygen levels during welding
[7]	2017	Shipbuilding energy consumption for tanker construction
[8]	2017	GHG emissions from shipbuilding processes
[9]	2018	Particulate matter causes disturbances in shipyard welders
[10]	2019	Development of green welding technology
[11]	2019	Shipyard welding emission for different electrode
[12]	2020	CO2 emission in the shipbreaking industries
[13]	2020	Diesel engine exhaust for shipyard transporter signal workers
[14]	2020	Carbon emission and noise - optimisation of ship plane block flow
[15]	2021	Blasting waste generation
[16]	2021	Multi-vehicle and one-cargo green transportation
[17]	2021	Metal fume $PM_{2.5}$
[18]	2021	Efficiency of dust and gas collecting units
[19]	2021	Sustainability manufacturing by friction stir welding (FSW)
[20]	2022	Particle release from refit operations
[21]	2022	Energy-related clean and green framework for shipbuilding
[22]	2022	Long-term metal fume exposure

The analysis of the listed sources sets the current state for the existing requirements and norms, as well as for the quantities of emissions and corresponding risks related to the various activities in the shipyard - the new building or repair of ships, which is presented below. The modern view of ship-related research requires consideration of the entire life cycle of the ship. In this sense, the Life Cycle Analysis (LCA) is widely used to assess environmental impacts associated with all the life cycle stages. Harmful emissions accompany the life cycles of the ship, and their quantity depends on the length of the cycles, but their impact on the environment and man is different. Emissions during ship recycling, apart from air, most often represent metals that enter the soil.

The following sections present existing norms and characteristics of emissions from various shipyard activities. A numerical example of estimating the emitted CO_2 while constructing a 9,800 DWT multi-purpose ship is presented here.

AIR POLLUTION REGULATIONS IN SHIPBUILDING AND REPAIR INDUSTRY

International regulations

A review of marine policies concerning air pollution [23] highlighted a few conclusions: the number of global, national, and port-level policies is limited. Current policies are focused on relative improvements, not overall emissions caps; current policies are unlikely to achieve pollutant reduction goals sufficiently.

IMO with its five committees, works in several directions [23], [24].

• Oil spill prevention and recovery.

• Emissions control represents two separate but related policy objectives:

- Air pollution control technologies, e.g., exhaust scrubbers for sulphur, specialised low-emission engine technologies and cleaner fuels;

[2] https://www.epa.gov/indoor-air-quality-iaq/what-are-volatile-organic-compounds-vocs.

- Climate change energy efficiency technologies, e.g., addressing GHGs, and/or in support of energy efficiency design index policies.

• Ballast water treatment to prevent or reduce the risk of aquatic species invasions.

• Other environmental issues:

- Hull fouling treatment to reduce the risk of aquatic species invasions;
- Noise, e.g., on-board noise controls for health and safety and underwater noise management;
- Regional integration of environmental protection (i.e., Polar Code).

A chronological summary of the individual IMO measures to reduce greenhouse gases from shipping can be seen in [25]. The Ballast Water Convention is in force in addition to the treatment of ballast water. Several other IMO instruments are in force regarding the operation of ships. Regarding emissions from shipbuilding production, different norms of individual organisations apply.

Air pollutant standards

The US Environmental Protection Agency (EPA)[3] sets National Ambient Air Quality Standards (NAAQS) for six common air pollutants: Carbon Monoxide (CO); Sulphur Dioxide (SO_2); Nitrogen Dioxide (NO_2); Particulate Matter (PM); Ground-level Ozone (O_3); Lead (Pb).

CO is a colourless, odourless gas that could be harmful when inhaled in large amounts. CO is a product of burning. SO2 is the component of the larger group of sulphur oxides (SO_x). Other gas, such as SO_3, is found in the atmosphere at a much lower concentration than SO_2. The most significant sources of SO_2 emissions are fossil fuel combustion at power plants and other industrial facilities. Nitrogen Dioxide (NO_2) is one of the group oxides of nitrogen or nitrogen oxides (NO_x). NO_2 primarily gets in the air from the burning of fuel. Particle pollution includes PM_{10} - inhalable particles, with diameters generally 10 micrometres and smaller; and $PM_{2.5}$ - fine inhalable particles, with diameters generally 2.5 micrometres and smaller. PM in the atmosphere results from complex reactions of chemicals such as SO_2 and NO_x, pollutants emitted from power plants, industries, and transport. All fore mentioned air pollutants are a product of maritime transport too.

Ground-level or “bad” ozone is not emitted directly into the air. Still, it is created by chemical reactions between NOx and Volatile Organic Compounds (VOCs) in the presence of heat and sunlight. The significant sources of lead in the air are ore and metals processing and piston-engine aircraft operating on leaded aviation fuel. Other sources are waste incinerators, utilities, and lead-acid battery manufacturers. The highest air concentrations could be registered near lead smelters.

Table 2 shows National Ambient Air Quality Standards (NAAQS) levels. Units of measure for the levels are parts per million (ppm) by volume, parts per billion (ppb) by volume, and micrograms per cubic meter of air ($\mu g/m^3$). Primary standards provide public health protection (protecting the health of “sensitive” populations such as asthmatics, children, and the elderly). Secondary standards protect public welfare, including protection against decreased visibility and damage to animals, crops, vegetation, and buildings.

[3] https://www.epa.gov/

NAAQS levels of air pollutants [27]

Table 2

Pollutant		Primary/ Secondary	Averaging Time	Level	Form
Carbon Monoxide (CO)		primary	8 hours	9 ppm	Not to be exceeded more than once per year
			1 hour	35 ppm	
Sulphur Dioxide (SO_2)		primary	1 hour	75 ppb	99th percentile of 1-hour maximum daily concentrations averaged over 3 years
		secondary	3 hours	0.5 ppm	Not to be exceeded more than once per year
Nitrogen Dioxide (NO_2)		primary	1 hour	100 ppb	98th percentile of 1-hour maximum daily concentrations averaged over 3 years
		primary and secondary	1 year	53 ppb	Annual Mean
Particle Pollution (PM)	$PM_{2.5}$	primary	1 year	12.0 μg/m³	Annual mean averaged over 3 years
		secondary	1 year	15.0 μg/m³	Annual mean averaged over 3 years
		primary and secondary	24 hours	35 μg/m³	98th percentile averaged over 3 years
	PM_{10}	primary and secondary	24 hours	150 μg/m³	Not to be exceeded more than once per year on average over 3 years
Ozone (O_3)		primary and secondary	8 hours	0.070 ppm	Annual fourth-highest daily maximum 8-hour concentration averaged over 3 years
Lead (Pb)		primary and secondary	Rolling 3-month average	0.15 μg/m³	Not to be exceeded

To respond to the real and continued threat of air pollution to public health, the WHO issued in 2021 updated air quality guidelines [28]. Interim targets are incremental steps in reducing air pollution toward the air quality guideline levels in areas with high air pollution.

Table 3 presents the recommended Air Quality Guidelines (AQG) and interim targets. Interim targets are incremental steps in reducing air pollution toward the air quality guideline levels in areas with high air pollution.

Recommended AQG levels and interim targets of WHO [28]

Table 3

Pollutant	Averaging time	Interim target				AQG level
		1	2	3	4	
CO, μg/m³	24-hours*	7	-	-	-	4
SO_2, μg/m³	24-hours*	125	50	-	-	40
NO_2, μg/m³	Annual	40	30	20	-	10
	24-hours*	120	50	-	-	25
$PM_{2.5}$, μg/m³	Annual	35	25	15	10	5
	24-hours*	75	50	37.5	25	15
PM_{10}, μg/m³	Annual	70	50	30	20	15
	24-hours*	150	100	75	50	45
O_3, μg/m³	Peak season**	100	70	-	-	60
	8-hours*	160	120	-	-	100

* 99th percentile (i.e., 3-4 exceedance days per year); ** Average daily maximum 8-hour mean O_3 concentration in the six consecutive months with the highest six-month running-average O_3 concentration.

The VOC diffuse emissions should comply with European Directive 1999/13/EC [26]. For discharges of the VOCs assigned or need to carry the risk phrases R45, R46, R49, R60, R61[4], where the mass flow of the

sum of the compounds is more significant than, or equal to, 10 g/h, an emission limit value of 2 μg/Nm$^{3(5)}$ shall be complied with. For discharges of halogenated VOCs assigned the risk phrase R40, where the mass flow of the sum of the compounds causing the labelling R40 is more significant than, or equal to, 100 g/h, an emission limit value of 20 μg/Nm^3 shall be complied with.

Oxygen deficiency is a significant problem when inert gases such as argon and helium are used to shield welding arcs in aluminium structures. A specific analysis of the emissions presented in [6] shows that the various aluminium welding activities in the shipbuilding environment represent a small risk of oxygen deficiency relative to the regulatory limit. The limits according to US National Institute for Occupational Safety and Health (NIOSH) are presented in **Table 4**, and the limit value is 19.5%. According to [30] any atmosphere-supplying respirator is necessary for the concentration of oxygen less than 16%. Constant monitoring of oxygen deficiency is required, considering the intentional loss of argon containment during welding and the inadvertent loss due to leaks and other accidents.

Effects of Acute Exposure to an Oxygen-Deficient Atmosphere [29]

Table 4

Effect	Concentration, %
No symptoms	16 to 20.9
Increased heart and breathing rate, some loss of coordination, increased breathing volume, impaired attention and thinking	16
Abnormal fatigue upon exertion, emotional upset, faulty coordination, impaired judgment	14
Very poor judgment and coordination, impaired respiration that may cause permanent heart damage, nausea and vomiting	12
Nausea, vomiting, lethargic movements, perhaps unconsciousness, inability to perform vigorous movement or loss of all movement, unconsciousness followed by death	< 12
Convulsions, shortness of breath, cardiac standstill, spasmatic breathing, death in minutes	< 6
Unconsciousness after one or two breaths	< 4

Shipbuilding production is also related to shipyard transport, and the effect of diesel engine exhaust emissions on workers is also a research subject. Although not carrying a significant risk [13] the diesel engine exhaust emissions and other ones could cause problems. Some of the limits from the list of indicative occupational exposure limit values (IOELVs) [31] from Commission Directive 2017/164/EU are shown in Table 5.

Indicative occupational exposure limit values for selected engine exhaust pollutants [31]

Table 5

Substance	8 h TWA[6] μg/m^3	STEL[7] μg/m^3
CO	23	117
NO	2.5	-
NO_2	0.96	1.91
SO_2	1.3	2.7

The exposure limit value for diesel engine exhaust emissions has been set at 0.05 μg/m^3, measured as elemental carbon (EC).

[4] Risk phrases: R40 -Limited evidence of a carcinogenic effect; R45-May cause cancer; R46-May cause inheritable genetic damage; R49-May cause cancer by inhalation; R60-May impair fertility; R61-May cause harm to the unborn child

[5] Hence the term N means 'normal' for condition of the volume i.e., a temperature of 25 degree centigrade, and 1 atm pressure.

[6] eight hours' time-weighted average (TWA).

[7] Short-term exposure limit (STEL). A limit value above which exposure should not occur and which is related to a 15-minute period unless otherwise specified.

SHIPBUILDING AND REPAIR ACTIVITIES AND RESULTING POLLUTION

Shipyards are usually located in environmentally sensitive areas and build only 20-30% of each vessel, as the rest is subcontracted [32]. Activities usually take place outdoors or on purpose-built premises. Typical activities in the shipbuilding process are presented in Figure 1.

Key environmental, health and safety risk issues

The main and other potential environmental, health and safety risk issues according to [32] are summarised in Table 6.

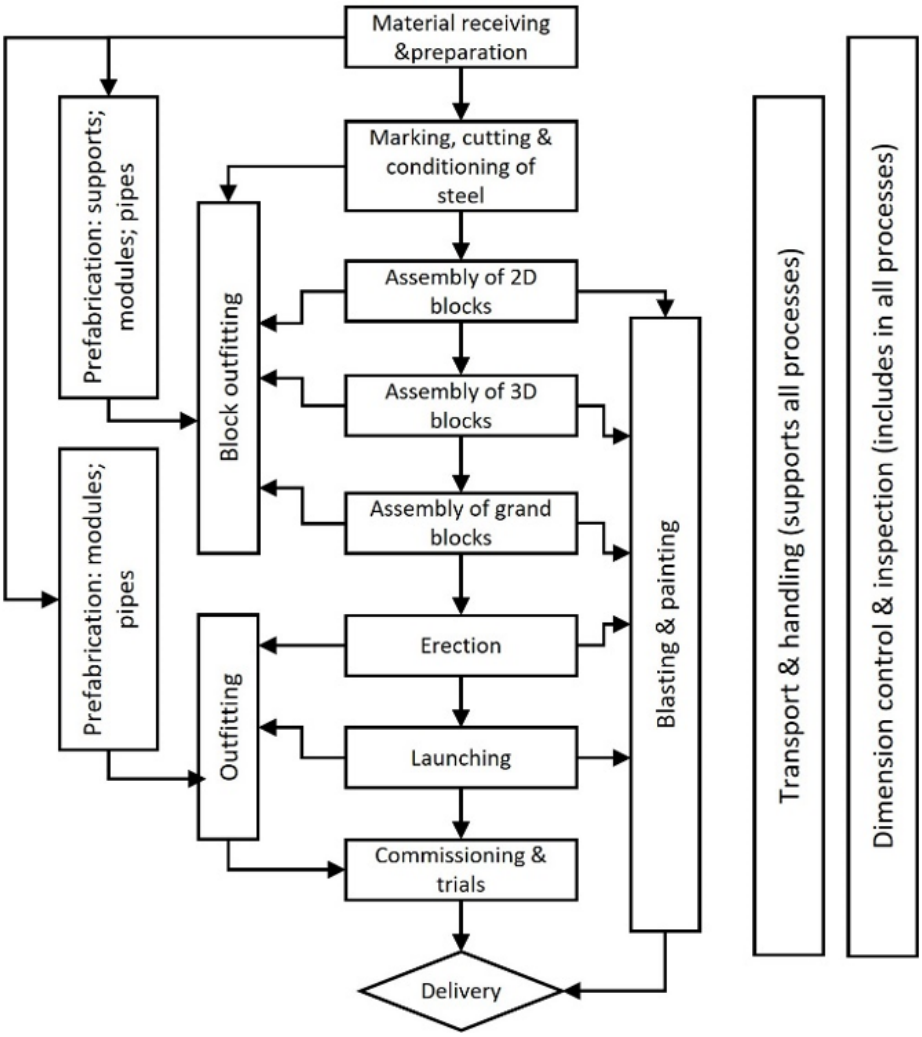

Fig. 1.
Scheme of typical shipbuilding process (adopted from [32])

Environmental, health and risk issues and corresponding sources

Table 6

Issue	Sources
MAIN ENVIRONMENTAL AND HEALTH AND SAFETY RISKS/LIABILITY ISSUES	
Water pollution	Oil spills during fitting operations. Running water picked up oil and debris that had accumulated on the dock. Seawater contacts of the hull painted with "anti-fouling" paints.
Wastewater	Discharge (acid/alkali) from galvanising and other metal preparation baths to the water. Water used in cleaning processes;
Air emissions	Blasting grit used in shipyards (typically is a slag). Paint stripping[8]
Solid waste	Spent grit from blasting. Sludge from wastewater treatment.
Hazardous materials	Solvents used to formulate bottom paints and coatings for corrosion resistance. Volatile organic compounds (VOCs) included in the solvents.
Liquid wastes	Wash water, oily water from bilges and tank cleaning. Engine fluids such as oil, hydraulic fluids, lubricants, and anti-freeze. Hydrocarbons, glycols, and other pollutants from fuelling facilities.
Noise	Pneumatic hammers. Gouging tools. Chipping machines.
Falls from height	Frequent work above ground on a scaffolding
Falling objects	Falling objects from different levels in height. Failure of fixtures and conveyance gantries. Hit by moving objects.
Confined spaces	Formation of vapours in closed spaces.
Slips, trips, and falls	Uneven surfaces, unsteady walkways, and wet decks.
OTHER POTENTIAL ENVIRONMENTAL AND HEALTH, AND SAFETY RISKS/LIABILITY ISSUES	
Ground Contamination	Poor management of materials, waste, and discharges. Heavy metals and accidental discharges from spills and storage tanks. Leakages. Deteriorated drainage networks.
Radiation	Radioactive substances associated with submarine facilities.
Polychlorinated Biphenyls (PCBs) and Asbestos	PCBs used as electrical insulators, as constituents of hydraulic oils or dielectric fluids PCBs from electrical switchgear, transformers, and fluorescent light starters. Asbestos used as fireproofing and insulation.
Machinery	Metal cutting equipment. Other machines that require appropriate personal protective equipment.
Inhalation	Used solvents. Dust during shot blasting. Machining and welding activities
Occupational Dermatitis	Contact with antioxidants, chromates, and solvents.

Volatile organic compounds (VOC) emissions

VOCs from painting solvents are one of the essential sources of pollutant outputs for the shipyard, with an adverse effect on human health. The VOC emissions for a 3,500 DWT tanker and general cargo carrier built in a Turkish shipyard are studied in [5]. There are different norms for the emissions depending on the part of the painting region. The most significant VOC emissions are released for the side shell between the flat bottom and the waterline level and for freeboard regions. Both ships' total amounts are 420.78 and 493.44 g/m^3,

[8] Stripping 280m^2 of hull surface area, for example, may require an estimated 60 tonnes of grit [32].

respectively. This same study shows that the painting process of a 3,500 DWT vessel causes around 5.5 tonnes of VOC emissions or 1.57 kg/DWT.

The amount of VOC emissions in ship construction and repair in the French shipyard *Chantiers de l'Atlantique* is analysed in [4]. The VOC emissions are evaluated based on the volume of docks for construction and different zones for repair. The emissions from repair are about ten times higher than ones for construction, reaching 278 $\mu g/m^3$ against 26.5 $\mu g/m^3$. Based on the available data on paints and VOC quantities used in shipyards, current toxicological knowledge, and exposure hypotheses, human chronic and acute health risks due to VOC emitted by dry docks are of no concern.

Air emissions during ship construction

Welding is an essential process in shipbuilding, and air emissions cause remarkable problems for workers' health and the environment. A recently provided study [11] analyses the emissions from three types of electrodes at two welding processes, i.e., shielded metal arc welding (SMAW) and flux cored arc welding (FCAW). Some of the main characteristics of the studied electrodes are presented in Table 7. The results for total suspending particulate (TSP)[9] at the construction of a chemical tanker and container ship are shown in Table 8. TSP fume emissions per DWT are 0.247 kg/DWT and 0.082 kg/DWT for chemical tankers and container ships.

Environmental, health and risk issues and corresponding electrodes [33]

Table 7

Electrode type	Main constituent	Shielding gas created
Rutile	Titania (TiO_2)	Mainly CO_2
Basic	Calcium compounds	Mainly CO_2
Cellulosic	Cellulose	Hydrogen + CO_2

Air emissions at different types of welding electrodes [11]

Table 8

Electrode type	Average fume formation rates, $g.min^{-1}$	Emission factor, $g.kg^{-1}$	TSP for 7100 DWT chemical tanker, kg	TSP for 26,200 DWT container ship, kg
Rutile	0.166	7.03	19.11	43.68
Basic	0.285	10.5	12.55	23.58
Cellulosic	0.617	26.0	0.83	6.06
FCAW	0.413	17.2	1,720	2,064
		TOTAL	1752.5	2137

In addition to analysis of specific emission levels, research into the effect of shipbuilding on the environment and man is carried out by assessing the required energy.

The bottom-up analysis of Korea's GHG emissions from shipbuilding processes is discussed in [8]. The results are based on the simplified Reference Energy System (RES), where five energy forms, i.e., electricity, LPG, LNG, bunker fuel, and diesel, are considered for six processes - cutting, plate forming, welding, crane operations, painting, and sea trial. The Tons Oil Equivalent (TOE) per unit Compensated Gross Tonnage (CGT) for the six processes is shown in Table 9 and Figure 2.

[9] TSP refers to the totality of small solid matter released in the atmosphere. TSP are a primary contributor to air pollution, smog formation and environmental contamination (https://www.corrosionpedia.com/).

Average energy intensity, TOE/CGT [8]

Table 9

Process	Average Energy intensity, TOE/CGT
Cutting	0.0045
Plate forming	0.0069
Welding	0.0034
Crane	0.0016
Painting	0.0059
Sea trial	0.0130
TOTAL	0.0353

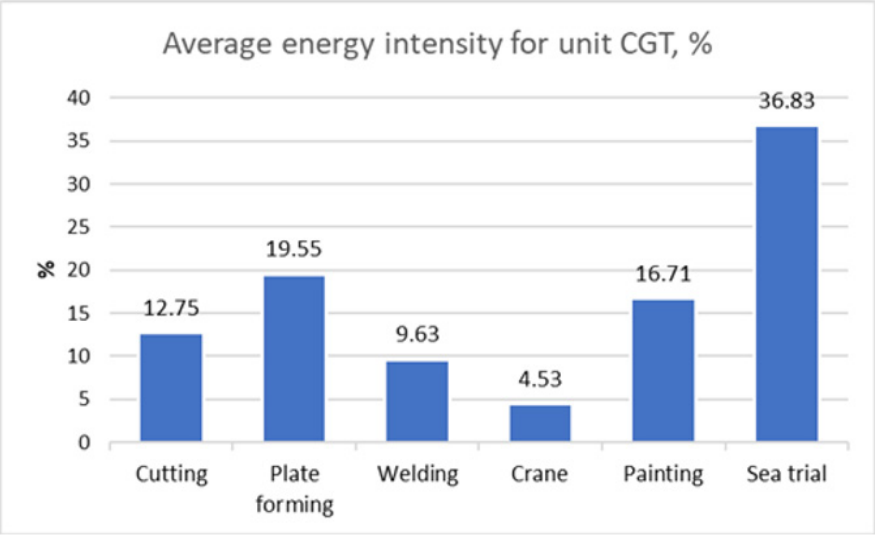

Fig. 2.
Average energy intensity, % for unit CGT [8]

The amount of GHG emissions from shipbuilding processes is relatively small (only 0.4 ~ 0.5% of national emissions), but individual shipbuilders should be aware of the economic and environmental impacts. A way to reduce GHG emissions is shown in [34]where the use of aluminium honeycomb sandwich for ship construction demonstrated less energy consumption and carbon footprint, compared to the whole steel solution, with 57% energy saving and 71% carbon footprint reduction compared to conventional steel ship structure.

The study presented in [35]analysed the energy consumed in the shipbuilding process in India. The used energy is grouped as follows:

• Direct Materials (energy contained in the materials of a ship and their transportation);

• Direct (energy consumed in the construction of the ships such as electricity consumed due to welding, cutting, use of cranes, transportation of blocks etc.); and

• Indirect or overhead (energy consumed in the shipyard which cannot be billed to a particular ship, such as electricity and fuel consumed in administration, design, planning, transportation of personnel etc.).

Energy consumed in construction for O_2 gas, CO_2 gas, LPG, Paint, electrodes, and electrical power for fabrication of 1-tonne net ship steel is estimated to be 2.73 GJ. The study also evaluated the energy for extracting one tonne of steel at dismantling ships, which is 1.17 GJ.

One tonne of oil equivalent (TOE) equals 41.868 Giga Joules (GJ). One GJ is equal to 277.778 kWh. The CGT is calculated according to [36]:

(1) $$CGT=A.GT^{B}$$

where:

GT is the Gross tonnage, A is a coefficient = 27 and 29, and B is a coefficient = 0.64 and 0.61 for general cargo ships and bulk carriers, respectively.

Based on information from Table 9 for the total amount of consumed energy in kWh, it is possible to estimate the CO_2 footprint by the Greenhouse Gas Equivalencies Calculator presented in [37].

The same approach to conversion of consumed energy of 1-tonne hull steel to CO_2 equivalent is used for the second approach. The CO_2 footprint for constructing a 9,790 DWT multi-purpose ship is shown in Table 10.

CO_2 footprint for construction of 9,790 DWT multi-purpose ship

Table 10

L = 113.75 m; B = 20.00 m; D = 10.40 m; DWT = 9,790 tonnes; GT = 7,775; CGT= 8,345; W_{st} = 2,370 tonnes.		
	Based on TOE/CGT	Based on GJ/tonne
Total consumed energy, kWh	3,191,943.3	2,070,251.7
CO_2 equivalent, tonnes	1,381	896

CONCLUSIONS

The current study reviewed state of art related to the shipyard activity gas emissions and their impact on environmental pollution. Different shipyard manufacturing processes were analyzed, and the level of generated pollution and existing norms and characteristics were presented. An example of the CO_2 footprint for building a 9,790 DWT multi-purpose ship, conditional on the installed shipbuilding and repair technology implemented in one shipyard, is also presented. The next step of this study is to analyze the process of new shipbuilding and repair and generated gas emissions in shipyard conditions and associated costs and carbon footprint. It will also rank the impact of different shipyard processes and suggest measures to mitigate their effect.

ACKNOWLEDGMENTS

This work was performed within the Research Plan of the Technical University of Varna, funded by the State Budget under the contract NP13 for 2022.

REFERENCES:

[1] MP/CONF. 3/34, (1997) CONSIDERATION AND ADOPTION OF THE PROTOCOL OF 1997 TO AMEND THE INTERNATIONAL CONVENTION FOR THE PREVENTION OF POLLUTION FROM SHIPS, 1973, AS MODIFIED BY THE PROTOCOL OF 1978 RELATING THERETO.

[2] G a r b a t o v, Y.; Georgiev, P. (2022). Stochastic Air Quality Dispersion Model for Defining Queuing Ships Seaport Location. Journal of Marine Science and Engineering 2022, 10, 140, doi:10.3390/jmse10020140.

[3] G a r b a t o v, Y.; Georgiev, P. (2022). Short Sea shipping greenhouse gas emissions and dispersion. In Trends in Maritime Technology and Engineering, Guedes Soares, C., Santos, T., Eds.; Taylor and Frances: UK, London, 2022; Volume 2, pp. 35-43.

[4] M a l h e r b e, L., & Mandin, C. (2007). VOC emissions during outdoor ship painting and health-risk assessment. Atmospheric Environment, 41(30), 6322-6330. https://doi.org/10.1016/J.ATMOSENV.2007.02.018.

[5] C e l e b i, U. B., & Vardar, N. (2008). Investigation of VOC emissions from indoor and outdoor painting processes in shipyards. Atmospheric Environment, 42(22), 5685-5695. https://doi.org/10.1016/J.ATMOSENV.2008.03.003

[6] M c M a n u s, N., & Haddad, A. N. (2015). Oxygen Levels During Welding: Assessment in an Aluminum Shipbuilding Environment. Professional Safety, 60(07), 26-32.

[7] N i a n, V., & Yuan, J. (2017). A method for analysis of maritime transportation systems in the life cycle approach - The oil tanker example. Applied Energy, 206, 1579-1589. https://doi.org/10.1016/J.APENERGY.2017.09.105

[8] C h u n g, Y., Paik, C., Kim, H., & Kim, Y. J. (2017). Bottom-up Analysis of GHG Emissions from Shipbuilding Processes for Low-carbon Ship Production in Korea. Journal of Ship Production and Design, 33(03), 221-226. https://doi.org/10.5957/JSPD.33.3.160013.

[9] C h u a n g, H. C., Su, T. Y., Chuang, K. J., Hsiao, T. C., Lin, H. L., Hsu, Y. T., Pan, C. H., Lee, K. Y., Ho,

S. C., & Lai, C. H. (2018). Pulmonary exposure to metal fume particulate matter cause sleep disturbances in shipyard welders. Environmental Pollution, 232, 523–532. https://doi.org/10.1016/J.ENVPOL.2017.09.082.
[10] X u e, S., Wang, B., Zhang, L., & Long, W. (2019). Development of Green Welding Technology in China During the Past Decade. Cailiao Daobao/Materials Reports, 33(9), 2813-2830. https://doi.org/10.11896/cldb.19050104.
[11] M e r t, T., Celebi, U. B., Bilgili, L., & Ekinci, S. (2019). Shipyard welding emission estimation for different electrode and ship types. Fresenius Environmental Bulletin, 28(2), 891-894.
[12] M i t r a, N., Ahmad Shahriar, S., Lovely, N., Khan, S., Rak, A. E., Kar, S. P., Khaleque, A., Mohd Amin, M. F., Kayes, I., & Abdus Salam, M. (2020). Assessing energy-based co<inf>2</inf> emission and workers' health risks at the shipbreaking industries in Bangladesh. Environments - MDPI, 7(5). https://doi.org/10.3390/environments7050035.
[13] S h i n, J., Kim, B., & Kim, H.-R. (2020). Characteristics of Occupational Exposure to Diesel Engine Exhaust for Shipyard Transporter Signal Workers. International Journal of Environmental Research and Public Health, 17(12), 4398. https://doi.org/10.3390/ijerph17124398.
[14] G u o, H., Li, J., Yang, B., Mao, X., & Zhou, Q. (2020). Green scheduling optimisation of ship plane block flow line considering carbon emission and noise. Computers & Industrial Engineering, 148, 106680. https://doi.org/10.1016/J.CIE.2020.106680.
[15] Q i, C., Weinell, C. E., Dam-Johansen, K., & Wu, H. (2021). A review of blasting waste generation and management in the ship repair industry. Journal of Environmental Management, 300, 113714. https://doi.org/10.1016/J.JENVMAN.2021.113714.
[16] J i a n g, Z., Chen, Y., Li, X., & Li, B. (2021). A heuristic optimisation approach for multi-vehicle and one-cargo green transportation scheduling in shipbuilding. Advanced Engineering Informatics, 49, 101306. https://doi.org/10.1016/J.AEI.2021.101306.
[17] L a i, C. H., Ho, S. C., Pan, C. H., Chen, W. L., Wang, C. C., Liang, C. W., Chien, C. Y., Riediker, M., Chuang, K. J., & Chuang, H. C. (2021). Chronic exposure to metal fume PM2.5 on inflammation and stress hormone cortisol in shipyard workers: A repeat measurement study. Ecotoxicology and Environmental Safety, 215, 112144. https://doi.org/10.1016/J.ECOENV.2021.112144
[18] M a k a r o v a, V., & Tkalich, V. (2021). Evaluation of the Efficiency of Dust and Gas Collecting Units of Woodworking Shops in Shipbuilding Industry. IOP Conference Series: Earth and Environmental Science, 666(4). https://doi.org/10.1088/1755-1315/666/4/042049.
[19] M a j e e d, T., Wahid, M. A., Alam, M. N., Mehta, Y., & Siddiquee, A. N. (2021). Friction stir welding: A sustainable manufacturing process. Materials Today: Proceedings, 46, 6558–6563. https://doi.org/10.1016/J.MATPR.2021.04.025.
[20] L ó p e z, M., López Lilao, A., Ribalta, C., Martínez, Y., Piña, N., Ballesteros, A., Fito, C., Koehler, K., Newton, A., Monfort, E., & Viana, M. (2022). Particle release from refit operations in shipyards: Exposure, toxicity, and environmental implications. Science of The Total Environment, 804, 150216. https://doi.org/10.1016/J.SCITOTENV.2021.150216.
[21] V a k i l i, S., Ölçer, A. I., Schönborn, A., Ballini, F., & Hoang, A. T. (2022). Energy-related clean and green framework for shipbuilding community towards zero-emissions: A strategic analysis from concept to case study. International Journal of Energy Research. https://doi.org/10.1002/er.7649.
[22] W a n g, Y.-F., Kuo, Y.-C., & Wang, L.-C. (2022). Long-term metal fume exposure assessment of workers in a shipbuilding factory. Scientific Reports, 12(1). https://doi.org/10.1038/s41598-021-04761-z.
[23] G ö s s l i n g, S., Meyer-Habighorst, Ch., Humpe, A. (2021) A global review of marine air pollution policies, their scope and effectiveness, Ocean & Coastal Management, Volume 212, 2021, 105824, ISSN 0964-5691, https://doi.org/10.1016/j.ocecoaman.2021.105824.
[24] C o r b e t t, J., Johnstone, N., Strodel, K., Daniel, L. (2016), Environmental Policy and Technological Innovation in Shipbuilding, OECD Science, Technology and Industry Policy Papers, No. 28, OECD Publishing, Paris. http://dx.doi.org/10.1787/5jm25wg57svj-en.
[25] https://sustainabledevelopment.un.org/content/documents/26620IMO_ACTION_TO_REDUCE_GHG_EMISSIONS_FROM_INTERNATIONAL_SHIPPING.pdf.
[26] EC, OJ (1999) Council Directive 1999/13/EC of March 11, 1999, on the limitation of emissions of volatile organic compounds due to the use of organic solvents in certain activities and installations, L 85/1.[27] https://www.epa.gov/criteria-air-pollutants/naaqs-table.

[28] WHO. (2021). WHO global air quality guidelines. Particulate matter (PM2.5 and PM10), ozone, nitrogen dioxide, sulphur dioxide and carbon monoxide. Geneva: World Health Organization; 2021. License: CC BY-NC-SA 3.0 IGO.
[29] NIOSH. (2005). NIOSH respirator selection logic (NIOSH Publication No. 05-100). Retrieved from www.cdc.gov/niosh/docs/2005-100/pdfs/05-100.pdf.
[30] OSHA. (1998). Respiratory protection (29 CFR 1910.134). Retrieved from www.osha.gov/pls/oshaweb/owadisp.show_document?p_table=STANDARDS&p _id=12716.
[31] https://echa.europa.eu/indicative-oelvs-dir-2017-164.
[32] EBRD. Shipbuilding and shipyards Sub-sectoral Environmental and Social Guidelines-438., European Bank for Reconstruction and Development. https://www.ebrd.com/downloads/policies/environmental/transport/shipbuilding.pdf (last visited August 1, 2022).
[33] https://www.twi-global.com/technical-knowledge/job-knowledge/comparison-of-the-use-of-rutile-and-cellulosic-electrodes-142#:~:text=Rutile%20electrodes%20have%20a%20medium,purpose%20electrodes%20(TWI%20website).
[34] P a l o m b a, G.; Scattareggia Marchese, S.; Crupi, V.; Garbatov, Y. (2022) Cost, energy efficiency and carbon footprint analysis of hybrid light-weight bulk carrier. Journal of Marine Science and Engineering 2022, 10, 957, doi:10.3390/jmse10070957.
[35] H a r i s h, Ch. R., Sunil, SK (2015). Energy Consumption and Conservation in Shipbuilding International Journal of Innovative Research & Development, July 2015, Vol 4 Issue 7 (Special Issue), pp. 26-31.
[36] OECD, (2007), Compensated gross ton (CGT) system. Retrieved from: https://www.oecd.org/industry/ind/37655301.pdf.
[37] https://www.epa.gov/energy/greenhouse-gas-equivalencies-calculator#results.

LIQUEFIED NATURAL GAS, AN ALTERNATIVE FOR RETROFITTING AGEING SHIPS

Dimitar YALAMOV*, Petar GEORGIEV*, Yordan GARBATOV**

Abstract.*Considering the long-term economic and energy scenarios, greenhouse gas emissions, carbon dioxide, methane, and nitrous oxide, are expected to increase concerning the emissions from around 90% in 2018 to 90-130% in 2050. Different mitigation solutions are employed, including liquefied natural gas (LNG) as an alternative fuel. The present work reviews the current state of the art of using LNG as an alternative to fossil fuels derived from crude oil (e.g., diesel) for retrofitting ageing ships. Reducing greenhouse gas emissions, especially for short sea shipping, is associated with several challenges related to employing an innovative ship propulsion system and developing a port supply infrastructure. Recently very intensive transportation activities have been observed in the region of the Black Sea, where the correlation between carbon emissions and transported cargo increased. Alternative solutions to mitigate the region's carbonisation are analysed and discussed here.*

Key words: *alternative fuels, existing ships, GHG emissions, LNG, retrofit.*

INTRODUCTION

With the growing concern over pollution and global warming around the world shipping industry has to adapt and be part of the solution for reducing the Carbon dioxide (CO_2)and Nitrogen oxide (NO_x) emissions.

Global CO_2 emissions in the 2020-2021 Coronavirus pandemic have declined by 7%, from 40,1 billion metric tonnes to 37 billion metric tonnes, the most significant decline since the first industrial revolution. Even before the pandemic, global emissions fell by about 15-20% due to moving utilities away from coal and using cleaner natural gas, wind and solar power and the retirement of coal power plants. During the pandemic, for example, the related economy in the USA's slowdown caused a reduction in green gas emissions of more than 10%. Most of the reductions were in the transport sector, which relies heavily on fossil fuels [1].

Alternative marine fuels are considered a perspective approach for reducing ship-related airborne pollutants. Alternative fuels are determined biogas, dimethyl ether, ethanol, liquefied natural gas (LNG), liquefied petroleum gas (LPG), methanol, ammonia, and biodiesel. A recent study in [2] compared alternative marine fuels from a life cycle perspective. The investigations focus on the effects on human health, the ecosystem, resource utilisation, emission inventory, and social costs. As a result, biogas was the best fuel in the short, medium, and long term; the methanol, ammonia, and biodiesel group performed worst. While biogas causes 0.9 tonnes of CO_2 production, methanol, ammonia, and biodiesels produce 1.5, 4.8, and 1.6 (average) CO_2, respectively. The study proved that although LNG is more dominant than other alternative fuels, within the framework of the LCA approach (environmental effects and availability), biogas is in a brighter position in the future, and it is recommended to focus more on biogas technologies.

While LNG is today the most available alternative, numerous analyses and studies have been done on the effect of its use. Results showed [3] that particulate matter (PM), black carbon (BC), nitric oxides (NO_x), and carbon dioxide (CO_2) were reduced by about 93%, 97%, 92%, and 18%, respectively, when switching from diesel to NG. SEA-LNG[1] is a multi-sector industry coalition established to demonstrate LNG's benefits as a viable marine fuel. A report [4] presents today's 23% cut in CO_2-eq/kWh engine power for LNG fuel over oil-based marine fuels for 2-stroke SS engine and 14% for 4-stroke MS engine (Figure 1).

[1] https://sea-lng.org/

***Technical University of Varna, Varna, Bulgaria,**
**** Centre for Marine Technology and Ocean Engineering (CENTEC), Instituto Superior Técnico, Universidade de Lisboa, Lisbon, Portugal**

Natural gas is a mixture of gases consisting mainly of methane, ethane, and propane. Methane's chemical composition is CH_4, with one carbon molecule attached to four hydrogen molecules. Burning it releases carbon dioxide and water vapour. Other components like butane, pentane and nitrogen may be found in various portions depending on the source of origin. Natural gas is liquefied (LNG) to facilitate its storage and transport. This process reduces the volume of the gas by about 600 times. Depending on the gas composition, the liquification process under atmospheric pressure occurs at temperatures of about -162°C (111K). Due to the shallow temperatures, this process is defined as cryogenic and cryo-liquid. The composition of LNG may vary significantly, influencing the kind of gas storage and combustion properties. Table 1 shows the properties of LNG.

While natural gas is used as fuel alternatively to conventional liquid fuel reducing CO_2 emission by up to 23-25%, NO_x up to 90% and the gas is practically free of any sulphur compounds. Therefore, engines fuelled with gas do not require additional pre or after-processing to fulfil IMO sulphur requirements. There are also no particulate matter (PM) emissions.

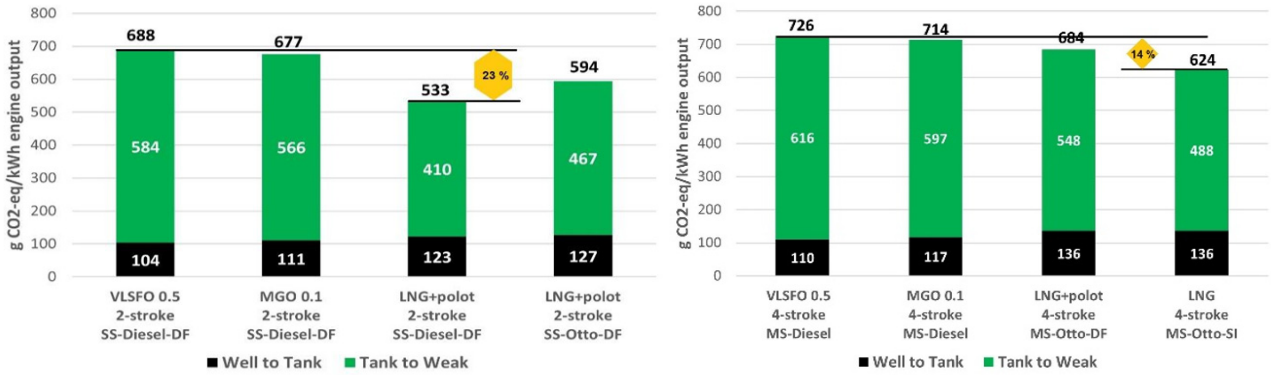

Fig. 1.
Relative CO_2 emissions for different fuels for 2-stroke SS (left) and 4-stroke MS engine (right) (adapted from [4])

Properties of LNG

Table 1

Physical parameter	Value
Density [kg/m^3]	410 - 500
Specific calorific value [MJ/kg]	42–58
Toxicity	Nontoxic
Typical storage pressure	Close to atmospheric
Typical storage temperature [°C]	-162

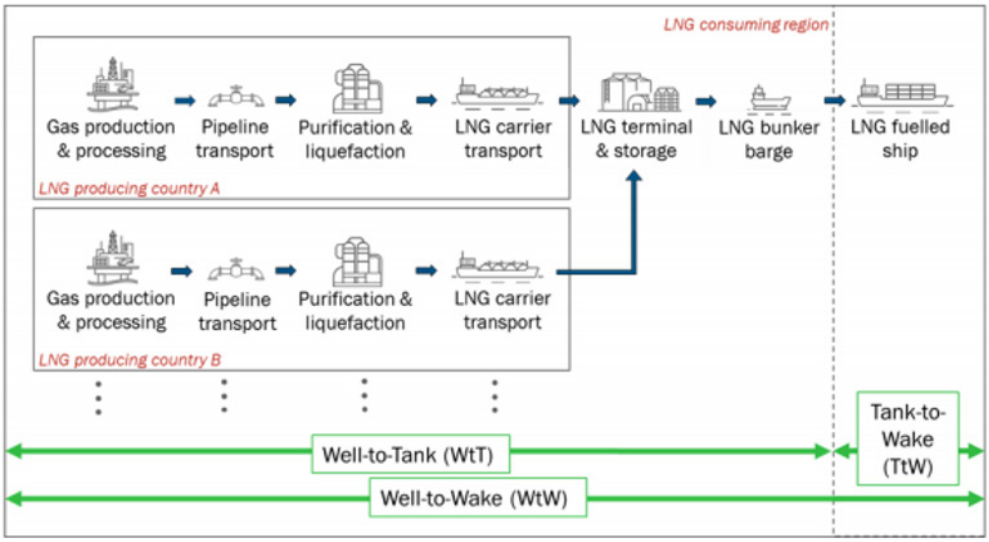

Fig. 2.
Well-to-Wake analysis - LNG supply and combustion [5]

The environmental performance of LNG as a marine fuel is analysed using a lifecycle approach known as "well-to-wake" (WtW) for ships (Figure 2). A range of parameters is used to describe the entire lifecycle of a particular fuel type and is usually expressed as CO_2 equivalent emission per unit of supplied energy (CO_2eq/MJ). Ship operators and engine manufacturers often refer to the Tank-to-Wake (TtW) emissions that occur during fuel combustion within the marine engine, including engine efficiency only. However, (TtW) approach does not present the whole environmental impact of the specific fuel and, in some cases, may give a false impression that one fuel is or is not more harmful than others.

The objective of the present work is to review the current state of the art in using LNG as an alternative to fossil fuels for ageing ships in the Black Sea region and the level of introducing an innovative ship propulsion system and developing a port supply infrastructure for a sooner transition to the standards for the emission control areas (ECAs), or sulphur emission control areas (SECAs). In this respect, several studies evaluating the short sea shipping in the Black Sea [6-8] and the air pollution generated by ships [9-10] demonstrated the need for adapting and retrofitting ships' circulating in this region to satisfy the current standard for the air pollution generated by ships.

CHALLENGES IN SHORT SEA SHIPPING IN THE BLACK SEA

Maritime transport in the Black Sea is an essential backbone for trade. Both the number and size of ships have increased in recent years and currently account for up to 4% of global cargo traffic. Shipping is a very effective means of transportation, measured in terms of emissions per tonne of cargo. However, shipping can still negatively impact the environment, such as emissions into the air and sea. Shipping in the Black Sea is expected to grow in the coming years.

On the other hand, the Black Sea ecosystem is under pressure due to its semi-enclosed waters, pollution from the lack of strict control, and countries following different rules for environmental protection.

Given the importance of maritime transport for the Black Sea region and the need to protect the marine environment, the Black Sea countries should act together to minimise pollution from ships while preserving the positive effects of maritime transport.

Many new technologies and measures are currently being developed in the shipping sector to reduce the negative environmental impacts of maritime transport. This industry has great opportunities and significant growth potential in achieving both environmentally friendly and clean shipping and a robust maritime economy in the Black Sea region.

The impact of the pandemic in 2020/2021 has proven positive and effective for the environment and climate goals: about a 10% reduction. The transport sector, shipping, made the most significant contribution. Action by the World's largest emitting countries is not enough. As a result, a fundamental transformation to

a green policy is urgently needed. The pandemic and eventual recovery provide a golden opportunity for this transformation.

Figure 3 presents the average size (GT) of ships engaged in Short Sea Shipping calling the main EU ports, i.e., ports handling more than one million tonnes of goods, or 200 000 passengers annually based on inward declarations. These data briefly represent the profile of the ships, which is related to a possible retrofit. The maximum average GT is around 7,500, and the ships have a minimum tonnage of over 5,000. They are all included in the EMSA MRV (Monitoring, Reporting and Verification) system.

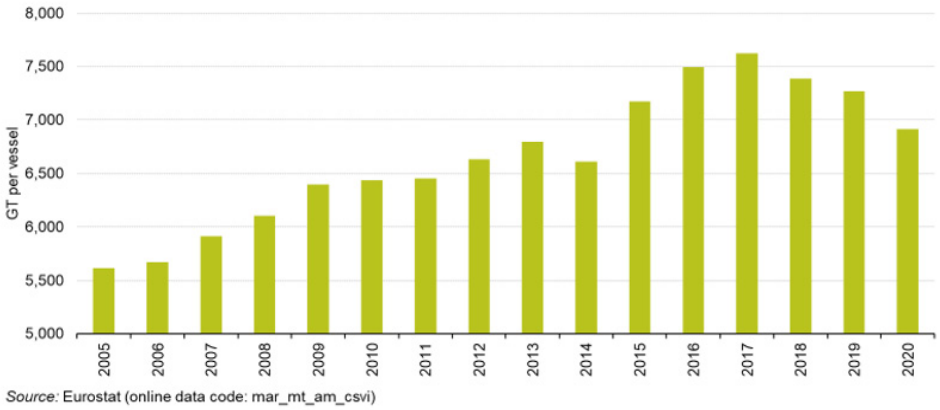

Fig. 3.
Average size of vessels calling at main ports, EU, 2005-2020[2].

The analysis of more than 200 dry cargo ships (MPVs and mini-bulk carriers) in the range of 2,100 to 9,300 DWT vessels used for SSS in the Mediterranean and Black Sea region found a very good relationship between the GT e and the DWT of the ships [9].

(1) $$GT = 0.6044 * DWT^{1.0164}$$

From this relation, it can be estimated that for ships with DWT greater than 7150, the GT is more significant than 5000 tonnes, i.e., the MRV system is mandatory. This study highlighted that 12% of the SSS fleet is over 20 years old, and 485 of about 4,300 active units (11%) are considered sub-standard [11].

In addition, Türkiye increased the Bosphorus passage fee five times [15]. The new fee of 4 dollars per net tonnage will enter into force of regulation on 7 October 2022.

RETROFITTING OF AGEING SHIPS

There is a growing wish from the shipping industry to meet sustainability goals and emission reduction targets, as well as growing demand from ship owners. The new and adaptive regulations, such as the International Maritime Organization (IMO) Energy Efficiency Existing Ship Index (EEXI) and impending future emission regulations, can stimulate the deployment of current and future retrofitting options.

In January 2021, LNG-fuelled new building orders accelerated dramatically, approaching 30% of the gross tonnage ordered (Figure 4). Even for some segments, such as the ultra-large container vessels, more than 50% of the order book is either LNG-fuelled or LNG-ready.

[2] https://ec.europa.eu/eurostat/statistics-explained/index.php?title=Maritime_freight_and_vessels_statistics.

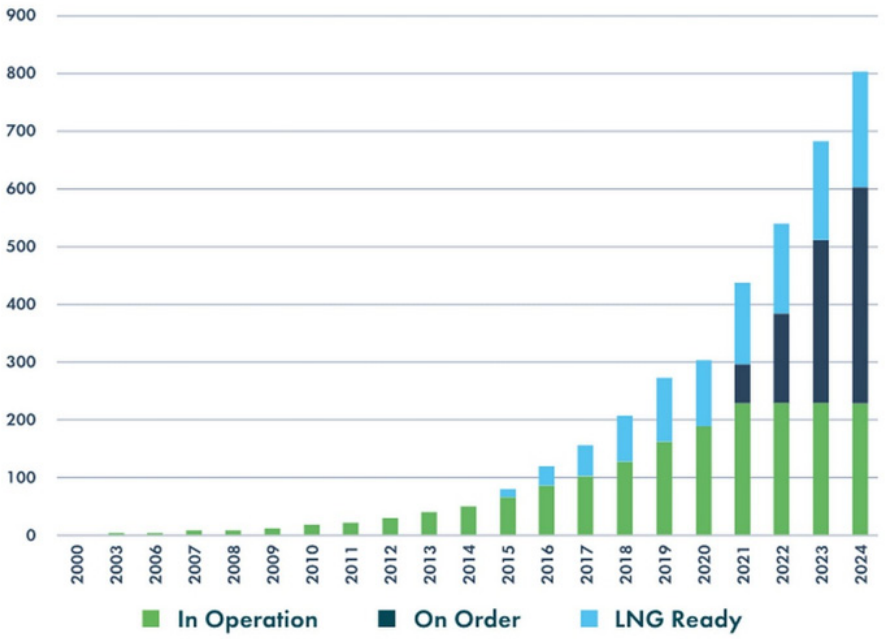

Fig. 4.
LNG fuelled vessels [4]

The Transition Strategy analysis found that vessels retrofitted to run on scalable zero-emission fuels could comprise nearly half the global fleet by 2050. Engines have different design specifications for each fuel, requiring different technologies. Most new ships operating LNG and LPG engines can be retrofitted to run on a dual fuel [16].

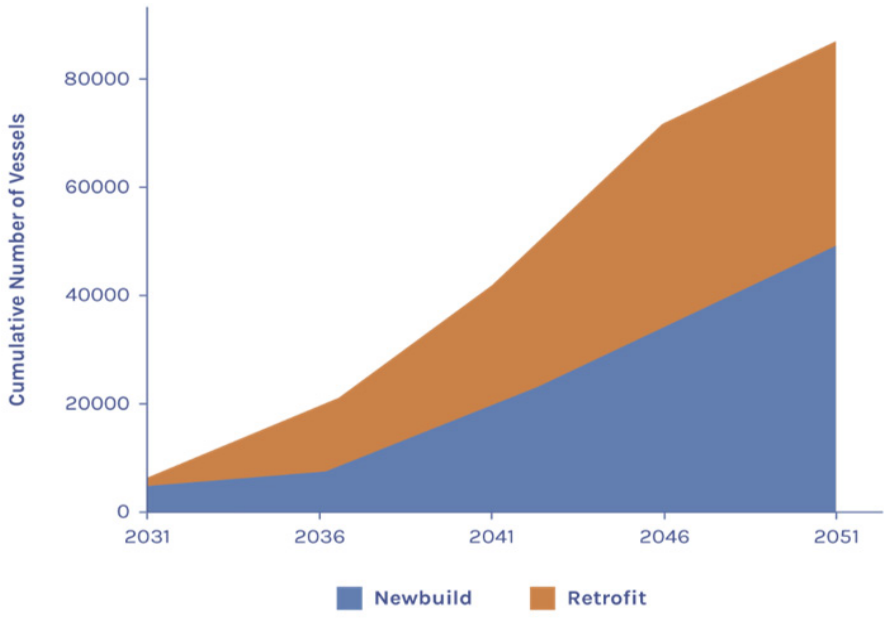

Fig. 5.
New built and retrofitted ships with zero-emission fuels [17]

Natural gas-fuelled engines are expected as an imperative substitute for diesel engines, and the utilisation of dual-fuel engines appears particularly promising. The last ten years have proven that using LNG is the most viable, safe, and adaptive method to be implemented on ships to lower environmental impact and stricter IMO regulations. Ship operators' interest in reducing operating costs through dual fuel or gas technology has grown significantly. International policies and regulations, as listed below, have a crucial role in the development of

the use of LNG as fuel in the maritime industry:

- IMO International Code for the Construction and Equipment of Ships Carrying Liquefied Gases in Bulk (IGC Code).
- IMO Interim Guidelines on Safety for Natural Gas-Fuelled Engine Installations in Ships MSC 285(86) (IGF Interim Guidelines)
- International Association of Classification Societies Unified Requirement M59: Control and Safety Systems for Dual Fuel Diesel Engines.
- IMO International Code of Safety for Ships using Gases or other Low-flashpoint Fuels - IGF Code.
- Classification Societies Rules for Gas Fuelled Ships.
- ISO Guidelines for systems and installations for the supply of LNG as fuel to ships.
- ISO Standard Installation and Equipment for Liquefied Natural Gas - Ship to shore interface and Port.

While the retrofitting of ageing ships could be a challenge and considered an expensive operation, many ships' engines can converter much easier without laying up the ships for a more extended period.

Some of the Man, Caterpillar and MAK engines can be converted to dual-fuelled LNG ships holding on to significant components such as the engine block, crankshaft, air cooler and turbocharger. Therefore, the following parts are to be renewed:

- Cylinder liners,
- Cooling water jackets,
- Pistons,
- Cylinder heads,
- Gas fuel line,
- Engine electronics,

Additionally, the following equipment is introduced:

- Big end bearing temperature monitoring,
- Primary bearing temperature monitoring,
- Timing sensors to the camshaft gear wheel and flywheel.

Next to the engine itself, many components must be placed near and next to the engine to make it possible to run the engine on gas.

- GVU (Gas Valve Unit). This unit controls the pressure of the gaseous fuel towards the engine and ensures safe operation with double block and bleed valves and ventilation possibilities.
- IFM unit (Ignition Fuel Module). This unit ensures enough filtered fuel oil is delivered to the pilot fuel injection system. In its turn, the pilot fuel injection system ignites the gaseous fuel.
- Vacuum pump unit. The fuel gas line on the engine and between the GVU outlet and the engine is double walled. This unit creates an under pressure in the double wall barrier to monitoring any leakage. The extracted air is monitored for CH content and blown off outside.
- Exhaust ventilation module. In the event of an emergency shutdown of the engine in gas mode, the exhaust pipe after the turbocharger is to be flushed to prevent the accumulation of an explosive mixture in the exhaust pipe.
- Slow turn device. Due to the engine's construction, no indicator valves or over-pressure valves are mounted on the cylinder heads. To detect water on the piston, a slow turn device is mounted to slowly turn the engine before starting.

These major components are required to convert the engine from diesel to Dual Fuel mode. Besides this, the ship is to be equipped with:

- Gas storage tanks,
- Master gas valve on deck,
- Transfer pumps suitable for LNG
- Safety devices according to the IGF codes, such as Ex safety zones
- Double wall gas piping throughout enclosed spaces.
- Inert gas production, storage, and deployment equipment

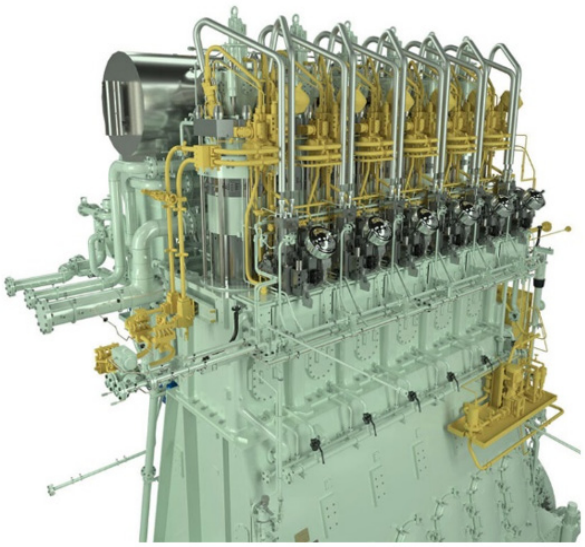

Fig. 6.
MAN-ME-C type engine retrofitted to dual LNG fuel operation [18]

PORT INFRASTRUCTURE

LNG bunkering infrastructure is developing rapidly. The Bunker Navigator[3] map-based tool overviews key LNG bunkering developments and how this growing infrastructure relates to major global shipping routes. Table 2 presents the European LNG bunkering port with some parameters.

List of European bunkering ports

Table 2

No	Port	Type of LNG Bunkering:	Status	Bunkering Capacity	Start Date
			Baltic Sea		
1	Hammerfest (Polarbase)	TTS	OP	90 tonnes/h	April 2017
2	Stockholm	TTS, STS	OP	20,000 m³ storage tank	2011
3	Gothenburg	STS	OP		September 2016
4	Klaipeda	TrTS, TTS	OP	Total 5,000 m³	2020
5	Gdynia	TrTS	OP		September 2016
6	Gdansk	TrTS	OP		September 2016
7	Świnoujście	TrTS	OP		September 2016
8	Szczecin	TrTS	OP		September 2016
9	Hamburg	TrTS,TST*	OP	5,500 cum storage	2017
			Atlantic Ocean		
10	Emden	STS	OP	5,800 cum	November 2020
11	Amsterdam	TrTS, STS*	OP		2013
12	Rotterdam	TTS,STS,TrTS	OP	1000 cum/h	August 2016
13	Antwerp	TTS, STS	OP		2012
14	Zeebrugge	TrTS,TTS,STS	OP		2015
15	Dunkerque	STS	PL		2020?
16	Isle of Grain	PTS	PL		2020
17	Le Havre	TrTS	OP		May 2016
18	Bilbao	STS	OP	Bunkering vessel 600 m³	February 2018
19	Murgados	STS	PL	10,000 m³	2023
20	Sines	STS	PL		2022
21	Huelva	STS	OP		February 2018
22	Gibraltar		PL	5,000 m³storage	2021
			Mediterranean Sea		
23	Valencia	TrTS	OP		July 2018
24	Barcelona	TrTS,STS	OP	6,000 m³	January 2017
25	Marseille	TrTS, STS*	OP		January 2018
26	Oristano, Sardinia	TrTS,STS	UC	7,500 m³	1 H 2021
27	La Spezia	STS	OP	7,551 m³	2020
28	Piraeus	STS	PL	3,000 - 4,000 m³	2022
29	Limassol	STS	PL	3,000 - 4,000 m³	2022

Note: TrTS = Truck-to-Ship; TTS=Tank-to-Ship; STS=Ship-to-Ship; OP=Operational; PL= Planned; *= planned

[3] https://sea-lng.org/bunker-navigator/

While the major European ports are well prepared with facilities for LNG bunkering the capacity and demand for LNG bunkering will increase significantly in the next years with the increased number of dual fuelled LNG new ships. LNG is rapidly becoming more common as a maritime fuel and port infrastructure for LNG bunkering must grow rapidly to cover the needed capacity. The global LNG bunkering market size was valued at $0.38 billion in 2019, and is projected to reach $5.14 billion by 2027 [20].

At the moment there are four options regarding the supply of LNG to ships and while for the bigger ships the solution is supply by land bunkering-TPS(Terminal pipeline to Ship) and supply STS(Ship to ship),using LNG barge vessels, for the short sea shipping in Black sea the most convenient methods of bunkering will be: supply by tanker tracks-TST (Truck Ship transfer) and supply by standard containers -CTS (Container to Ship)

The Black Sea coastal fleet has a total displacement of about 53 million dwt (from over 2 billion dwt, world merchant fleet 2020). Over 4800 merchant vessels are in operation worldwide, or more than 4% of all ships.

There are 57 commercial ports overall, including 18 major ports. The Black Sea port traffic capacity is close to 700 million tonnes. While bulk cargo has historically been the focus of marine transport, the Black Sea container port system was among the World's fastest expanding markets in 2014 with a cargo growth rate of 6% per year. In 2018, 2.92 million Twenty-foot Equivalent Unit (TEU) containers were moving annually.

Due to the Bosporus strait's navigational limitations, the size of the ships visiting Black Sea ports increased over the past 15 years from 2,500 TEU in 2003 to 10,000 TEU, which is the maximum size, while ships up to 18,000 TEU are already making port calls in the Mediterranean. The ports of Istanbul, Piraeus, Damietta, Port Said, Gioia Tauro, Malta, and other smaller Black Sea ports are used for trans-shipment.

The Black Sea region, including the Caspian Sea, is a significant crossroads where more than 34% of the EU's imports of natural gas and oil come from this region. At the same time, most of these are generated onshore, and recent developments have also led to the development of offshore regions, meaning that 8% of Romania's total production comes from offshore crude [20].

There is no doubt that port infrastructure in the Black Sea is not well developed for servicing LNG ships, and more efforts in this direction are expected. The building of LNG storage port terminals will dramatically change the conditions and will increase the interest of charterers using LNG ships and ship Owners to convert their ageing ships using dual fuel

CONCLUSIONS

The present work performed a very intensive review of state of the art on applying the LNG as an alternative for short sea shipping in the Black Sea region. It has been identified that the ports of the Black Sea are not part of existing emission control areas (ECAs) or sulphur emission control areas (SECAs). Recently very intensive transportation activities have been observed in the region of the Black Sea, where relatively aged sheep are still operating.

Alternative solutions to mitigate the region's carbonisation are analysed and concluded that the transition to zero-emission fuels would see key milestones reached within the next decade. The shipping industry must prepare for this transition immediately, avoiding losing assets from ships not complying with the latest requirements. It has been noted that one of the challenging problems is the underdeveloped port infrastructure that also needs to accompany the zero-emission transition.

It seems that, for the moment, the most promising and workable decision is to retrofit existing ships or build new ships with LNG dual-fuel engines and thus systems ready for ammonia, bio-LNG, or synthetic methane. Such a decision makes sense since the existing vessels should meet the latest International Maritime Organisation (IMO) and European Union Emissions Trading Scheme (EU-ETS) legislation demand for reducing emissions and the intention to change the rules all the time. Such a decision should be taken as an opportunity to protect the climate and nature of our planet and be part of sustainable life

Although retrofitting can be a significant investment, it will pay off in the long run as charter companies increasingly begin to favour ships with improved environmental performance. In this context, initiatives such as Poseidon principles [21] and the Maritime Cargo Charter are essential, encouraging financial institutions and charterers to favour ships with a lower environmental footprint.

The step further step is to develop an approach for evaluating the retrofitting of existing commercial ship propulsion system into a green energy one, including the cost-benefit analysis with particular attention to savings from reduced fuel expenses, the societal impacts due to the reduced gas emissions, human health impacts resulting from air quality, and climate change.

ACKNOWLEDGEMENTS

This work was performed within the Research Plan of the Technical University of Varna, funded by the State Budget under the contract NP13 for 2022.

REFERENCES:

[1] https://abcnews.go.com/US/covid-19-brought-emissions-2020-happen-pan-demic/story?id=74362220.
[2] Bilgili, L. (2021). Comparative assessment of alternative marine fuels in life cycle perspective. In Renewable and Sustainable Energy Reviews (Vol. 144): Elsevier Ltd. https://doi.org/10.1016/ j.rser.2021.110985.
[3] Peng, W., Yang, J., Corbin, J., Trivanovic, U., Lobo, P., Kirchen, P., Rogak, S., Gagné, S., Miller, J. W., & Cocker, D. (2020). Comprehensive analysis of the air quality impacts of switching a marine vessel from diesel fuel to natural gas. In Environmental Pollution Vol. 266, pp. 115404: Elsevier.
[4] SEA-LNG (2022). LNG - a fuel - in transition. A view from the bridge. January 2022. Retrieved from https://sea-lng.org/wp-content/uploads/2022/01/LNG-2022_A-view-from-the-bridge_V937.pdf.
[5] SPHERA. (2021). 2nd Life Cycle GHG Emission Study on the Use of LNG as Marine Fuel. Sphera Solutions GmbH, 2021.
[6] Georgiev, P.; Naydenov, L.; Garbatov, Y. Carbon emissions from container shipping in the Black Sea. In Sustainable Development and Innovations in Marine Technologies, Ergin, S., Guedes Soares, C., Eds.; 2023; pp. 85-92.
[7] Georgiev, P.; Angelov, A.; Garbatov, Y. Shipyard construction, repair, and recycling emissions impact on environmental pollution. In Proceedings of the Black Sea, 2022.
[8] Damyanliev, T.; Georgiev, P.; Denev, Y.; Naydenov, L.; Garbatov, Y.; Atanasova, I. Short Sea shipping and shipbuilding capacity of the East Mediterranean and Black Sea regions. In Developments in Maritime Technology and Engineering, Guedes Soares, C., Santos, T.A., Eds.; Taylor and Frances: UK, London, 2021; Volume 1, pp. 749-758.
[9] Atanasova, I.; Damyanliev, T.P.; Georgiev, P.; Garbatov, Y. Analysis of SME ship repair yard capacity in building new ships. In Progress in Maritime Technology and Engineering, Guedes Soares, C., Santos, T.A., Eds.; Taylor & Francis Group: London, 2018; pp. 431-438.
[10] Garbatov, Y.; Georgiev, P. Air pollution and economic impact from ships operating in the port of Varna. *Atmosphere* 2023, Revised.
[11] IDEAS. (2016). European Coaster Fleet Analysis in View of Substandard Shipping & Easy Classification. [Online] http://denizstrateji.com/: IDEAS Institute.
[12] UNCTAD. (2022). The war in Ukraine is in two of the Black Sea countries, but its impact is global. 22 June https://unctad.org/news/war-ukraine-raises-global-shipping-costs-stifles-trade.
[13] UNCTAD. (2022). The impact on trade and development of the war in Ukraine. UNCTAD Rapid Assessment. 16 March. https://unctad.org/system/files/official-document/osginf2022d1_en.pdf.
[14] Bosack, M. McA. (2022). Understanding the Black Sea Grain Initiative, Parley Policy Cable No. 14 (28 July 2022), Retrieved from: https://www.parleypolicy.com/post/understanding-the-black-sea-grain-initiative.
[15] https://en.portnews.ru/news/334558/.
[16] https://www.globalmaritimeforum.org/content/2021/10/A-Strategy-for-the-Transition-to-Zero-Emission-Shipping.pdf.
[17] https://www.weforum.org/agenda/2022/04/3-actions-decarbonize-shipping-industry/.
[18] https://www.offshore-energy.biz/man-es-dual-fuel-retrofits-for-shipping-decarbonisation/.
[19] https://www.digitaljournal.com/pr/lng-bunkering-market-estimated-to-hit-5-14-billion-by-2027.
[20] https://blackseablueconomy.eu/sites/default/files/cma_factsheet_maritime_transport.pdf.
[21] https://www.poseidonprinciples.org/finance/#principle3.

MACHINERY AND PROPULSION SYSTEMS

INFLUENCE OF ENVIRONMENTAL PARAMETERS ON THE HYDRAULIC POWER REQUIRED FOR THE OPERATION OF BULK CARRIER BILGE SYSTEM

Vladimir YORDANOV*

Abstract. *This paper deals with the structure and elements of bulk carrier bilge system and their hydraulic calculation has been performed. Based on the hydraulic calculations of the system in tropical and northern operating conditions, a study of the influence of the environmental parameters on the hydraulic power required for the operation of the bilge system is carried out. For this purpose, analytical dependencies of the density and viscosity of sea water from it's temperature, developed by the author are used.*

Key words: *Bulk carrier, bilge system, hydraulic calculation, influence of the environmental parameters.*

INTRODUCTION

The bilge system is used to pump out any bilge water that may accumulate in ship's spaces - engine room, steering gear room, cargo holds, dry compartments, cofferdams, double bottom tunnel, chain locker, echo-sounder trunk, log trunk, boatswain store, emergency fire pump room and others. In normal conditions of navigation, bilge water is accumulated because of leaks in water systems and ship hull, washing the decks and devices in compartments, fire extinguishing, after an irrigation of rooms and also owing to condensation of water vapour. To remove the bilge water from inside the ship, it is necessary that the parameters of its drainage system meet the requirements of the classification organizations. The elements of the bilge system depend on the type and size of the ship. The capacity of a bilge system is defined by the diameter of the bilge main bilge pipe and bilge pump power. The bilge pump power variation of a bulk carrier under different environmental conditions is investigated in the paper.

DIAGRAM OF BILGE SYSTEM, ELEMENTS AND PARAMETERS

The researched bilge system refers to 43000 tdw bulk carrier with the following main dimensions: length overall - Loa = 186.45 m, breadth moulded - B=30 m, draught moulded - T=11.79 m, depth moulded - D=16.20 m . The lenth of cargo holds are the following: L1=27,20 m, L2=27,54 m, L1=27,54 m, L4=27,54, L5=27,54.

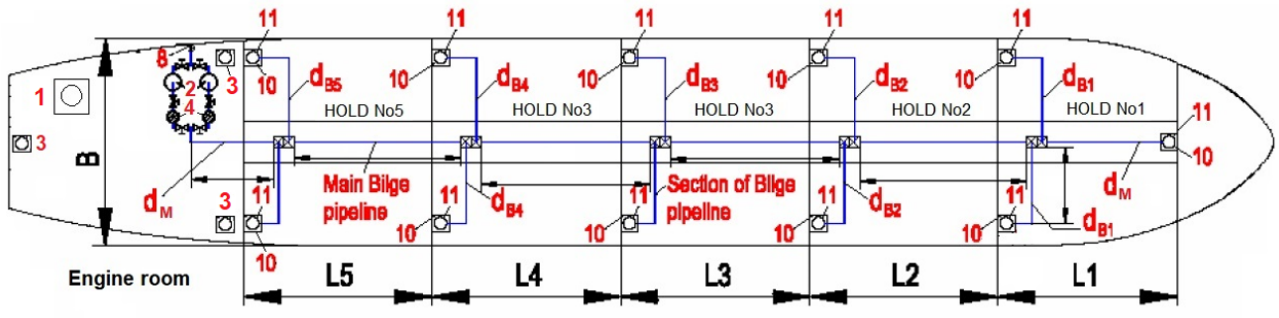

Fig. 1.
Diagram of bilge system for bulk carrier with deadweight 43000 t

Vladimir Yordanov, Assist. Prof., Dr., Technical University of Varna, Bulgaria,
Phone: +359 879 690 184; E-mail: v_jord2@abv.bg

The elements of bilge system (fig. 1) are the following: 1 - bilge separator with degree of cleaning 15 ppm (15 parts of oil per million parts of water by volume) ; 2 - main bilge pump, centrifugal, bronze body, self-priming; 3 - bilge well in engine room; 4 - filter; 8 - outlet connection with non-return valve through which bilge water is pumped outboard or to shore through international shore connections on the both ship sides on open deck; 10 - bilge well in cargo holds; 11 - sucker. Outside cargo holds and engine room, the other spaces like small enclosed spaces and steering gear compartments are with suitable means of drainage, either by hand or power pump bilge suctions. The bilge wells shall have a capacity of at least 0.15 m^3. One of the bilge pumps may be a bilge ejector if there is a separate pump delivering sufficient water for operating the ejector.

The parameters of bilge piping system are [1, 2, 3]:

(1) $$d_M = 1{,}68 .[L . (B+D)]^{0,5}$$

(2) $$d_{Bi} = 2{,}15 .[l_i . (B+D)]^{0,5}$$

where:

d_M - internal diameter of main bilge line , in mm

B - greatest moulded breadth of ship or maximum breadth of cargo hold for ore carriers, in metres

D - moulded depth to bulkhead deck, in metres

L - the distance on the waterline at draught T, from the forward side of the stern to the after side of the rudder post or not less than 96% , and not greater than 97% of the extreme length on the waterline, in metres

d_{Bi} - internal diameter of i-branch bilge suction, in mm

l_i - length of i-watertight compartment, in metres

In no case the diameter d_{Bi} of any suction to be less than 50 mm. The direct bilge suctions in the main and auxiliary engine rooms are not to be of a diameter less that required for the main bilge line.

The capacity Q of each main bilge pump is to be not less than required by the following formula (on condition that the bilge water velocity in the main bilge line is not less than 2 m/s):

(3) $$Q = 2.3600.10^{-6} (\pi /4).d^2_M$$

(4) $$Q = 0{,}005655. d^2_M$$

where:

Q - capacity of each main bilge pump , in m^3/h

d_M - internal diameter of main bilge line , in mm.

The hydraulic power required for the operation of the bilge system and bilge pump power depends on the pump capacity Q and head of the pump H needed to overcome the hydraulic losses in the system.

(5) $$P_{BilgePump} = \frac{Q.H.\rho.g}{3600.1000.\eta} \qquad [kW]$$

where:

$P_{Bilge\ Pump}$ - bilge pump power in kW, Q - capacity of main bilge pump in m^3/h, H - pump differential head in m, ρ - bilge water density in kg/m^3, g = 9,81 - gravity in m^2/s, η - pump efficiency.

Determination of the hydraulic losses and required power of the bilge system is carried out according to the developed diagram (fig.2), with the main pipeline divided into 5 partss starting at point 1. The following parameters are calculated for each part (i = 1 - 5):

(6) $$V = Q_{i-j} / (fi . 3600)$$

(7) $$fi = \pi. (d_i)^2/4$$

(8) $$P_{FR} = \lambda.l.\rho.V^2 / (2 . d_i)$$

(9) $$P_{LR} = \boldsymbol{Sx}_i \rho.V^2 / 2$$

(10) $$Re = V.d / \boldsymbol{\nu}$$

where:

V - water velocity from point i to point j; fi - internal area of cross section of the pipe in i-part, m^2;
d_i - internal diameter of the pipe in i-part, m; P_{FR} - total hydraulic resistance from friction in in i-part, Pa;
P_{LR} - hydraulic local resistance in i-part, Pa; Re - Reynolds number
l - length of the straight section from point i to point j (see fig.2)
ρ - mass density of the bilge water, kg/m^3; x_i - coefficient of local resistance in i-part
v - kinematic viscosity of water, m^2/s; λ - coefficient of hydraulic friction.

Calculation of coefficient of hydraulic friction λ

Table 1

I – 0<Re<2300 $\lambda = 64/Re$ II – 2300<Re<3200 $\lambda = 2{,}7.Re^{-0{,}53}$ III – 3200 < Re<Re` Re`=23/ε $\lambda = 0{,}316Re^{-0{,}25}$	IV – Re` <Re <Re" Re"=560/ε $\lambda = 0{,}1(1{,}46.K/d+100/Re)^{-2}$ V – Re" <Re $\lambda = (1{,}14+2\lg d/K)^{-2}$

The coefficient of hydraulic friction λ is determined by empirical dependences from table 1, where the equivalent geometric roughness is denoted by K (K=0,3 mm-for pipes in operation), and the relative roughness by $\varepsilon = K/d_i$. The parameters of cargo holds and pipelines are shown in table 2.

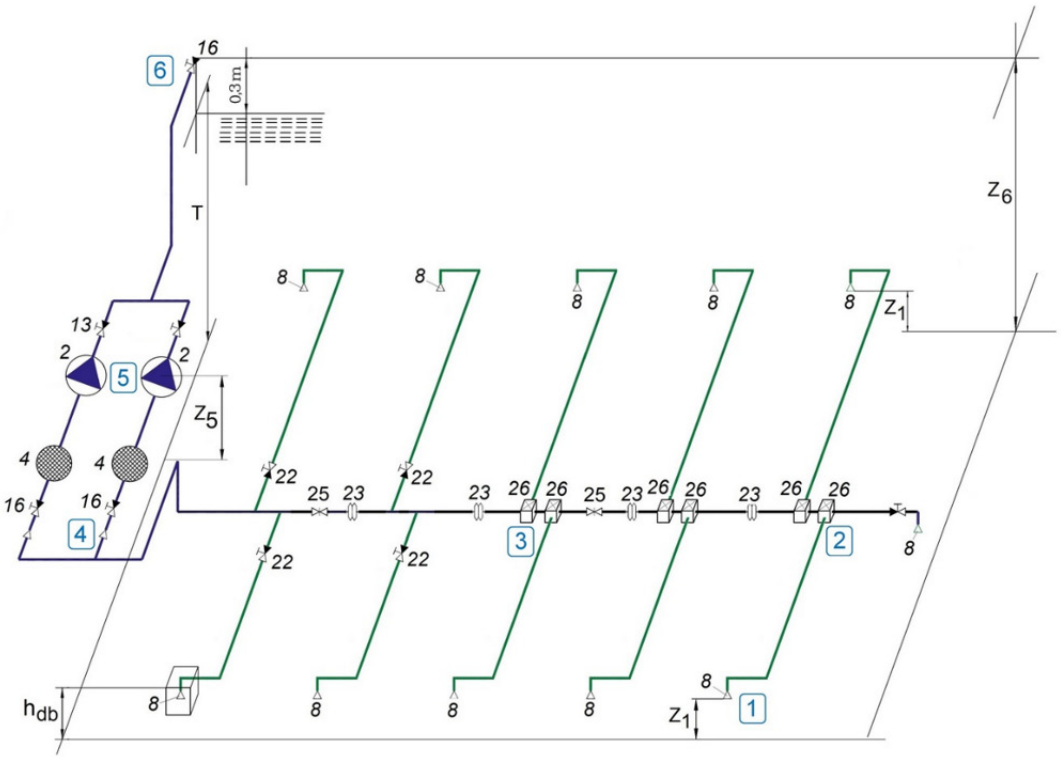

№ of part	1-2	2-3	3-4	4-5	5-6
Sum-L_{i-j} [m]	13,400	55,080	63,75	2,000	55,080

Fig. 2.
Diagram of the bilge system with 5 parts and lengths Sum-L of the corresponding straight pipes from point i to point j

Cargo holds and pipelines parameters

Table 1

		L 177	L1 27,2	L2 27,54	L3 27,54	L4 27,54	L5 27,54	S mm	D mm
calculated	dm	176,92						6	194
	d_{B1}		101,22					5	133
	d_{B2}			101,69				5	133
	d_{B3}				101,69			5	133
	d_{B4}					101,69		5	133
	d_{B5}						101,69	5	133
		dm	d_{B1}	d_{B2}	d_{B3}	d_{B4}	d_{B5}		
		182	123	123	123	123	123		
		standart pipes d=D-2.S							

Sea water parameters are determined as follows (at an average of salinity of 35 grams per liter) [4].

(11) $$\nu_{SW}=[1{,}31.10^{-6}.(t_{SW})^4-2{,}1.10^{-4}.(t_{SW})^3+1{,}45.10^{-2}.(t_{SW})^2-0{,}619.t_{SW}+18{,}5].10^{-7}$$

(12) $$\rho_{SW}=1{,}71.10^{-18}.(t_{SW})^4+1{,}85.10^{-5}.(t_{SW})^3-5{,}51.10^{-3}.(t_{SW})^2-5{,}05.10^{-2}.t_{SW}+1030$$

The designations in the the above equations are the following: ν_{SW} - kinematic viscosity of sea water in m^2/s; t_{SW} - temperature of sea water in ^oC; ρ_{SW} - density of sea in kg/m^3.

RESULTS OF HYDRAULIC CALCULATION OF THE BILGE SYSTEM

The hydraulic calculation of the drying system is carried out under two variants of the environmental parameters:

1/ in winter conditions, as the sea water temperature is 2 °C;

2/ in summer conditions, as the sea water temperature is 32 °C.

On the basis of the analytical dependences (11)-(12) developed by the author for the kinematic viscosity and mass density of sea water the following results were obtained:

1/in winter conditions t_{SW}=2 °C:

ν =17,3573.10^{-5} [m^2/s] ρ_{SW}=1027,875 kg/m^3

2/in summer conditions t_{SW}=32 °C:

ν =8,1046.10^{-5} [m^2/s] ρ_{SW}=1021,34 kg/m^3

The results of the hydraulic calculation are presented in tabular form at three pump capacities (Q/3, 2.Q/3 and Q) for each of the five parts of the bilge system and at two variants of the environmental parameters as follows.

Obtained results for system parameters under winter conditions

Table 2

Parameter	Part of bilge pipeline		
	1-2	1-2	1-2
$Q_{i-j}=Q$	Q/6	Q/3	Q/2
d	0,123	0,123	0,123
Sum-L_{i-j}	13,400	13,400	13,400
$f=\pi.d^2/4$	0,0119	0,0119	0,0119
Sum (ξ_{LR})	2,970	2,970	2,970
Q_{i-j}	31,21860815	62,4372163	93,655824
V	0,730	1,460	2,189
Re	51717,213	103434,425	155151,638
λ	0,027225971	0,02594007	0,0254656
ρ	1027,875	1027,875	1027,875
P_{FR}	811,925	3094,309	6834,861
P_{LR}	812,998	3251,991	7316,980
$P_{i-j}=P_{FR}+P_{LR}$	1624,923	6346,301	14151,842

Parameter	Part of bilge pipeline		
	5-6	5-6	5-6
$Q_{i-j}=Q$	Q/3	(2/3).Q	Q
d	0,182	0,182	0,182
Sum-L_{i-j}	22,500	22,500	22,500
$f=\pi.d^2/4$	0,026	0,026	0,026
Sum (ξ_{LR})	3,550	3,55	3,55
Q_{i-j}	62,437216	124,87443	187,31165
V	0,667	1,333	2,000
Re	69903,485	139806,971	209710,456
λ	0,0248887	0,0236376	0,0231728
ρ	1027,875	1027,875	1027,875
P_{FR}	702,815	2669,946	5889,240
P_{LR}	810,879	3243,517	7297,913
$P_{i-j}=P_{FR}+P_{LR}$	1513,694	5913,463	13187,153

The additional designations in table 2, 3 and 4 are the following: P_{SUCT} - pressure losses in the suction part of the pipeline, Pa; P_{S-CH} - losses of hydraulic pressure in the suppercharge part of the pipeline, Pa; P_{TPL} - total pressure losses in the main pipeline of the bilge system, Pa, Q - capacity of main bilge pump, m^3/h. These parameters are defined as follows:

(11) $$P_{SUCT} = P_{1-2} + P_{2-3} + P_{3-4} + P_{4-5} + \rho.g.\ (Z_5 - Z_1)$$

(12) $$P_{S-CH} = P_{5-6} + \rho.g.(Z_6 - Z_5)$$

(13) $$P_{TPL} = P_{SUCT} + P_{S-CH}$$

where:

Z_1 , Z_5 , Z_6 are the vertical coordinates of the corresponding points of the system from the main line, determining the hydrostatic pressure.

Obtained results for system parameters under summer conditions

Table 3

Parameter	Part of bilge pipeline		
	1-2	1-2	1-2
$Q_{i-j} = Q$	Q/6	Q/3	Q/2
d	0,123	0,123	0,123
Sum-L_{i-j}	13,400	13,400	13,400
$f = \pi . d^2/4$	0,0119	0,0119	0,0119
Sum (ξ_{LR})	2,970	2,970	2,970
Q_{i-j}	31,21860815	62,4372163	93,655824
V	0,730	1,460	2,189
Re	110760,959	221521,917	332282,876
λ	0,025847985	0,02516813	0,0246789
ρ	1021,340	1021,340	1021,340
P_{FR}	765,930	2983,140	6581,590
P_{LR}	807,829	3231,316	7270,460
$P_{i-j}=P_{FR}+P_{LR}$	1573,759	6214,456	13852,051

Parameter	Part of bilge pipeline		
	5-6	5-6	5-6
$Q_{i-j} = Q$	Q/3	(2/3).Q	Q
d	0,182	0,182	0,182
Sum-L_{i-j}	22,500	22,500	22,500
$f = \pi . d^2/4$	0,026	0,026	0,026
Sum (ξ_{LR})	3,550	3,55	3,55
Q_{i-j}	62,437216	124,87443	187,31165
V	0,667	1,333	2,000
Re	149709,867	299419,734	449129,602
λ	0,0235475	0,0228802	0,0222375
ρ	1021,340	1021,340	1021,340
P_{FR}	660,715	2567,966	5615,614
P_{LR}	805,724	3222,895	7251,514
$P_{i-j}=P_{FR}+P_{LR}$	1466,439	5790,861	12867,128

Obtained results for system parameters from point 1 to point 6

Table 4

Q	62,4372163	124,8744326	187,3116489
P_{FR}	5289,010	20102,459	44350,627
P_{LR}	4894,804	19579,216	44053,235
sumP_{FR+LR}	10183,814	39681,674	88403,862
P_{SUCT}	29744,540	54842,631	96291,129
P_{S-CH}	97709,849	102109,618	109383,307
P_{TPL}	127454,389	156952,249	205674,437

in winter conditions

Q	62,4372163	124,8744326	187,3116489
P_{FR}	4974,834	19341,654	42354,303
P_{LR}	4863,684	19454,734	43773,152
sumP_{FR+LR}	9838,518	38796,389	86127,455
P_{SUCT}	29312,511	53945,959	94200,758
P_{S-CH}	97050,994	101375,416	108451,684
P_{TPL}	126363,505	155321,376	202652,442

in summer conditions

The comparison of the two variants in winter and summer conditions is carried out according to the required pressure to overcome the hydraulic losses in the bilge system.and according to the following indicators in %:

(14) $$dP_{FR} = 100.(P_{FRW-W} - P_{FR-S})/P_{FR-S}$$

(15) $$dP_{FR+LR} = 100.(P_{FR+LR-W} - P_{FR+LR-S})/P_{FR+LR-S}$$

(16) $$dP_{SUCT} = 100.(P_{SUCT-W} - P_{SUCT-S})/P_{SUCT-S}$$

(17) $$dP_{S-CH} = 100.(P_{S-CH-W} - P_{S-CH-S})/P_{S-CH-S}$$

(18) $$dP_{TPL} = 100.(P_{TPL-W} - P_{TPL-S})/P_{TPL-S}$$

where:

dP_{FR} - relative difference in pressure required to overcome friction losses in the main pipeline; dP_{FR+LR} - relative difference in the required pressure to overcome the hydraulic losses from friction and from the local resistances in the main pipeline; dP_{SUCT} - relative difference in the required pressure to overcome hydraulic pressure losses in the suction part of the main pipeline; dP_{S-CH} - relative difference in the necessary pressure to overcome hydraulic pressure losses in the supercharge part of the main pipeline; P_{TPL} - relative difference in the required hydraulic pressure to overcome the total pressure losses in the main pipeline of the bilge system.

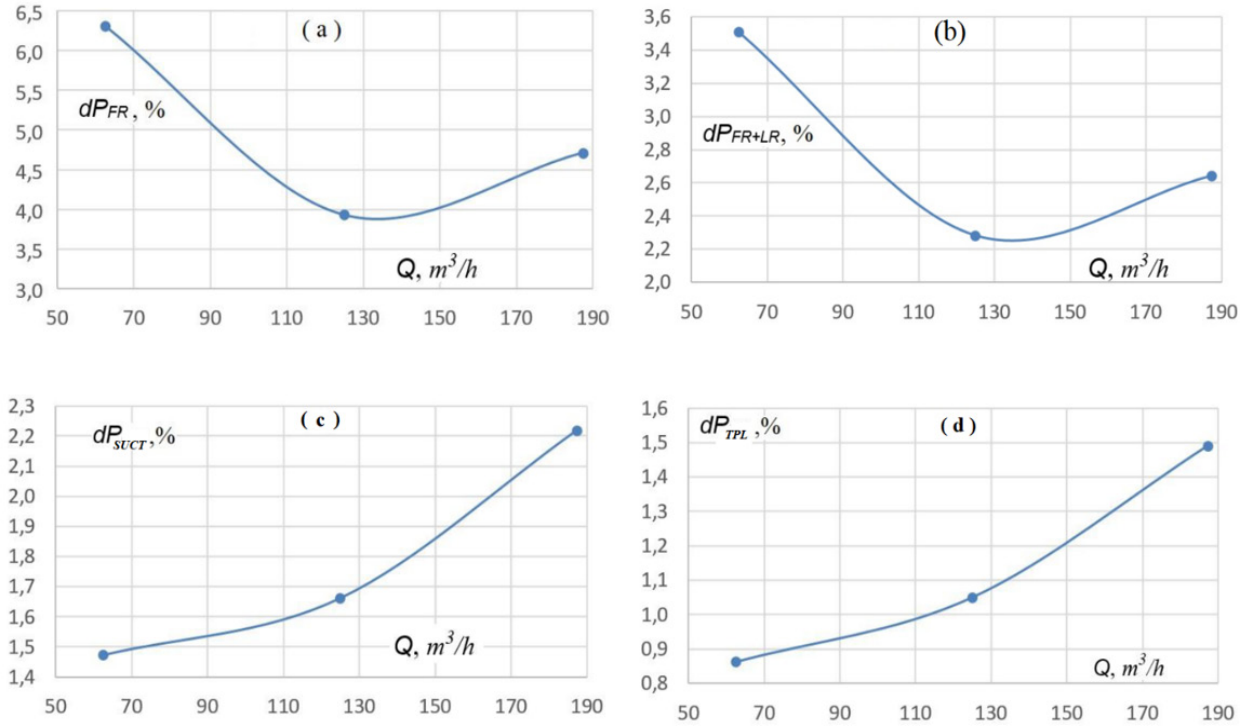

Fig. 3.
Comparison of the different indicators of the required hydraulic pressure in the main pipeline of the bilge system

CONCLUSIONS

1. Environmental parameters have the strongest influence on the required pressure to overcome friction losses in the main pipeline (fig. 3.a). During the transition from summer to winter operating conditions, a relative increase of this pressure is about 4.7÷6.3% . Taking into account the total hydraulic losses from friction and from local resistances during the transition from summer to winter conditions, the relative increase in required pressure is about 2.6% at 100% pump flow load.

2. During the transition from summer to winter conditions, the influence of the environmental parameters on the total hydraulic losses (from friction and from local resistances) in the suction part of the main pipeline pipeline (fig.3.c) is such, that it leads to an increase of these losses up to 2.2%. The increase of these hydraulic losses in the supercharge pipeline (which is of shorter length) is about 0.86%, and with the consideration of the total hydraulic losses before and after the bilge pump, their increase and the corresponding increase in the required hydraulic power for operation of the bilge system constitutes about 1.5% (fig.3.d).

REFERENCES:

[1] H a r a l a n o v, H., Petrov, N. *Ship systems* (guide for course design), TU-Varna, Varna, 1987. (in Bulgarian).
[2] *R u l e s and Regulations for the Classification of Ships.* Lloyd's register, January 2016.
[3] *R U L E S for Classification of Ships*. DNV GL AS, July 2017.
[4] Y o r d a n o v, V., Danilovskiy, A., Aung, H. Improvement of models for automated design of engine room arrangement on a transport ship. Fourteenth International Conference on Marine Sciences and Technologies, Black Sea 2018, Prpceedings, Varna, Bulgaria, ISSN 1314-0957, pp. 107-113.

VARNA SCIENTIFIC AND TECHNICAL UNIONS

SIXTEENTH INTERNATIONAL CONFERENCE ON MARINE SCIENCES AND TECHNOLOGIES

Correction by LARGO CITY Ltd. - DOBRICH
Computer layout by Donika Sarkoleva-Zlateva
Total print: 30, Format 60/84/8

LARGO CITY Ltd. - DOBRICH
DESIGN, PRE-PRESS AND PRINTING

ISSN 1314 - 0957